

Aus der Medizinischen Poliklinik – Innenstadt
der Ludwig-Maximilians-Universität München
Komm. Direktor: Prof. Dr. med. Martin Reincke

Role of pro-inflammatory and homeostatic chemokines in diabetic nephropathy

Dissertation

zum Erwerb des Doktorgrades der Humanbiologie
an der Medizinischen Fakultät der
Ludwig-Maximilians-Universität zu München

vorgelegt von

Sufyan G. Sayyed

Malegaon, India

2010

Mit Genehmigung der Medizinischen Fakultät
der Universität München

Berichterstatter: PD Dr. med. Hans-Joachim Anders

Mitberichterstatter: Priv. Doz. Dr. Uli C. Brödl

Mitberichterstatter: Priv. Doz. Dr. Wolfgang Neuhofer

Dekan: Prof. Dr. med. Dr. h.c. M. Reiser,
FACR, FRCR

Tag der mündlichen Prüfung: 12. 02. 2010

ACKNOWLEDGEMENTS

I can not resist myself from expressing my heart felt deep sense of gratitude and respect for my PhD supervisor PD Dr. Hans-Joachim Anders, for his keen interest in my research, constant encouragement, concrete suggestions and meticulous guidance that helped me at each and every step of my research work during my PhD. Above all his kindness and support to me through out my tenure at Klinische Biochemie, LMU. I feel myself extremely lucky to be one of his students.

I would like to acknowledge Prof. S. Klussmann and Dr. D. Eulberg (Noxxon Pharma, Berlin) as well as Dr. Pius Litcher (Novartis Pharma, Basel) for providing me experimental drug molecules for the research work carried out during my PhD work.

My sincere thank goes to Dr. Bruno Luckow and Dr. Peter Nelson for their constant encouragement of my research work and constructive suggestions throughout my stay at Klinische Biochemie.

I wish to express my profound gratitude to Ewa Radomska, Dan Draganovici and Jana Mandelbaum for providing skillful technical assistance to carry out the research work successfully.

My special thanks go to Dr. Volha Ninichuk for providing her valuable support and guidance in addition to her great help at the time of my transition to this lab.

I am really grateful to all my friends who always cared for me and made my stay a delightful and helped me at every stage of my PhD. To the few names which I really hold close to my heart Mr. Ramanjaneyulu Allam, Dr. Rahul Pawar, Mr. Onkar Kulkarni, Mr. Anil Gaikwad, Dr. Julia Lichtnekert, Ms. Anela Taubitz, and Dr. Nagendrana Ramnigam.

I wish to express my heartiest thanks to my lab colleagues for their delightful and stimulating companionship during my stay at Klinische Biochemie, LMU.

I would like to take this opportunity to mention here few of best pals of my life who were and are always there whenever I called them for any kind of help and support namely, Paraksh, Moin, Lalit, Joney, Shahid, Hamid, Imran, Nafees, Sandeep, Majid and Mushtaque.

There are no words to express my feeling, love and affectionate gratitude to all my family members for their faith, love, inspiration, selfless sacrifices and constant encouragement throughout my life.

Date:

SUFYAN G. SAYYED

Place: München

SUFYAN ALI GHAZANFAR ALI SAYYED, M.S. Pharm.

Med. Poliklinik, Klinische Biochemie,
Ludwig-Maximilians University (LMU),
Schiller straÙe-42, Munich- 80336,
Germany
hisufy@gmail.com

DECLARATION

I here by declare that the present work embodied in this thesis was carried out by me under the supervision of OA PD Dr. Hans Joachim Anders, Internist-Nephrologe-Rheumatologe, Medizinische Poliklinik-Innenstadt Klinikum der Universität München. This work has not been submitted in part or full to any other university or institute for any degree or diploma.

Sufyan G. Sayyed

Date:

Dedicated to
MY LOVING SISTER "RAHILA"

CONTENTS	PAGE
1. Introduction.....	4
1.1. Diabetic nephropathy and different stages	5
1.2. Pathophysiology	6
1.2.1. <i>Histomorphological changes observed in human diabetic nephropathy</i> ..	6
1.2.2. <i>Molecular mechanisms involved in progression and development of diabetic nephropathy</i>	7
1.2.2.1. <i>Metabolic pathways in the development of DN</i>	9
1.2.2.2. <i>Hemodynamic pathways</i>	11
1.2.2.3. <i>Involvement of growth factors</i>	13
1.2.2.4. <i>Inflammation and diabetic nephropathy</i>	15
1.2.2.5. <i>Chemokines and chemokine receptors in diabetic nephropathy</i>	18
1.2.2.5.1. <i>Pro-inflammatory chemokines and receptors</i>	20
1.2.2.5.2. <i>Homeostatic chemokines and their receptors</i>	25
2. Summary and hypothesis.....	29
2.1. Role of pro-inflammatory chemokines in diabetic nephropathy	29
2.2. Role of homeostatic chemokines in diabetic nephropathy	29
3. Materials and methods.....	30
3.1. Equipments and instruments.....	30
3.2. Other Equipments	30
3.3. Chemicals and reagents	31
3.4. Miscellaneous	33
3.5 Experimental procedures	34
3.5.1. <i>Animals</i>	34
3.5.2. <i>Animal model</i>	35
3.5.3. <i>Drugs and formulations</i>	36
3.5.4. <i>Experimental designs</i>	39
3.5.5. <i>Blood and urine sample collection</i>	40
3.5.6. <i>Body weight and blood glucose</i>	40
3.5.7. <i>Urinary albumin</i>	41
3.5.8. <i>Urinary creatinine measurement</i>	41
3.5.9. <i>Urinary albumin to creatinine ratio</i>	42
3.5.10. <i>Cytokines</i>	42
3.5.11. <i>Glomerular filtration rate determination</i>	43
3.5.12. <i>Fluorescence activated cell sorting</i>	45
3.5.13. <i>Immunostaining</i>	47
3.5.14. <i>Periodic acid Schiff staining</i>	48
3.5.15. <i>Silver staining</i>	48
3.5.16. <i>Histopathological evaluations</i>	49
3.5.17. <i>RNA analysis</i>	50
3.5.18. <i>In vitro methods</i>	53
3.6. Computer programs	55
3.7. Statistical analysis.....	55
4. Results.....	56
4.1. Animal model validation	56
4.1.1. <i>Glomerulosclerosis is aggravated upon uninephrectomy</i>	56
4.1.2. <i>Glomerulosclerosis was associated with macrophage infiltration in kidney</i>	57

4.1.3. <i>Uninephrectomy in db/db mice resulted in increased albuminuria and decreased glomerular filtration rate</i>	58
4.2. Role of pro-inflammatory chemokines in diabetic nephropathy	58
4.2.1. <i>CCL2/MCP-1 blockade at different stages of disease progression</i>	58
4.3. Inhibition of the homeostatic chemokine CXCL12 in diabetic nephropathy ..	72
4.3.1. <i>Plasma levels of CXCL12</i>	72
4.3.2. <i>CXCL12 blockade prevents proteinuria in db/db mice</i>	73
4.3.3. <i>Effect of CXCL12 blockade on glomerulosclerosis in db/db mice</i>	73
4.3.4. <i>CXCL12 blockade and tubulointerstitial pathology in db/db mice</i>	75
4.3.5. <i>Effect of CXCL12 blockade on infiltrating macrophages in 1K db/db mice</i>	77
4.3.6. <i>Effect of CXCL12 blockade on stem cell mobilization</i>	78
4.3.7. <i>Effect of CXCL12 blockade on macrophage polarization in kidney</i>	80
4.3.8. <i>CXCL12 is mainly produced by podocytes in db/db mice</i>	81
4.3.9. <i>Effect of CXCL12 blockade on podocytes in glomeruli</i>	84
4.3.10. <i>Effect of CXCL12 blockade on body weight and blood glucose</i>	85
5. Discussion	86
5.1. Role of pro-inflammatory chemokines in diabetic nephropathy	86
5.2. Role of homeostatic chemokines in diabetic nephropathy	90
6. Summary and conclusions	94
7. Zusammenfassung	96
8. References	98
9. Abbreviations	115
Appendix	119
CURRICULUM VITAE	122

List of tables

<i>Table 1: Percentage incidence and prevalence of diabetes in German dialysis population,</i>	4
<i>Table 2: Different stages of diabetic nephropathy</i>	5
<i>Table 3: Effect of uninephrectomy on albuminuria and glomerular filtration rate ..</i>	58

List of Figures

Figure 1: Incidence trends of different renal disease in the German dialysis population	5
Figure 2: Renal biopsies from microalbuminuric type 2 diabetic patients	7
Figure 3: Different molecular mechanisms involved in the development and progression of diabetic nephropathy	8
Figure 4: Metabolic pathways associated with diabetic nephropathy.	11
Figure 5: Hemodynamic and pro-inflammatory pathways associated with diabetic nephropathy.	13
Figure 6: Chemokines and chemokine receptors.	19
Figure 7: Pictures showing surgical procedure for uninephrectomy in mice.	35
Figure 8: Schematic representation of Spiegelmer generation.	37
Figure 9: Representative agarose gel for RNA integrity check.	51
Figure 10 : PAS stains for renal sections.	56
Figure 11 : Renal sections from 24 week old mice with or without uninephrectomy were stained for Mac2.	57
Figure 12: Serum CCL2 levels.	59
Figure 13: Urinary albumin to creatinine ratio.	60
Figure 14: Ki 67 staining of kidney sections.	61
Figure 15: Renal sections from mice of all groups were stained for Mac2.	62
Figure 16: PAS staining of renal sections.	63
Figure 17: The mRNA expression levels of CCL2.	64
Figure 18: Glomerular filtration rate.	65
Figure 19: Body weight and blood glucose levels.	66
Figure 20: Urinary albumin to creatinine ratio.	67
Figure 21: Mac2 staining of renals sections.	68
Figure 22: PAS staining for renal sections.	69
Figure 23: Silver staining of renal sections..	70
Figure 24: Body weight and blood glucose levels.	71
Figure 25: Serum CXCL12 lelvels	72
Figure 26: Urinary albumine to creatinine ratio.	73
Figure 27: PAS staining for renal sections.	74
Figure 28: Silver staining for renal sections.	75
Figure 29: Ki 67 staining of renal sections.	76
Figure 30: Meca32 staining of renal sections.	77
Figure 31: Mac2 staining for renal sections.	78
Figure 32: FACS analysis of bone marrow, blood and kidney cell preparations.	79
Figure 33: Macrophage marker expression profile in kidney.	80
Figure 34: The mRNA expression levels of CXCL12.	81
Figure 35: CXCL12 stains of renal sections at different age.	82
Figure 36: Fluorescence microscopy on renal sections..	83
Figure 37: WT1 positive cells on glomerula tuft and in periphery.	84
Figure 38: Body weight and blood glucose levels.	85

1. Introduction

Diabetes is a metabolic disorder of multiple causes characterized by chronic hyperglycemia and disorders of carbohydrate, fat and protein metabolism associated with defect in insulin secretion (type 1) or inability of the secreted insulin for its action (type 2).

Diabetes mellitus is one of the major health concerns in developing as well as developed countries. The number of people affected with diabetes world wide is projected to increase from 171 million in the year 2000 to 366 million by year 2030 world wide ¹. In Germany, about 7 million people are known to have manifested diabetes mellitus, 2 to 3 million are thought to have undetected disease and about 10 million people are diagnosed having impaired glucose tolerance. It is suspected that in the near future every third person in German population of age group over 65 years will suffer from diabetes mellitus ². Uncontrolled and prolonged hyperglycaemia in diabetic patients often leads to several macro and micro vascular complications. Major microvascular complications include diabetic retinopathy, neuropathy and nephropathy. Diabetic nephropathy is one of the most common complications affecting more than 30 % of diabetic patients suffering for prolonged periods ³. Diabetic nephropathy is leading cause of end stage renal diseases (ESRD) in US, Europe and Japan ⁴. Diabetic nephropathy is one of the leading cause of morbidity and mortality almost 30-40 % of ESRD patients in US are either type 1 or type 2 diabetic patients. A prospective study from Germany has reported that 5-year survival rate was less than 10 % in elderly population with type 2 diabetes, and no more than 40% in younger population with type 1 diabetes. In Heidelberg, 59% of patients admitted for renal replacement therapy in 1995 had diabetes (Figure 1).

Table 1: Percentage incidence and prevalence of diabetes in German dialysis population, data obtained from QUASI-Niere registry (2005)

Diabetes type 1 / 2	1996	1997	1998	1999	2000	2001	2002	2003	2004
Incidence (%)	30.6	30.7	32.4	33.9	35.7	35.6	35.9	36.2	34.2
Prevalence (%)	21.6	22.3	23.2	24.1	25.0	25.7	26.3	26.8	27.1

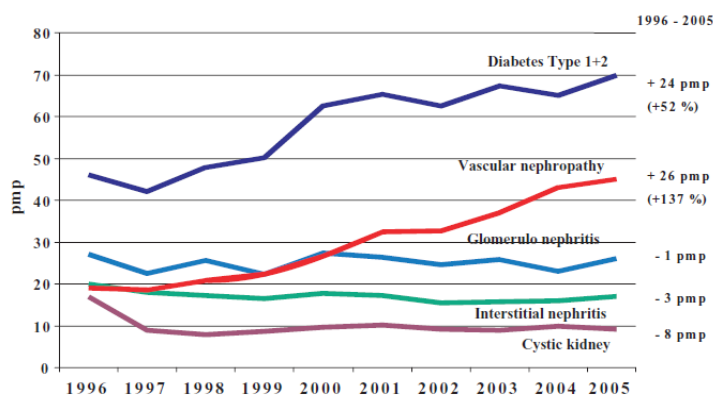


Figure 1: Incidence trends of different renal disease in the German dialysis population (data from QUASI-Niere registry 2007)

1.1. Diabetic nephropathy and different stages

Diabetic nephropathy is characterized by persistent albuminuria (> 300 mg/d or >200 mcg/min), a relentless decline in the glomerular filtration rate (GFR) and elevated arterial blood pressure, which is confirmed on at least 2 occasions 3-6 months apart. Based on the GFR decline, renal physiology and albumin excretion progression of DN has been classified into five different stages as suggested by K/DOQI (Table 2) ⁵.

Table 2: Different stages of diabetic nephropathy

	Designation	Characteristics	GFR *	Albumin Excretion	Chronology	Prevalence in German diabetic population
Stage 1	Hyperfunction and hypertrophy	Glomerular Hyperfiltration	> 90	May be increased	Present at the time of diagnosis	30-37 %
Stage 2	Silent stage	Thickened GBM Expanded mesangium	60-90	< 200 mg/d	First five years	17-19 %
Stage 3	Incipient stage	Microalbuminuria	30-59	30-300 mg/d	6-15 years	19-22 %
Stage 4	Overt diabetic nephropathy	Macroalbuminuria	15-29	> 380 mg/d	15-25 years	1-2 %
Stage 5	Uremic	ESRD	<15/ dialysis	Decreasing	25-30 years	28 %

*ml/min/1.73 m², GBM; glomerular basement membrane, ESRD; end stage renal disease.

1.2. Pathophysiology

1.2.1. Histomorphological changes observed in human diabetic nephropathy

The key changes observed clinically in diabetic nephropathy are augmentation of extracellular matrix, thickening of the glomerular basement membrane, and expansion of mesangium. Where as light microscopy has shown increased solid spaces of the tuft, most frequently observed are as coarse branching of solid (Periodic Acid Schiff positive) material (diffuse glomerulopathy). Large acellular nodules are observed also know as Kimmelstiel-Wilson lesions/nodules (Figure 2). The glomeruli and kidneys are typically normal or increased in size thus, distinguishing DN from most other forms of chronic renal insufficiency, wherein renal size is reduced (except renal amyloidosis and polycystic kidney disease). Immune deposits are not observed. The renal vasculature typically displays evidence of atherosclerosis, usually due to concomitant hyperlipidemia and hypertensive arteriosclerosis. Electron microscopy provides a more detailed definition of the structures involved. In advanced disease, the mesangial regions occupy a large proportion of the tuft, with prominent matrix content. Further, the basement membrane in the capillary walls (i.e. the peripheral basement membrane) is thicker than normal. The severity of diabetic glomerulopathy is estimated by the thickness of the peripheral basement membrane and mesangium and matrix expressed as a fraction of appropriate spaces (e.g. volume fraction of mesangium/glomerulus, matrix/mesangium, or matrix/glomerulus) (Figure 2).

Three major histological changes occur in the glomeruli of persons with diabetic nephropathy. First, mesangial expansion is directly induced by hyperglycaemia, perhaps via increased matrix production or glycosylation of matrix proteins. Second, thickening of GBM occurs. Third, glomerular sclerosis is caused by intraglomerular hypertension (induced by renal vasodilatation or from ischemic injury induced by hyaline narrowing of the vessels supplying the glomeruli). These different histologic patterns appear to have similar prognostic significance (www.emedline.com).

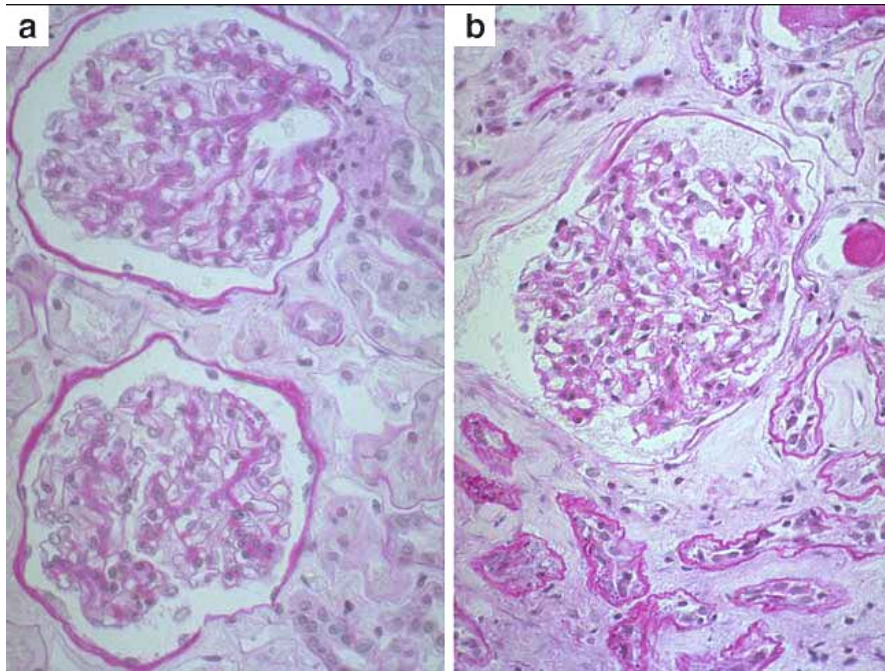


Figure 2: Renal biopsies from microalbuminuric type 2 diabetic patients (periodic acid–Schiff stain). (a) Normal glomerular, tubular, interstitial and vascular structures. This would be classified as Category I. (b) Mild mesangial expansion relative to the severity of interstitial fibrosis and tubular atrophy. This would be classified as Category III.J (images taken from www.emedline.com)

1.2.2. Molecular mechanisms involved in progression and development of diabetic nephropathy

Diabetic nephropathy is one of the major causes of morbidity and mortality in diabetic population. As is the case with other diabetic complications hyperglycemia is the underlying cause for development of DN. However, the relative significance of each of the proposed molecular mechanisms that have been described is yet to be defined (Figure 3).

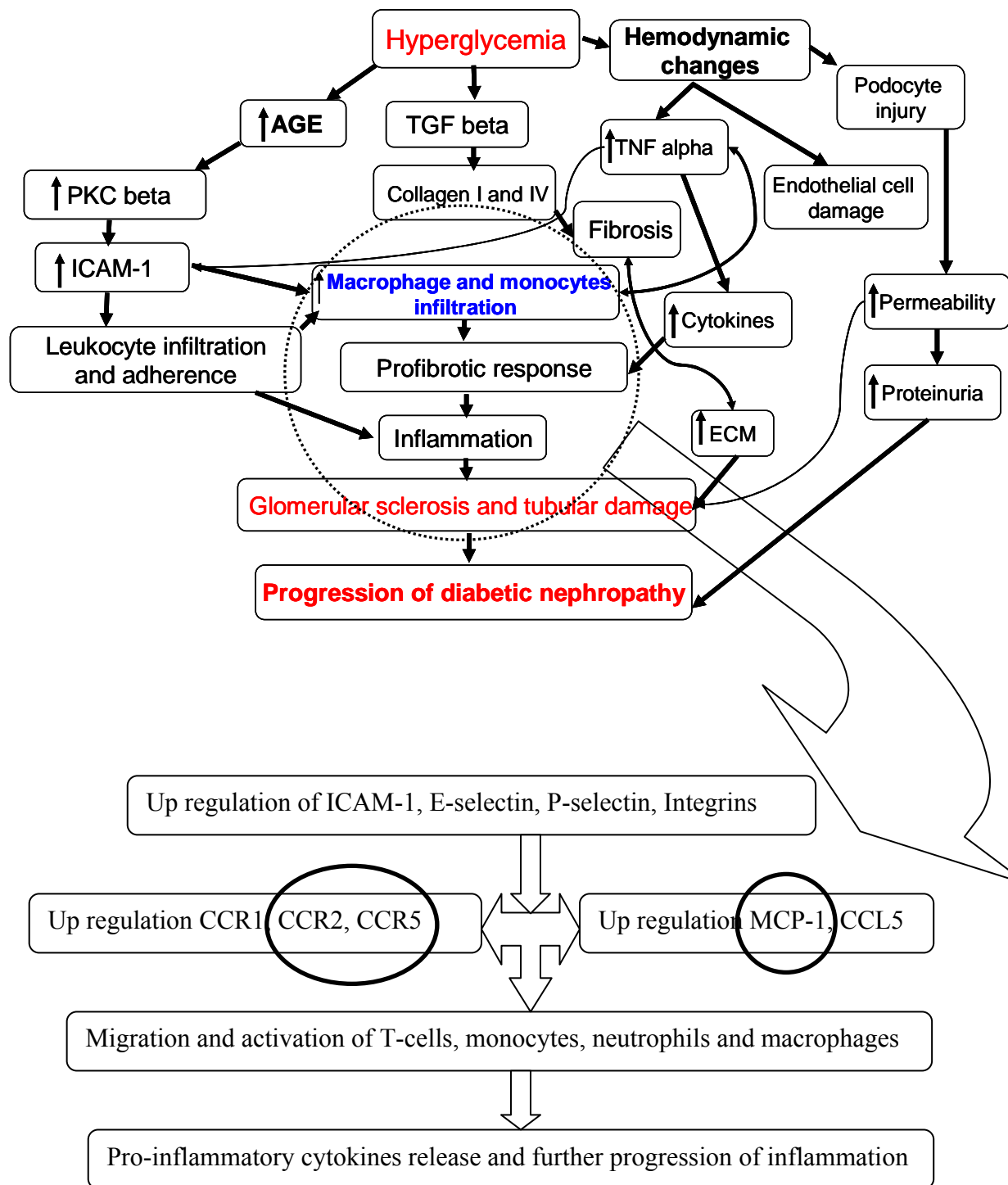


Figure 3: Different molecular mechanisms involved in the development and progression of diabetic nephropathy

1.2.2.1. Metabolic pathways in the development of DN

1.2.2.1.1. Hyperglycemia

Prolonged hyperglycemia in diabetic patients is the root cause of all microvascular complications which develop at the later stage of the disease including diabetic nephropathy. Clinical studies such as Diabetes Control and Complication Trial (DCCT) ⁶ and UK Prospective Diabetes Study (UKPDS) ⁷ have shown that intensive glycaemic control retards the progression and development of microalbuminuria and overt nephropathy. However, achieving and maintaining normal blood glucose levels in diabetic patients still remains a challenge. High glucose induced up regulation of angiotensin II (Ang II) production and several other growth factors such as transforming growth factor beta (TGF- β), vascular endothelial growth factor (VEGF) in mesangial cells and in proximal tubular cells has been confirmed in *in-vitro* studies ⁸. In addition high glucose induces the production of superoxide by the mitochondrial electron transport chain ⁹, can activate nuclear factor kappa B (NF- κ B), in part through the stimulation of protein kinase C (PKC) activity in endothelial cells ⁹, thus contributing to the progression and development of diabetic nephropathy.

1.2.2.1.2. Peroxisome proliferator activator receptor gamma

Peroxisome proliferator-activator receptors (PPARs) are members of the nuclear hormone receptor superfamily of ligand-binding transcription factors ^{10, 11}. Dysregulation of the function or activity of PPARs has been implicated in obesity, insulin resistance, dyslipidemia, inflammation and hypertension ^{12, 13}. Studies in humans have shown that thiazolidinediones (TZDs) ameliorate microalbuminuria / albuminuria associated with type 2 diabetic nephropathy ¹⁴. Moreover, it has been shown that administration of TZDs to insulin resistant- or type 1 diabetic rats ameliorated albuminuria, glomerular matrix deposition, glomerulosclerosis and tubulointerstitial fibrosis that are hallmarks of diabetic nephropathy ^{15, 16}. Several *in vitro* studies have also shown to ameliorate diabetes-induced mesangial and tubulointerstitial damage with TZDs as well ^{17, 18}.

The mechanism of protective effect of TZDs for diabetic nephropathy is thought to be due to anti-inflammatory properties independent of their insulin-sensitizing action

indicative of role of PPAR- γ receptor in inflammation associated with diabetes. Recently, Tang *et al.* have reported interleukin-8 (IL-8) and soluble intercellular adhesion molecule-1 (sICAM-1) activation by stimulation with advanced glycation end products (AGEs) is partially ameliorated by PPAR- γ ligation in human proximal tubular epithelial cells^{18,19}.

1.2.2.1.3. Advanced glycation end products

Under hyperglycemic conditions several proteins undergo non-enzymatic glycation resulting in Amadori's products known as advanced glycation end products (AGEs). There are different types of AGEs that have been reported in diabetes. AGEs are known to be one of the major contributors in the progression of DN and other complications associated with diabetes. Almost all renal structures are susceptible to accumulate AGEs including basement membranes, mesangial and endothelial cells, podocytes and tubules²⁰. Accumulation of AGEs such as *N*- ϵ -carboxymethyllysine (CML) and pentosidine in the kidney leads to the progressive alteration in renal structure and loss of renal function that is seen in long-term diabetes in humans¹⁸ and rodents²¹. There are several studies confirming inhibition of AGE formation prevents the development and progression of experimental diabetic nephropathy^{18,22}. AGEs are involved in the pathogenesis of diabetic nephropathy *via* multifactorial mechanisms²³. AGEs have been reported to induced apoptotic cell death, VEGF stimulation, activation of TGF- β -Smad signaling pathways and MCP-1 production in mesangial cells²⁴⁻²⁶ (Figure 4).

1.2.2.1.4. Polyol pathway

The polyol pathway consists of two enzymes, aldose reductase (AR) and sorbitol dehydrogenase (SDH), which together convert glucose to fructose *via* sorbitol. Aldose reductase, catalyzes reduction of glucose to sorbitol, while SDH converts sorbitol into fructose using NAD⁺ cofactor²⁷. The polyol pathway is activated under hyperglycemic conditions, and is considered to play an important role in the development of diabetic nephropathy. Intracellular sorbitol accumulation and decline in nicotinamide adenine dinucleotide phosphate (NADPH) contents caused by increases in AR flux has been postulated to induce osmotic damage and oxidative

stress, respectively. Some human studies have shown that AR inhibition attenuates hyperfiltration in normo-albuminuria and prevents the course of microalbuminuria in type 1 diabetic patients²⁸. Although many potent AR inhibitors have been identified and developed (minalrestat, zenarestat, eparlestat and zopolrestat¹⁸), none are currently marketed for clinical use for diabetic nephropathy. Many of the candidates failed to gain acceptance due to an inadequate therapeutic index and relatively high toxicity (Figure 4).

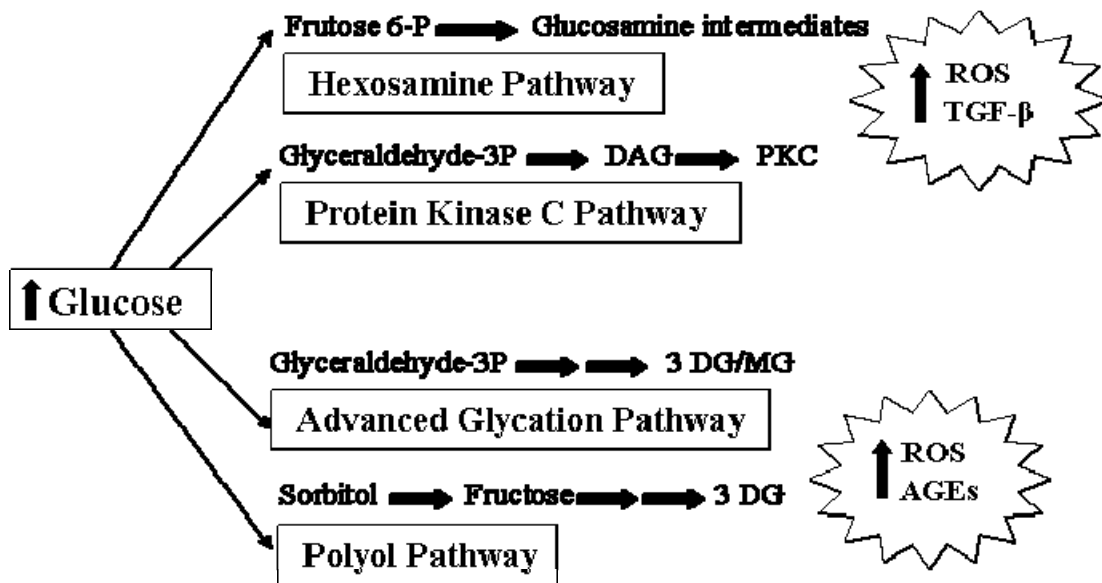


Figure 4: Metabolic pathways associated with diabetic nephropathy. (Taken with little modifications from Imtiaz et. al²⁹) 6-P; 6-phosphate, DAG; diacylglycerol, PKC; protein kinase C, ROS; reactive oxygen species, 3DG; 3-deoxyglucosone, MG; methylglyoxal, AGE; advanced glycation end products.

1.2.2.2. Hemodynamic pathways

Hemodynamic changes associated with diabetes are responsible for increased glomerular pressure and hyperfiltration resulting in stress related glomerular damage, loss of podocytes, hypertrophy and glomerular changes in diabetic kidneys (Figure 5).

1.2.2.2.1. Renin angiotensin system

Besides its well known hemodynamic actions including direct effects on glomerular hemodynamics, recent studies have suggested that the intrarenal renin angiotensin

system (RAS) is an important regulator of renal function and structure^{18, 26}. Angiotensin II (Ang II) exerts growth stimulatory and profibrogenic effects, most likely *via* up-regulation of growth factors such as TGF- β , platelet derived growth factor (PDGF), connective tissue growth factor (CTGF) and vascular endothelial growth factor (VEGF) and also can act as a pro-inflammatory factor³⁰. Recently, a close relationship between the RAS and AGE systems in diabetic nephropathy has been described. Post infusion accumulated AGEs in glomeruli and tubules were significantly ameliorated by valsartan treatment, an angiotensin II type 1 receptor (AT1R) antagonist³¹. Moreover, Ang II infusion has shown to accelerate the accumulation of AGEs in glomeruli and tubules as well.

These studies further strengthen the data implicating the RAS in diabetic complications. Hemodynamic changes resulting can cause podocyte damage leading to proteinuria. The role of another Ang II receptor subtype, the Ang II type 2 (AT2) receptor (AT2R), remains to be explored. However, this receptor subtype was recently shown to mediate the biological effects of Ang II; it is involved in the expression of RANTES and osteopontin as well as modulation of NO release and prostaglandin E2 (PGE2) production¹⁸.

1.2.2.2.2. Endothelin pathway

Vascular complications associated with diabetes contribute to the development of diabetic nephropathy. Diabetic nephropathy is associated with enhanced renal synthesis of endothelin (ET), one of the most potent endogenous vasoconstrictors³². There are two receptor subtypes for ET, namely A and B. ET typeA receptors are found predominantly in vascular smooth muscle cells, mediating vasoconstriction and cell proliferation³³. In contrast, ET typeB receptors are usually found on endothelial cells, and mediate vasodilatation *via* NO³⁴. Therefore, there may be potential benefits of specifically blocking the ET typeA receptor while preserving the vasodilator function of the ET typeB receptor. Darusentan is a new, non-peptide, selective ET receptor antagonist that acts predominantly on ET typeA receptors³⁵. Experimentally in STZ-treated rats, a longterm treatment with darusentan completely abolished overexpression of glomerular fibronectin and type IV collagen, and reduced protein excretion by about 50% as compared to untreated

diabetic rats ³⁶ indicates potential role ET typeA receptor antagonists in the treatment of diabetic nephropathy.

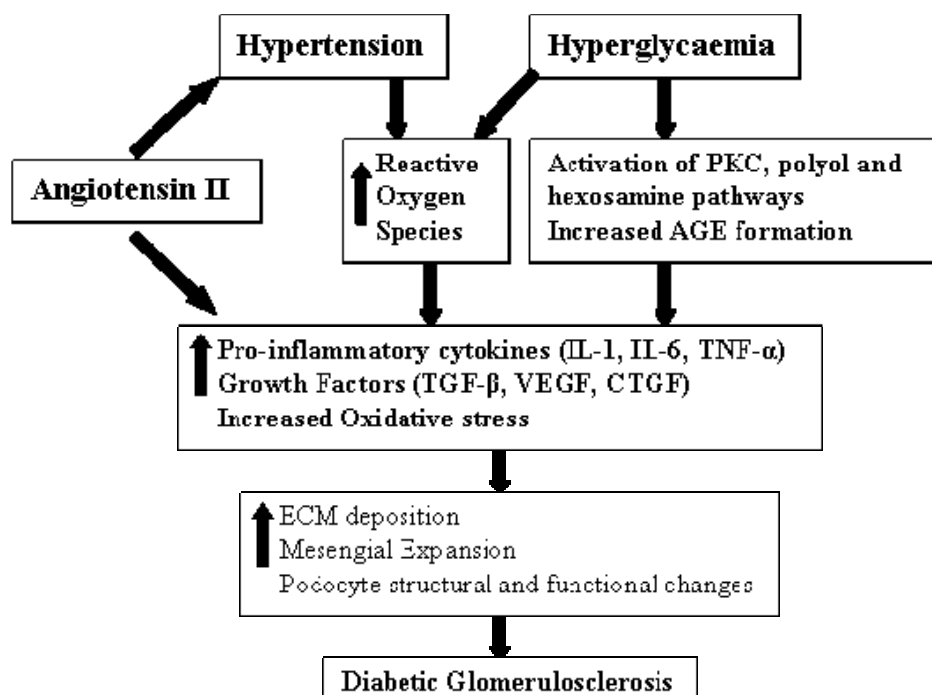


Figure 5: Hemodynamic and pro-inflammatory pathways associated with diabetic nephropathy. (Taken with little modifications from Imtiaz et. al ²⁹) PKC; protein kinase C, AGE; advanced glycation end products, TNF- α ; tumor necrosis factor alpha, VEGF; vascular endothelial growth factor, CTGT; connective tissue growth factor, ECM; extra cellular matrix.

1.2.2.3. Involvement of growth factors

1.2.2.3.1. Transforming growth factor (TGF- β) Elevated levels of TGF- β have been well documented in the diabetic kidney. It is well known to accelerates the development and progression of diabetic renal injury ³⁷. Several *in vivo*- and *in vitro* studies have implicated TGF- β as a key mediator in advanced diabetic renal disease, which mediates Ang II induced pro-sclerotic action, at least in part ^{37, 38}. Ziyadeh *et al.* have shown the effects of long-term administration of a neutralizing TGF- β antibody on the renal function and renal histology of *db/db* mice, an experimental model of type 2 diabetes ³⁷. Treatment with neutralizing TGF- β antibody completely prevented the increases in plasma creatinine, collagen and fibronectin expression, and the mesangial matrix expression in *db/db* mice. Therefore, inhibition of TGF- β expression may be useful in diabetic nephropathy. Use of TGF- β antibodies in humans remains uncertain since TGF- β and its expression is yet not fully characterized.

1.2.2.3.2. Connective tissue growth factor (CTGF) Increased CTGF expression has been confirmed in the plasma of type 1 diabetic patients with nephropathy, and also in glomeruli from diabetic rodents³⁹. CTGF act as a downstream factor of TGF- β in the development of diabetic nephropathy^{18, 40}. Experimental evidences have suggested an active role of CTGF in early- and late-stage morphologic changes in diabetic nephropathy including the damage resulting from hyperglycemia and hypertension, leading to proteinuria and fibrosis. Recent study with FG-3019 has shown normalized kidney filtration and weight in *db/db* mice upon treatment with a recombinant monoclonal antibody designed to bind and neutralize CTGF⁴¹.

1.2.2.3.3. Platelet derived growth factor (PDGF) PDGF is a polypeptide that was originally purified from human platelets as a potent mitogen for fibrosis, osteoblasts, smooth muscle and mesangial cells⁴². PDGF has been suggested to play a role in the pathophysiology of various fibroproliferative diseases of the kidney^{43, 44}. Upregulation of the PDGF pathway has been shown in experimental diabetic nephropathy and in the kidneys from patients with diabetes⁴⁵. Furthermore, amelioration of diabetic nephropathy by an inhibitor of advanced glycation, aminoguanidine, was associated with reduced renal PDGF expression⁴⁶. The inhibition of PDGF, *in vitro*, resulted in a significant reduction in mesangial cell proliferation, and largely prevented the increased deposition of ECM associated with the disease⁴⁷. Increased mesangial cell proliferation is well documented in DN and inhibition of PDGF may retard mesangial cell proliferation and ECM deposition and might improve the disease progression⁴⁸.

1.2.2.3.4. Vascular endothelial growth factor (VEGF) VEGF is a cytokine which plays a major role in development of diabetic nephropathy and has been extensively studied. VEGF is found to be upregulated early in type 1 diabetic rodents, especially in podocytes⁴⁹. Blockade of VEGF by neutralizing antibodies in type 1 diabetic rats abolished hyperfiltration and suppressed the urinary albumin excretion (UAE) rate⁵⁰. In addition, VEGF contributes to renal matrix accumulation, since treatment with anti-VEGF antibodies has attenuated GBM thickening and mesangial expansion in *db/db* mice⁵¹. Recently, one study has demonstrated that a neutralizing VEGF antibody prevents glomerular hypertrophy in Zucker diabetic fatty rat (a model of obese type 2 diabetes)⁵². VEGF regulates transcription of chemokines like CXCL12

which may contribute to the disease progression. VEGF upregulation has been correlated with DN and inhibition of VEGF may retard mesangial cell proliferation and matrix accumulation.

1.2.2.4. Inflammation and diabetic nephropathy

Over the past decade, a number of important research developments in the area of diabetic nephropathy have contributed to understanding of the disease. Beyond the hemodynamic and metabolic abnormalities, inflammatory processes and immune cells are involved in development and progression of diabetic nephropathy⁵³. There are increasing evidences, which suggests that immune cells participate in the vascular injury in the conditions of DN, and their migration into the kidney is a crucial step in the progression of this disease⁵⁴. Increased glomerular and interstitial infiltration of macrophages/monocytes has been confirmed in diabetic rodents as well as human renal biopsies, and recent studies demonstrate that macrophage-derived products can induce further inflammation in the diabetic kidney⁵⁵⁻⁵⁷. Furthermore, activated T lymphocytes have been associated with DN⁵⁸. One of the most striking features of leukocytes from patients with diabetes is the activated status of blood neutrophils^{59,60}.

Little is known about the migration patterns of different types of immune cells into renal tissues in DN. Homing of neutrophils is thought to be a hallmark of acute kidney inflammation, and recruitment of macrophages and T cells indicates chronic inflammatory processes^{57, 61}. Although the detailed mechanisms of leukocyte migration to renal tissues are not completely understood, there is evidence that selectins, integrins and chemokines participate in this recruitment⁵⁴. Upregulation of ICAM-1 expression has been confirmed in human renal biopsies as well as in rodents which facilitates neutrophils/macrophage infiltration into kidney. Hyperglycemia induced PKC activation further contributes to chemokine expression in renal cells and in immune cell infiltrates. Therapeutic intervention targeting protein kinase C can disrupt this positive amplification loop by reducing renal chemokine expression, subsequent recruitment of immune cells, and tubular injury in experimental and human diabetic nephropathy^{62, 63}. The relevance of these experimental data for human disease was supported by transcriptome analysis of

human renal biopsy samples from patients with diabetic nephropathy that identified a specific NF- κ B promoter-dependent inflammatory stress response in progressive diabetic nephropathy ⁶⁴. The contribution of inflammation to the progression of diabetic nephropathy has become increasingly anticipated.

1.2.2.4.1. T Lymphocyte recruitment to kidney

Although trafficking of naive, effector, and memory T cells into peripheral lymph nodes, spleen, skin, gut, and liver has been the subject of extensive studies the mechanisms of T cell homing into the kidney under different pathologic conditions are not fully identified. The fundamental appreciation of the importance of the leukocyte recruitment in the induction of endothelial dysfunction has significantly changed the view of the pathogenesis of DN. Because naive as well as effector T cells constitutively express LFA-1, and ICAM-1 expression is found on renal endothelial, epithelial, and mesangial cells ^{65, 66}, it is likely that this interaction will play a significant role during T cell migration into kidney. Indeed, homing of CD4⁺ T cells into glomeruli of diabetic kidney was decreased in ICAM-1 deficient-db/db mice compared with normal db/db mice ⁶⁷. It should be noted that the activation of CD4⁺ and CD8⁺ T cells by AGEs can initiate IFN- γ secretion by T cells ⁶⁸, which can induce further inflammation and oxidative stress within renal tissues. T cell accumulation is also found in the juxtaglomerular apparatus of patients with type 1 diabetes ⁵⁸. The functional role of T cells within this compartment is not clear yet, but this T cell influx is common among young patients with type 1 diabetes, especially those with accelerated duration of diabetes, and correlates with glomerular filtration surface and albumin excretion rate ⁵⁸. A T helper-1 (Th1) response precedes and accompanies type 1 diabetes ⁶⁹; therefore, it is possible that accumulation of Th1 cells will be prevalent in diabetic kidney. Little is known about the homing of Th1 cells during the development and progression of kidney diseases. It has been reported that the homing of effector Th1 cells in glomeruli is P-selectin and ICAM-1 dependent and associated with increased levels of IFN- γ and MIF in crescentic Th-1-mediated glomerulonephritis ⁷⁰. Although the mechanisms of Th1 cell migration in models of DN have not been reported yet, elevated levels of ICAM-1 and P-selectin within the diabetic kidney were found. Further studies will

elucidate the possible role of these adhesion molecules in the migration into the diabetic kidney ⁵⁴.

1.2.2.4.2. Neutrophil recruitment

Neutrophil influx is associated with the acute response to inflammation or injury. Neutrophils secrete enzymes and products of oxidation that can harm the local microenvironment and induce tissue damage. The role of neutrophils in the development of DN is not well understood; however, there is some evidence that neutrophils might be involved in this pathologic process. Abnormal activation of blood neutrophils has been reported in patients with type 1 and type 2 diabetes ^{59, 60} suggesting possible involvement of neutrophils in diabetic nephropathy. Takahashi et al. ⁶⁰ showed that spontaneous adhesion of neutrophils from patients with diabetes is increased significantly compared with adhesion of neutrophils from patients with normoalbuminuria as well as healthy control subjects and was associated with increased ICAM-1 expression. The precise molecular mechanisms that orchestrate trafficking of neutrophils in diabetic kidney are not yet defined, but studies with other models of kidney pathology suggest that selectins and integrins might participate in this process. Expressions of both E- and P-selectin was increased in the glomeruli and interstitial capillaries of human diabetic kidneys compared with kidneys of other glomerular diseases ⁷¹.

1.2.2.4.3. Macrophage recruitment

Infiltrating glomerular and interstitial macrophages are hall mark of renal vascular inflammation, and their accumulation is a characteristic feature of DN ^{55, 56}. Infiltrated M/M (Monocytes/Macrophages) release various substances including lysosomal enzymes, nitric oxide, reactive oxygen intermediates or TGF-beta which are essential mediators of renal damage ⁷². Adoptive transfer studies show that macrophages can induce proteinuria and mesangial proliferation in a model of experimental glomerulonephritis ⁷³. Therefore, it is possible that infiltrating macrophages might induce or accelerate the mesangial cell proliferation during the development of DN.

Detailed molecular mechanisms that direct macrophage migration are not fully characterized, but chemokines/chemokine receptors as well as integrins are involved in this process. Increased expression of ICAM-1 that serves as a ligand for LFA-1 was detected in models of type 1⁶⁵ and type 2 DN^{66,74}. ICAM-1 expression can also be induced by factors such as hyperglycemia⁷⁵, AGE⁷⁶, oxidative stress⁷⁷, and hyperinsulinemia⁷⁸. Diminished infiltration of macrophages, reduced expression of TGF- β and collagen IV in glomeruli, reduced urinary albumin excretion, glomerular hypertrophy, and mesangial matrix expansion are associated with reduced renal injury in diabetic ICAM-1 deficient mice⁷⁹. In a model of type 2 diabetes, Chow et al.⁶⁷ used ICAM-1 deficient db/db mice and showed significant reduction in albuminuria and a decrease in the number of glomerular and interstitial macrophages that was associated with reduced glomerular hypertrophy, hypercellularity, and tubular damage. Both studies indicate, a role of ICAM-1 in macrophage infiltration into renal compartment⁶⁷.

1.2.2.5. Chemokines and chemokine receptors in diabetic nephropathy

Chemokines are a large family of small secreted proteins of 8–14 kDa that control cell trafficking. They are structurally divided into four classes —C, CC, CXC, and CX3C—depending on the number and the relative position of their amino terminal cysteine residues⁸⁰. Individual chemokines are named using the acronyms of the structural class they belong to, followed by an L (for ligand) and their gene number^{81,82}.

Chemokine receptors are themselves classified according to the chemokine family they bind. The nomenclature of the receptors is analogous to that of chemokines, using the family acronym followed by an R (for receptor) and a number that corresponds to the order of its discovery⁸³. Chemokine receptors belong to class A of the G protein-coupled receptor (GPCR) superfamily. They are rhodopsin-like receptors with 7 transmembrane structure coupled with heterotrimeric G $\alpha\beta\gamma$ proteins⁸⁴. Upon ligand-receptor interaction, different intracellular signaling pathways are activated, ultimately leading to cell mobilization and activation^{82,85} (Figure 6).

1.2.2.5.1. Pro-inflammatory chemokines and receptors**1.2.2.5.1.1. Monocyte chemoattractant protein-1 (MCP-1/CCL2)**

CCL2 also known as MCP-1 is a member of CC class of chemokine which binds to CCR2, a chemokine receptor CCL2 is believed to play a key role in recruitment of M/M into different renal compartments. It is secreted by mononuclear and various non-leukocytic cells including renal resident cells^{88, 89}. Its role in experimental glomerulonephritis models⁹⁰ and human nephritis⁹¹, crescent formation and progressive tubulointerstitial lesions via M/M recruitment and activation has been reported. In patients with diabetic nephropathy urinary CCL2 levels were significantly elevated at different stages of DN, and were correlated with the number of CD68-positive infiltrating M/M in the interstitium^{92, 93}. Immunohistochemical and *in situ* hybridization analyses revealed CCL2 positive cells localize within tubulointerstitial lesions⁹². Furthermore, in Japanese patients with type 2 diabetes increased urinary CCL2 excretion was positively correlated with the tubular damage marker N-acetylglucosaminidase and albuminuria, indicating that increased tubular CCL2 expression contributes to renal damage⁹⁴. Recently CCL2 deficient mice with streptozotocin-induced diabetes demonstrated attenuated diabetic nephropathy, with marked reductions in glomerular and interstitial macrophage accumulation, histological damage, and renal fibrosis when compared with the wild-type⁹⁵. In db/db mice, CCL2 deficiency reduced renal M/M accumulation and the progression of diabetic renal injury independent of development of obesity, insulin resistance or type2 diabetes⁹⁶. High glucose mediated enhanced expression of CCL2 in human mesangial cells via NF- κ B activation has been confirmed in many *in-vitro* studies⁹⁷. In addition renal biopsies of patients with type 2 diabetes and overt nephropathy, showed a strong up-regulation of CCL2 mainly in the tubular cells which was positively correlated with NF- κ B activation in the same cells^{98, 99}. In cultured human mesangial cells, AGE mediated enhanced apoptotic cell death was associated with concomitant increased expression of CCL2²⁴. In another study mechanical stretching of human mesangial cells resulted in over expression of CCL2 via NF- κ B¹⁰⁰ which was accelerated in presence of high glucose medium¹⁰⁰. Some *in vitro* and *in vivo* data provides evidence that angiotensin II (Ang II) directly induces the expression of CCL2. This can be further supported by study showing treatment with the ACE inhibitor, enalapril and the AT1-receptor antagonist, candesartan

dramatically suppressed renal CCL2 expression in streptozotocin treated rats ¹⁰¹ and was associated with a marked reduction in renal M/M infiltration and proteinuria. A similar study has reported reduction in glomerular and tubular CCL2 expression and amelioration of renal damage with reduced M/M infiltration in Zucker rats upon treatment with olmesartan ¹⁰². Treatment with ACE inhibitors or AT1-receptor blockers led to a reduction of urinary CCL2 excretion, improvement of renal function, and reduction of oxidative stress in patients with type 1 and 2 diabetes ^{103, 104}. Addition of CCL2 to cultured macrophages resulted in enhanced secretion of TGF β 1, which in turn increased expression of collagen type I and III as well as fibronectin in renal interstitial myofibroblasts ¹⁰⁵. Furthermore, CCL2 also mediates collagen deposition in experimental glomerulonephritis by TGF- β ¹⁰⁶ independent of M/M infiltration ^{53, 107}. In addition one of the studies from our lab has demonstrated the effect of late onset of CCL2 blockade in uninephrectomized type 2 db/db mouse model ⁶¹. CCL2 blockade using mNOX-E36-3_PEG reduced the number of glomerular macrophages by 40% in 1K db/db mice which was associated with protection from diffuse glomerulosclerosis and significantly improved the glomerular filtration rate ⁶¹. Another study has reported administration of anti-CCL2 antibodies prevents glomerular sclerosis and interstitial fibrosis ⁹⁰.

Most of the pathological changes associated with diabetes including hyperglycemia, AGEs, hemodynamic changes and oxidative stress results in over expression of CCL2 in renal cells. CCL2 over expression plays a central role in disease progression and renal inflammation through M/M recruitment to different renal compartments. CCL2 activation serves as common pathway towards development and progression of DN. Thus targeting CCL2 in diabetic nephropathy may turn more beneficial than targeting each pathway.

1.2.2.5.1.2. Fractalkine (CX3CL1)

Fractalkine/CX3CL1 exists in membrane- bound as well as in soluble form, and therefore acts as a chemoattractant and adhesion molecule ¹⁰⁸. In diabetes mellitus, fractalkine/CX3CL1 expression is upregulated in human kidneys along the glomerular and peritubular capillaries ¹⁰⁹. The corresponding receptor for fractalkine, CX3CR1, is expressed mainly on monocytes ^{110, 111}. In the diabetic rat

kidney mRNA expression of fractalkine/CX3CL1 and CX3CR1 was found to be increased and some CX3CR1 positive cells are M/M¹⁰⁹. Up-regulation of fractalkine/CX3CL1 was induced in proximal tubular cells by protein overload through NF-κB and p38 mitogen activated protein kinase-dependent pathways¹¹². Moreover, AGEs¹¹³ and TNF-alpha¹¹⁴ also induce fractalkine/CX3CL1 in the kidney. In an *in vitro* study fractalkine/CX3CL1 mediated arrest and migration of CD16+ monocytes, suggesting that fractalkine might function as an arrest chemokine in the pathway of M/M adhesion before migration into the diabetic kidney¹¹⁵. However, the extent to which fractalkine/CX3CL1 is involved in the recruitment of T lymphocytes remains controversial. Fractalkine/CX3CL1, RANTES/CCL5 and gamma-interferon-inducible-protein (IP-10/CXCL10) have been identified as responsible chemokines for mediating attraction of T cells⁵³. The role of fractalkine in progression and development of diabetic nephropathy is yet to be explored.

1.2.2.5.1.3. RANTES / CCL5

Another important CC-chemokine in diabetic nephropathy, RANTES/CCL5, is a potent chemoattractant for M/M and granulocytes, but also for T cells, and is involved in enhanced chronic inflammation. CCL5 is expressed by various cell types including lymphocytes, fibroblasts, mesangial cells and renal tubular epithelial cells^{116, 117}. Molecular studies have identified NF-κB binding sites within the promoter region of the CCL5 gene¹¹⁸. In kidney, up-regulation of CCL5 predominantly in mesangial and tubular is induced by effectors such as, NFκB dependent pathways⁶⁴, protein overload¹¹⁹, activation of the RAS¹²⁰, enhanced glomerular filtration of growth factors such as TGF-β¹²¹, and cytokines such as TNF-α¹²². The exact role of CCL5 in directing the T lymphocyte recruitment into the diabetic kidney is not completely known. T cell clusters have been found in the juxtaglomerular apparatus in renal biopsies from patients with type 1 diabetes⁵⁸. Interestingly, T cell positive patients had a shorter duration of diabetes than T-cell negative patients and a lower albumin excretion rate, but the glomerular filtration rate was not different. These findings suggest that possibly T cells play a preservative role for renal function^{53, 58}. Treatment with AOP-RANTES a receptor blocker has shown inhibition of infiltrating macrophages in a rat model¹²³.

1.2.2.5.1.4. Interferon-gamma inducible protein (IP-10 / CXCL10)

Microvascular damage is a characteristic of diabetic nephropathy. A selective upregulation of IP-10/CXCL10 by endothelial cells in the tubulointerstitial area, co-localizing with infiltrating T cells, was found in a model of renal endothelial microvascular injury in rats. Despite extensive damage of glomerular vasculature, no IP-10/CXCL10 expression by glomerular endothelial cells was detected. In contrast, MCP-1/CCL2 mRNA was upregulated in the glomerulus and the tubulointerstitium¹²⁴. Treatment with a neutralizing anti-IP-10/CXCL10 antibody significantly reduced the number of infiltrating tubulointerstitial T cells without affecting M/M migration and led to improved renal function¹²⁴. This study demonstrates a role for IP-10/CXCL10 on T cell recruitment in renal endothelial microvascular injury in rats. However, there are no reports describing role of CXCL10 in development and progression of diabetic nephropathy⁵³.

1.2.2.5.1.5. CX3CR1

Chemokine C-X3-C motif receptor 1 (CX3CR1), the receptor for fractalkine, was found on infiltrating M/M, and on T cells in different renal compartments. In a model of streptozotocin treated rats, CX3CR1 was found to be upregulated in diabetic nephropathy¹⁰⁹. In glomerular disease with prominent M/M infiltration, the distribution of M/M matched the distribution of CX3CR1 and in interstitial infiltrates the distribution of CX3CR1 corresponded to the distribution of both T cells and M/M¹²⁵. The pattern of CX3CR1 expressing cells was consistent with its ligand fractalkine. The co-localization of CX3CR1 and fractalkine argues for the hypothesis that the CX3CR1/fractalkine complex mediates adhesion in the early extravasation cascade, whereas the ligands of CCR2 and CCR5 might guide inflammatory cells to more specific renal compartments¹²⁵.

1.2.2.5.1.6. CCR1

Chemokine C-C motif receptor 1 (CCR1) has been identified recently as playing a critical role in the recruitment of renal interstitial M/M⁵⁷. In one of the studies from our lab we used a CCR1 antagonist to block interstitial M/M recruitment in uninephrectomized db/db mice, an accelerated model for advanced nephropathy of

type 2 diabetes⁵⁷. CCR1 blockade reduced interstitial M/M infiltration, most likely by interfering with M/M adhesion to activated endothelial cells of peritubular capillaries in the renal interstitium⁵⁷. Furthermore, a reduction of proliferating tubular epithelial and interstitial cells, tubular atrophy, and interstitial fibrosis was observed⁵⁷ thus, indicating role of CCR1 in macrophage infiltration to interstitium. Glomerular macrophage infiltration was not affected with CCR1 blockade in mice.

1.2.2.5.1.7. CCR2

Chemokine C-C motif receptor 2 (CCR2) is CC chemokine receptor mainly expressed on monocytes, basophils, memory T cells and pDCs. CCR2, acts as receptor for CCL2 (MCP-1), CCL13 (MCP 4), CCL7 (MCP3) and CCL8 (MCP2), is mainly represented by the distribution of M/M in renal tissue¹²⁶. Inhibition of CCR2 by receptor antagonists as well as a CCR2 knockout mice model are characterized by a reduced degree of M/M infiltration and abolished renal fibrosis¹²⁷. CCR2 blockade prevents renal fibrosis in UUO kidney¹²⁷. Monocyte and macrophage trafficking is mediated through CCR2 in ischemia-reperfusion injury¹²⁸ as well as in monocytogenic infection¹²⁹. Similar effects could be shown by the delivery of a mutant of the MCP-1/CCL2 gene into mice¹³⁰. In CCR2 deficient mice tubular necrosis and the number of infiltrating M/M were significantly lowered after transient renal ischemia¹³¹. Targeted macrophage depletion has been shown to ameliorate mesangioproliferative glomerulonephritis in rats¹³² which was associated with reduction of infiltrating macrophage in glomerular compartment, alpha smooth muscle actin and fibronectin¹³². Recruitment of monocytes and macrophages to renal compartments is considered to be hallmark of DN development and progression. Thus targeting CCR2 blockade using some specific antagonist remains attractive for treating DN and yet to be explored.

1.2.2.5.1.8. CCR5

Chemokine C-C motif receptor 5 (CCR5) is a CC chemokine receptor which is mainly expressed on monocytes, T cells, NK cells, pDCs and immature DC. CCR5 acts as common receptor for many chemokines including CCL8 (MCP2), CCL4 (MIP 1 β), CCL3 (MIP 1 α S), CCL3L1 (MIP 1 α P) and CCL5 (RANTES).

Chemokine receptor CCR5 gene polymorphism has been reported in Indian patients with ESRD¹³³ as well as in Japanese diabetic nephropathy patients¹³⁴. Another study has reported overexpression of CCR5 on peripheral blood mononuclear cells in patients with type 2 diabetes¹³⁵. A human renal biopsy study of patients with various renal diseases showed that glomerular CCR5-positive cells were closely correlated with extracapillary lesions and urinary MIP-1 α /CCL3 levels, while interstitial CCR5-positive cells, mainly CD3-positive T cells, were correlated with interstitial lesions and urinary CCL5 levels⁹². NF- κ B mediated MIP 1 α -CCR5 signaling upregulation has been implicated in development of human crescentic glomerulonephritis¹³⁶ and in islet allograft rejection¹³⁷. Role of CCR5 gene polymorphism in renal allograft survival is also documented¹³⁸. CCR5 receptor antagonist AOP-RANTES has been reported to reduce number of infiltrating macrophages in glomerular compartment as well as reduced collagen IV deposition in a rat model of glomerulonephritis¹²³. Many studies have confirmed the role of infiltrating macrophages and immune cells in the development and progression of diabetic nephropathy. Targeting CCR5 receptor in order to achieve amelioration of disease by inhibiting infiltration of monocytes and T cells is quite attractive, but a recent study by Turner et al has reported CCR5 deficiency aggravates glomerulonephritis in mice which was associated with counter upregulation of CCL3, CCL5 and CCR1¹³⁹. Another study has reported renal as well as cardiac allograft rejections in CCR5 deficient mice¹⁴⁰. Both studies are indicative of CCR5 blockade results in counter upregulation of other chemokines and chemokine receptors. Inhibition of CCR5 in diabetic nephropathy remains to be explored yet.

1.2.2.5.2. Homeostatic chemokines and their receptors

Homeostatic chemokines are expressed in bone marrow and lymphoid tissues and are involved in hematopoiesis, immune surveillance and adaptive immune responses⁸⁶. The receptors for homeostatic chemokines (CXCR4, CXCR5 and CXCR7) are expressed on B cells, follicular-helper T cells, central-memory T cells, and mature dendritic cells. Some chemokine receptors bind specifically to only one ligand (e.g. CXCR4 and CXCL12, CXCR5 and BLA-1) while others share the binding domain with more than one chemokines (e.g. CCR7 binds to MIP-3 β , SLC).

1.2.2.5.2.1. CXCL12 / SDF-1 α

Chemokine C-X-C motif ligand 12 (CXCL12) also known as stromal cell-derived factor-1 alpha (SDF-1 α), was first identified as a lymphocyte homing chemokine ¹⁴¹. Until recently CXCR4 was reported to be the only receptor for CXCL12, recently CXCR7 has been confirmed as another receptor for CXCL12. Different effects of CXCL12 are mediated via its binding to CXCR4 and CXCR7 ¹⁴². CXCL12 is an extensively studied chemokine and has been reported to mediate beneficial as well as pathological responses in various conditions. CXCL12 and CXCR4 expression levels are highly modified under pathophysiological condition in different cells like hypoxia induced enhanced expression in microglia ¹⁴³, enhanced expression in cerebral ischemia in rat brain ¹⁴⁴ and increased CXCR4 expression in distal as well as proximal tubules in human renal biopsies from diabetic patients ¹⁴⁵.

In fact, some biological effects of CXCL12 support tissue reoxygenation and regeneration. For example, CXCL12 has shown to induce angiogenesis ¹⁴⁶, and promote cell survival ¹⁴⁷. CXCL12 supports vascular integrity similar to VEGF ¹⁴⁸ and recruits bone marrow-derived progenitor cells ¹⁴⁹⁻¹⁵¹. In this regard CXCL12 was shown to be a crucial mediator of repair in a number of different disease models like pancreatic beta cell loss in type 1 diabetes ¹⁴⁷, endovascular injury ¹⁵⁰, vascular occlusion ^{149, 152}, ischemic acute renal failure ¹⁵¹, stroke and myocardial infarction. Recently it has been reported that CXCL12-CXCR4 axis plays a key role in development of renal vasculature during embryogenesis ¹⁵³. This study by Takabatake et al. reported that CXCL12 secreting stromal cells surround CXCR4 positive epithelial components of early nephrons and blood vessels in embryonic kidney. In glomeruli CXCL12 secreting podocytes were found in close proximity to CXCR4 positive endothelial cells. Both CXCL12 and CXCR4 deficiency resulted in impaired vascular development ¹⁵³.

In contrast to the beneficial effects mediated by CXCL12 in tissue repair and regeneration, administration of CXCL12 antagonist to NZB mice has prevented the production of auto-antibodies ¹⁵⁴ indicating its potential in ameliorating lupus nephritis. Recently another study has reported beneficial effect of a peptide antagonist of CXCR4 in lupus nephritis ¹⁵⁵. A study has reported enhanced production of IL-6 by CXCL12 in microglia ¹⁵⁶. However, in chronic disease states injury response mechanisms are often maladaptive and rather promote disease

progression to organ failure. For example, CXCL12 was found to potentiate NF- κ B ligand-induced osteoclast differentiation and initiate pro-inflammatory responses implicating its involvement in rheumatoid arthritis¹⁵⁷. CXCL12-mediated fibrocyte recruitment aggravates bleomycin-induced pulmonary fibrosis^{152, 158-160} or CXCL12-driven neoangiogenesis drives diabetic eye disease¹⁴⁶, hemangioblastoma and renal cancer¹⁶¹. Furthermore, CXCL12 attracts circulating tumor cells as a tissue-based mechanism for cancer metastasis¹⁶². CXCL12 can also promote VEGF mediated tumor angiogenesis¹⁶³. In addition CXCL12 has been implicated to play important role in chronic allograft rejection in rats¹⁶⁴. These studies suggest that CXCL12 creates microenvironments that maintain niches for the homing of other cells including progenitor cell recruitment during repair. However, this function may also drive tissue- and disease-specific maladaptive disease pathomechanisms.

The role of CXCL12 in glomerular disease is still to be explored. Nephrotoxic serum nephritis specifically induces glomerular CXCL12 expression¹¹. In addition, transgenic over-expression of CXCR4 (by knocking out Von-Hippel-Lindau gene) induced podocyte proliferation and glomerular crescent formation in mice¹¹. In lupus-like immune complex glomerulonephritis of NZB/NZW mice glomerular CXCL12 expression mainly originated from podocytes¹⁵⁴. Blocking CXCL12 prevented glomerulonephritis which was attributed to less autoantibody production and T cell recruitment to glomeruli¹⁵⁴. So far nothing is known about CXCL12 in diabetic nephropathy. Diabetic nephropathy is devoid of either podocyte proliferation or autoimmunity, hence, the aforementioned studies hardly predict the predominant functional role of CXCL12 in diabetic nephropathy. We speculated that progressive remodelling of the glomerular structure to glomerulosclerosis, a morphological variant of wound healing, might involve CXCL12 signalling. Based on the available data from other disease states it is unclear whether CXCL12 predominantly protects from diabetic nephropathy (e.g. by maintaining tissue integrity and supporting regeneration) or it contributes to progression of diabetic nephropathy (e.g. by enhancing glomerulosclerosis).

1.2.2.5.2.2. CXCR4

Chemokine C-X-C motif receptor 4 (CXCR4) also known as Fusin, is one of the receptors for CXCL12. CXCR4-CXCL12 axis has been reported to initiate G-protein signaling and is responsible for several physiological and pathological responses. The expression of CXCR4 (and CXCL12) is controlled by hypoxia-regulated factor (Hif)- α , a transcription factor that orchestrates intrarenal expression in tissues when being exposed to hypoxia or oxidative stress¹⁶⁵. CXCR4 expression was enhanced in microglia under hypoxic condition¹⁴³. Another study has reported VEGF induced increased expression of CXCR4 in human endothelial cell¹⁶⁶.

1.2.2.5.2.3. CXCR7

Chemokine C-X-C motif receptor 7 (CXCR7) also known as RDC1, is highly conserved between mammalian species as revealed from the sequences from human, dog, mouse and rat¹⁶⁷. CXCR7 has shown high affinity for CXCL12 and ITAC. A characteristic of chemokine receptor is their signaling via pertussis toxin sensitive Gi-proteins¹⁶⁸, but coupling of CXCR7 to G-proteins has not been demonstrated yet. Most of the chemokine receptors contain a conserved DRYLAIV motif at N-terminus of the second intracellular loop which is assumed to be necessary but not sufficient for coupling to Gi-proteins. The sequence of CXCR7 is altered at two positions (A/S and V/T). Survival and efficient differentiation of B cells into antibody producing cells correlates with CXCR7 levels at the plasma membrane¹⁶⁹ at the same time proliferative activity of CXCR7 was also reported in fibroblasts¹⁷⁰ recently CXCL12 binding to CXCR7 has been shown to be responsible for renal progenitor cell adhesion to endothelial cells and for renal progenitor cell survival¹⁷¹. In a very interesting study recently Angelique, *et al* have shown CXCR7 heterodimerization with CXCR4 in CXCL12 mediated G-protein signaling¹⁷². Further studies in this field will be helpful in our understanding of CXCR7 as receptor for CXCL12.

2. Summary and hypothesis

2.1. Role of pro-inflammatory chemokines in diabetic nephropathy

Beyond hemodynamic and metabolic abnormalities associated with diabetes, the role of inflammation in development and progression of diabetic nephropathy is well accepted. Recruitment and activation of macrophages in different renal compartment is considered to be hallmark of all inflammation in diabetic nephropathy. Although recruitment of macrophages to the renal compartment has been extensively studied, the exact mechanisms involved are still to be explored. The chemokine-chemokine receptor interactions are implicated to be mainly responsible for trafficking and infiltration of different monocytes and macrophages. Contribution of macrophages to the development of DN can be addressed in either by inhibiting chemokines or chemokine receptor associated with diabetes.

We hypothesized that inhibition of CCL2 may inhibit macrophages infiltrating into different compartments in kidney and inhibition started at earlier stage of disease progression may show more beneficial effects than CCL2 blockade at late stage of DN. To address the involvement of additional chemokine receptors we hypothesized that blocking CCR5 and CCR2 simultaneously might have some additive or synergistic effects.

2.2. Role of homeostatic chemokines in diabetic nephropathy

Homeostatic chemokines are mainly involved in hematopoiesis, immune cell survival and adaptive immune responses. CXCL12 attracted our attention as it is being extensively studied and reported to be responsible for different functions like stem cell survival and homing and trafficking to different compartments. The role of CXCL12 in diabetic nephropathy has not been explored yet. CXCL12 is constitutively expressed by different renal cells. It may contribute to tissue repair and inhibit disease progression by stem cell recruitment or may cause increased tissue fibrosis and aggravate the disease.

We hypothesized that CXCL12 plays role in development and progression of diabetic nephropathy. In order to address this question we used CXCL12 blocker in a mouse model of diabetic nephropathy.

3. Materials and methods

3.1. Equipments and instruments

Balances:

Analytic Balance,
BP 110 S
Mettler PJ 3000

Sartorius, Göttingen, Germany
Mettler-Toledo, Greifensee, Switzerland

Cell Incubators:

Type B5060 EC-CO₂

Heraeus Sepatech, München, Germany

Centrifuges:

Heraeus, Minifuge T
Germany

VWR Internationl, Darmstadt,

Heraeus, Biofuge primo

Kendro Laboratory Products GmbH,
Hanau, Germany

Heraeus, Sepatech Biofuge A

Heraeus Sepatech, München, Germany

ELISA-Reader

Tecan, GENios Plus

Tecan, Crailsheim, Germany

Fluorescence Microscopes

Leica DC 300F

Leica Microsystems, Cambridge, UK

Olympus BX50

Olympus Microscopy, Hamburg,
Germany

TaqMan Sequence Detection System

ABI prism™ 7700 sequence detector
RTPCR

PE Biosystems, Weiterstadt, Germany

Light Cycler 480

Roche, Germany

3.2. Other Equipments

Cryostat RM2155
Germany

Leica Microsystems, Bensheim,

Cryostat CM 3000

Leica Microsystems, Bensheim,
Germany

Digital camera DC 300F

Leica Microsystems, Cambridge, UK

Glucometer Accu check sensor	Roche, Mannheim, Germany
Homogenizer ULTRA-TURRAX T25	IKA GmbH, Staufen, Germany
Microtome HM 340E	Microm, Heidelberg, Germany
pH meter WTW	WTW GmbH, Weilheim, Germany
Thermomixer 5436	Eppendorf, Hamburg, Germany
Vortex Genie 2™	Bender&Hobein AG, Zurich, Switzerland
Water bath HI 1210 Germany	Leica Microsystems, Bensheim, Germany

3.3. Chemicals and reagents

Chemicals for the molecular biology techniques

RNeasy Mini Kit	Qiagen GmbH, Hilden, Germany
RT-PCR primers	PE Biosystems, Weiterstadt, Germany
	Methion, Martinstreid, Germany

Elisa Kits

mouse RANTES/CCL5	R &D Systems, Minneapolis, MN, USA
mouse IL6 USA	R &D Systems, Minneapolis, MN, USA
mouse IP 10 USA	R &D Systems, Minneapolis, MN, USA
mouse MCP-1 USA	R &D Systems, Minneapolis, MN, USA
mouse Albumin	Bethyl Laboratories, TX, USA

Cell culture

DMEM-medium	Biochrom KG, Berlin, Germany
RPMI-1640 medium UK	GIBCO/Invitrogen, Paisley, Scotland, UK
FSC	Biochrom KG, Berlin, Germany
Dulbecco's PBS (1×) Cölbe, Germany	PAA Laboratories GmbH, Cölbe, Germany

Trypsine/EDTA (1×)	PAA Laboratories GmbH,
Cölbe, Germany	
Penicillin/Streptomycin (100×)	PAA Laboratories GmbH,
Cölbe, Germany	
Antibodies	
rat anti-F4/80	Serotec, Oxford, UK
anti-Ki-67	Dianova, Hamburg, Germany
anti-ssDNA	Chemicon, Hofheim, Germany
anti-mMECA-32	University of Iowa, Hybridoma Bank,
USA	
anti-mCCL5	PeptoTech, Rocky Hill, NJ, USA
goat anti-fibronectin	Santa Cruz, Heidelberg, Germany
rat anti-Mac2	Cederlane, Ontario, Canada
anti-ERHR3	DPC Biermann, Bad Nauheim,
Germany	
anti-CD3	BD Pharmingen, Hamburg, Germany
mouse F4/80 FITC conjugated	Caltag Laboratories, Bulingame, CA,
USA	
mouse anti CXCL12	} R &D Systems, Minneapolis, MN, USA
mouse anti CXCL12 FITC conjugated	
mouse anti WT1 PE conjugated	
mouse anti CXCR4	
mouse anti CD45	
Chemicals	
Aceton	Merck, Darmstadt, Germany
AEC Substrat Packung	Biogenex, San Ramon, USA
Bovines Serum Albumin	Roche Diagnostics, Mannheim,
Germany	
DEPC	Fluka, Buchs, Switzerland
DMSO	Merck, Darmstadt, Germany
Diluent C for PKH26 dye	Sigma-Aldrich Chemicals, Germany
EDTA	Calbiochem, SanDiego, USA

Eosin	Sigma, Deisenhofen, Germany
Ethanol	Merck, Darmstadt, Germany
Formalin	Merck, Darmstadt, Germany
Hydroxyethyl cellulose	Sigma-Aldrich, Steinheim, Germany
HCl (5N)	Merck, Darmstadt, Germany
Isopropanol	Merck, Darmstadt, Germany
Calcium chloride	Merck, Darmstadt, Germany
Calcium dihydrogenphosphate	Merck, Darmstadt, Germany
Calcium hydroxide	Merck, Darmstadt, Germany
MACS-Buffer	Miltenyi Biotec, Bergisch Gladbach, Germany
Beta mercapto ethanol	Roth, Karlsruhe, Germany
Sodium acetate	Merck, Darmstadt, Germany
Sodium chloride	Merck, Darmstadt, Germany
Sodium citrate	Merck, Darmstadt, Germany
Sodium dihydrogenphosphate	Merck, Darmstadt, Germany
Penicillin	Sigma, Deisenhofen, Germany
Roti-Aqua-Phenol	Carl Roth GmbH, Karlsruhe, Germany
Streptomycin	Sigma, Deisenhofen, Germany
Tissue Freezing Medium	Leica, Nussloch, Germany
Trypan Blue	Sigma, Deisenhofen, Germany
Oxygenated water	DAKO, Hamburg, Germany
Xylol	Merck, Darmstadt, Germany

3.4. Miscellaneous

Anti-FITC MicroBeads	Miltenyi Biotec, Bergish Gladbach, Germany
CellTiter 96 Proliferation Assay	Promega, Mannheim, Germany
Fluorescence-labeled microspheres (0.96 µm FluoSpheres)	Molecular Probes™/Invitrogen GmbH, Karlsruhe, Germany

LS ⁺ /VS ⁺ Positive selection columns (MACS)	Miltenyi Biotec, Bergish Gladbach, Germany
PKH26 Red Fluorescent Cell Linker kit	Sigma-Aldrich Chemicals, Steinheim, Germany
Preseparation filters	Miltenyi Biotec, Bergish Gladbach, Germany
SuperFrost® Plus microscope slides	Menzel-Gläser, Braunschweig, Germany
Silver Impregnation Kit	Bio-Optica, Milano, Italy
Needles	BD Drogheda, Ireland
Pipette's tip 1-1000µL	Eppendorf, Hamburg, Germany
Syringes	Becton Dickinson GmbH, Heidelberg, Germany
Plastic histocassettes	NeoLab, Heidelberg, Germany
Tissue culture dishes Ø 100x20mm	TPP, Trasadingen, Switzerland
Tissue culture dishes Ø 150x20mm	TPP, Trasadingen, Switzerland
Tissue culture dishes Ø 35x10mm	Becton Dickinson, Franklin Lakes, NJ, USA
Tissue culture flasks 150 cm ²	TPP, Trasadingen, Switzerland
Tubes 15 and 50 mL	TPP, Trasadingen, Switzerland
Tubes 1.5 and 2 mL	TPP, Trasadingen, Switzerland

- All other reagents were of analytical grade and are commercially available from Invitrogen, SIGMA or ROTH.

3.5 Experimental procedures

3.5.1. *Animals*

Male, 5 week old C57BLKS db/db or C57BLKS wild-type mice were obtained from Taconic (Ry, Denmark) and were housed in filter top cages with a 12 hour dark/light cycle. All mice had unlimited access to food (Sniff, Soest, Germany) and water for the complete duration of the study. Cages, bedding, nestles, food, and water were sterilized by autoclaving before use. All experimental procedures were performed according to the German animal care and ethics legislation and had been approved by the local government authorities.

3.5.2. Animal model

Db/db mice uninephrectomy: At the age of 6 weeks db/db and wild-type mice underwent uninephrectomy (1K mice) or sham surgery (2K mice) performed under general anesthesia using isoflurane (Harvard Anesthesia system, UK). Anesthetized mice were positioned laterally on the operation bed using adhesive tapes. Under deep anesthesia a flank incision of about 1-1.5 cm was made on the dorsolateral side just below the thoracic cage so as to reach kidney easily. A silk suture (2-0) was passed around the right kidney and after tying off all blood vessels and ureter the kidney was rapidly excised out using a curved scissors. In sham group of mice only incision was made and kidney was left as such. Skin incision was closed with silk suture and wound clamps (Figure 7). After surgery all mice received analgesic (1 drop of Novaminsulfon, Ratiopharm GmbH, Germany, 1:200, orally administered).

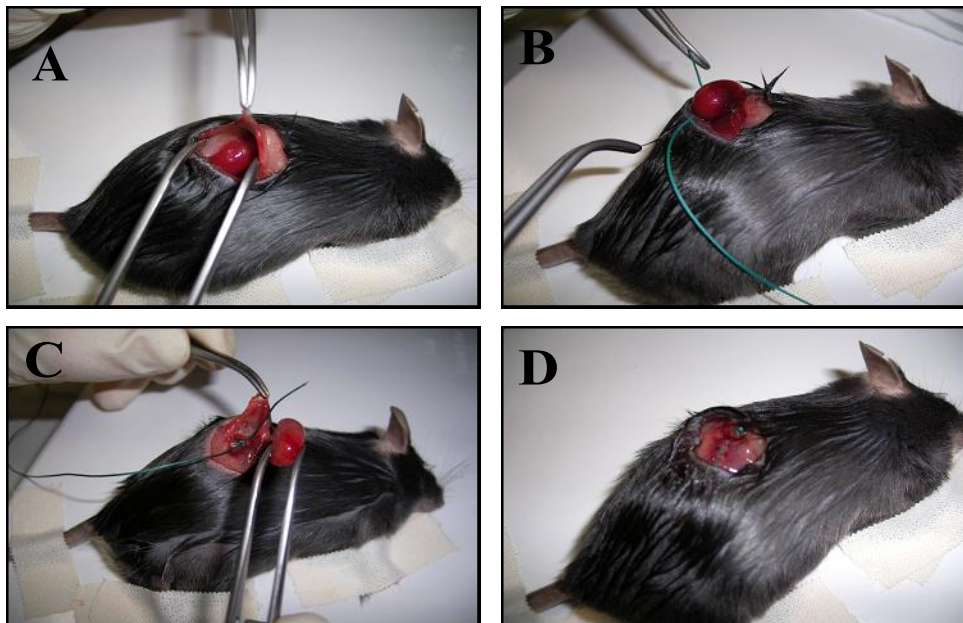


Figure 7: Pictures showing surgical procedure for uninephrectomy in mice. A: Making flank incision. B: Tying off the vessels and ureter with silk suture. C: Excision of the kidney after ligation. D: Wound closing with silk suture and wound clamps.

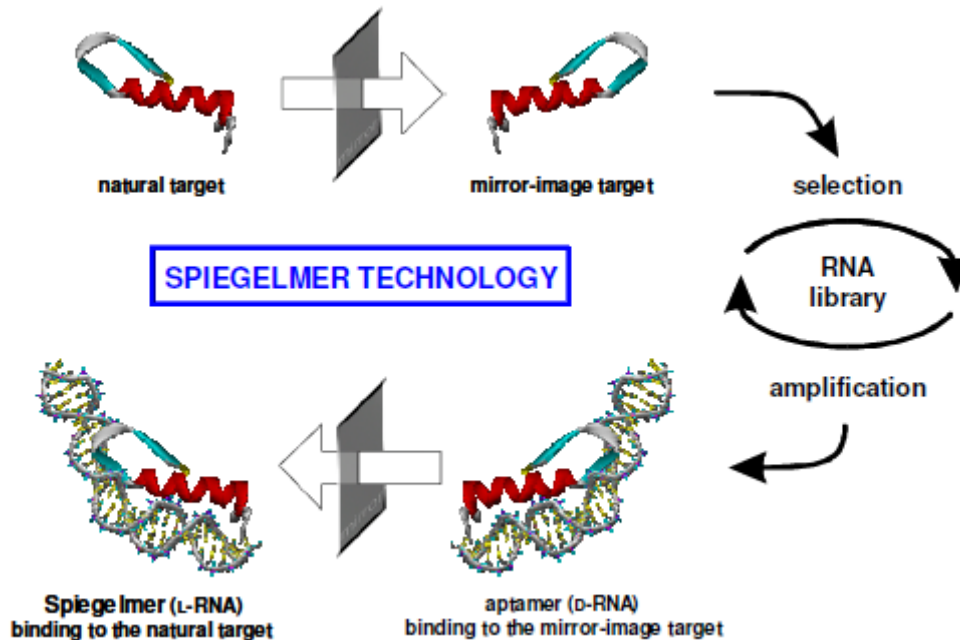
3.5.3. Drugs and formulations

To achieve CCL2 and CXCL12 antagonism we used a RNA-aptamers (Spiegelmer), a patented technology of NOXXON Pharma (Berlin). RNA-aptamer bind to the active site of target chemokines and makes them biologically non-functional.

An aptamer is a nucleic acid structure that can bind to a target molecule conceptually similar to an antibody that recognizes an antigen. Aptamers have binding characteristics similar to peptides or antibodies, with affinities in the low nanomolar to the picomolar range. However, there are several drawbacks to aptamers as useful therapeutic products. As relatively small molecules, aptamers demonstrate circulating half-lives in vivo in the order of minutes. This situation can be addressed by attaching large inert molecules to aptamers (e.g. polyethylene glycol) to reduce their elimination via the kidney and increase their presence in the circulation. Still, aptamers, as natural nucleic acid polymers, are prone to rapid degradation by nucleases that are present in all tissues in the body.

Spiegelmers are biostable aptamers, have all of the diverse characteristics of aptamers but possess a structure that prevents enzymatic degradation. While aptamers are created from the natural D-nucleotides, which are recognized by the nucleic acid degrading enzymes, Spiegelmers are synthesized as the mirror image L-oligonucleotide and are not degraded by any nucleases since there are no such enzymes in the body capable of interacting with these unnatural molecules¹⁷³. Spiegelmer technology is based on the simple concept that if an aptamer binds its natural target, the mirror image of the aptamer will identically bind the mirror image of the natural target (Figure 8). The process of aptamer selection is carried out against the mirror image target protein, an aptamer against this unnatural mirror image is obtained. More important, this Spiegelmer is now resistant to nuclease degradation. Spiegelmers should not be confused with antisense RNAs in that they do not directly interfere with transcription or translation of their target molecules¹⁷³. They are designed to bind specifically to extracellular proteins, either a receptor or its ligand, similar to the behavior of a monoclonal antibody, aptamer or peptide. Spiegelmers appear to be non-immunogenic, even under the most inductive

conditions for antibody formation in rabbits. These molecules are termed “Spiegelmer” from the German word “Spiegel” meaning “mirror” (www.noxxonpharma.com).



representation of Spiegelmer generation.
(Figure taken from www.noxxonpharma.com)

Study 1:

CCL2 / MCP-1 antagonist: mNoxE36 (Anti-Ccl2 Spiegelmer)

Ribonucleotide sequence:

5'- GGCGACAUUGGUUGGGCAUGAGGCGAGGCCCUUUGAU

GAAUCCGCGGCCA-3'-40 kDa PEG

Spiegelmer was dissolved in isotonic 5 % glucose solution for administration to mice.

Control Spiegelmer: Poc (scrambled sequence of RNA)

Ribonucleotide sequence:

5'-UAAGGAAACUCGGUCUGAUGCGGUAGCGCUGUGCAGA

GCU-3'-40 kDa PEG

Control Spiegelmer was dissolved in isotonic 5 % glucose solution for administration to mice.

Vehicle: 5% glucose solution was administered to vehicle group at the same concentration.

Study 2:

WM 7671: Orally bioavailable CCR2 and CCR5 dual antagonist
(Was obtained from Novartis Pharma.)

Dissolved in double distilled water and was administered orally

WM 7390: Orally bioavailable CCR2 and CCR5 dual antagonist
(Was obtained from Novartis Pharma.)

Dissolved in double distilled water and was administered orally

Vehicle: Distilled water

Study 3:

CXCL12 / SDF antagonist: mNOX-A12 (Anti-CXCL12 Spiegelmer):

Ribonucleotide sequence:

PEG 40 kDa-5'-GCGUGGUGUGAUCUAGAUGUAU UGGCUGAUCCUAGU
CAGGUACGC -3'

(5'-terminally modified with 40-kDa branched polyethylene glycol)

Spiegelmer was dissolved in isotonic 5 % glucose solution for administration to mice.

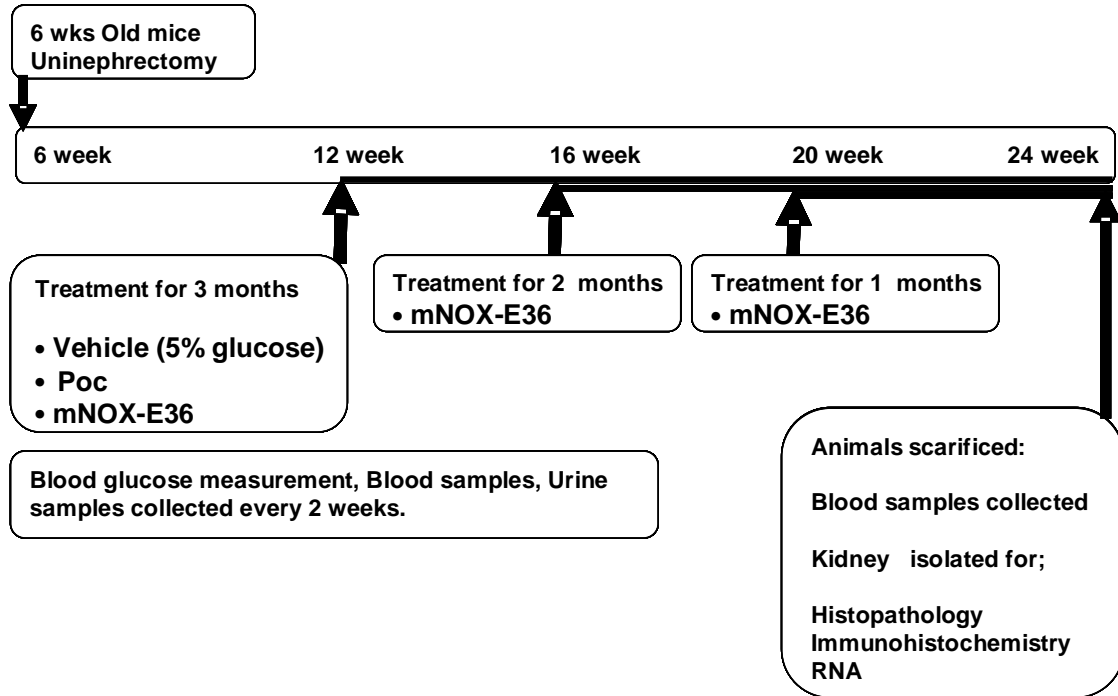
Control Spiegelmer: revmNOX-A12

Ribonucleotide sequence: reversed sequence of nucleotide as that of active Spiegelmer was used - 5'-terminally modified with 40-kDa branched polyethylene glycol.

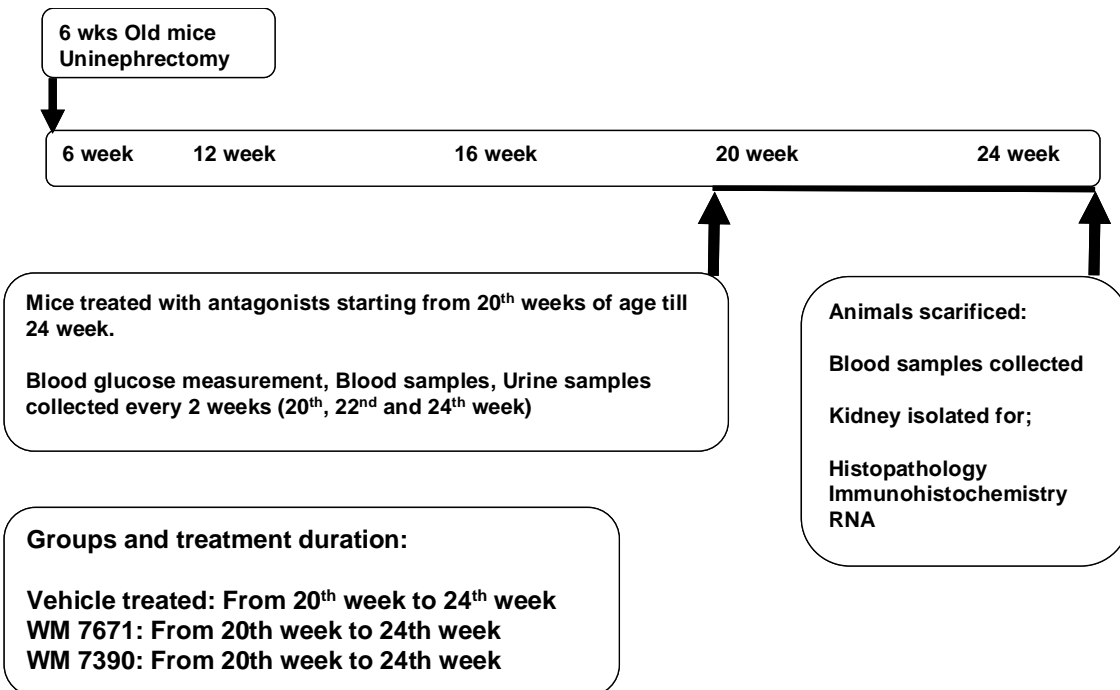
Vehicle: 5% glucose solution

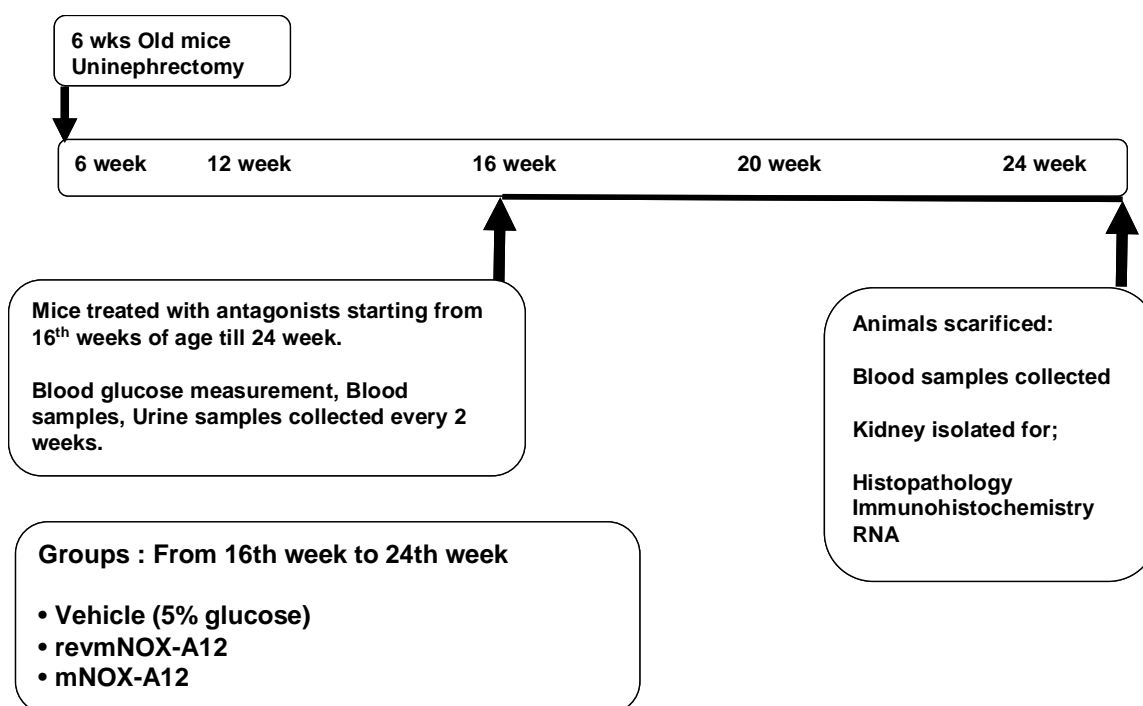
3.5.4. Experimental designs

Study 1:



Study 2:



Study 3:**3.5.5. Blood and urine sample collection**

Small blood samples (around 100 μ l) were collected under isoflurane anesthesia in microcentrifuge tubes containing EDTA (10 μ l of 0.5 M solution per 200 μ l of blood). Collected blood samples were centrifuged at 8000 rpm for 5 min and plasma was separated and stored at -20°C until used for different cytokine estimations.

Urine samples were collected every alternate week from each mouse in micro centrifuge tubes and were stored at -20°C until used for different biochemical estimations.

3.5.6. Body weight and blood glucose

Animals were weighed every week and blood glucose levels were monitored every alternate week using glucometer (Accu Check, Roche, Germany). Small blood samples were withdrawn by cutting tail tip from each mouse.

3.5.7. Urinary albumin

Urinary albumin levels were determined using albumin Elisa kit from Bethyl laboratories following manufacturer's instructions. Generally albumin levels in urine samples from db/db mice were quite high, so urine samples were diluted 1000 to 1500 times with water before estimation. In short, capture antibody (Anti-Mouse albumin, 1:100 dilution) was coated on polyethylene flat bottom 96 well plates (nunc plates) using carbonate-bicarbonate (pH 9.6) coating buffer. After overnight incubation of the capture antibody at 4 °C, plate was washed 3 times with wash buffer (Tris NaCl with Tween 20) and blocked with blocking solution (Tris, NaCl with 1% BSA, pH 8) at room temperature for 1 hour. After blocking was over the plate was washed 3 to 5 times with wash buffer and then diluted samples / standards were added in respective wells and further incubated for 1 hour. After incubation was over each well was washed 5 times with wash buffer and diluted HRP-conjugated detection antibody (using the suggested dilution) was added and the plate was incubated in dark for further 1 hour. After HRP-conjugate incubation was over each well was washed 5 to 7 times with wash buffer and TMB reagent (freshly prepared by mixing equal volumes of two substrate reagents) was added and incubated in dark till colour reaction was completed followed by addition of stop solution (2 M H₂SO₄). The absorbance was read at 450 nm within 10 min of stop solution addition. The albumin content in each sample was determined using the equation of regression line generated by plotting absorbance of different standards against their known concentrations.

3.5.8. Urinary creatinine measurement

Urinary creatinine levels were measured using enzymatic reaction (Jaffe' reaction using biochemical kit from Diasys). Urine samples were diluted 5 to 10 times (depending on the expected concentration range) with distilled water. Different dilutions of standard were prepared using the stock provided with the kit. Working monoreagent was prepared by mixing 4 part of reagent 1 (R1) and 1 part of reagent 2 (R2) provided with the kit. 10 µl of each of the diluted samples and standards were added to a 96 well plate with flat bottom (Nunc maxisorb plate). 200 µl of monoreagent was added to each well and absorbance for was read at 490 nm immediately after and 1 (A1) and 2 (A2) min of addition using elisa plate reader.

The change in absorbance (ΔA) was calculated as $\Delta A = [(A_2 - A_1) \text{ sample or standard}] - [(A_2 - A_1) \text{ blank}]$. And creatinine content of samples was calculated as:

$$\text{Creatinine (mg/dl)} = \Delta A \text{ sample} / \Delta A \text{ standard} * \text{Concentration of standard (mg/dl)}$$

3.5.9. Urinary albumin to creatinine ratio

Urinary albumin to creatinine ratio was calculated after converting values for albumin and creatinine to similar units (mg/dl). Albumin content for each sample calculated (mg/dl) was divided by creatinine content (mg/dl) for the same sample.

3.5.10. Cytokines

All cytokine levels in serum samples obtained from mice or supernatant collected from *in-vitro* cells stimulations were estimated using ELISA kits following the manufacturer's instructions.

3.5.10.1. CCL2 measurement

CCL2 levels in serum samples were measured using a commercially available Elisa kit (BD Biosciences, Cat: 555260). Polyethylene 96 well plate was coated with 100 μ l of capture antibody (Anti-Mouse CCL2, 1: 250 dilution) using coating buffer (Phosphate buffer, pH 6.5), after over night incubation at 4 $^{\circ}$ C. Each well was washed 3 time with wash buffer (PBS with Tween- 20) and plate was blocked using assay diluent (PBS with 10 % FBS) for further 1 hour at room temperature. Each well was washed 3 times and prepared standard (ranging from 1000 to 15.6 pg/ml, prepared by serial dilution of the stock provided) and diluted serum samples (20 times diluted in assay diluant) were added to respective well and incubated at room temperature for further 2 hours. After sample incubation was over each well was washed 5 times with wash buffer using elisa plate washer and 100 μ l of HRP-Conjugated detection antibody (1:250 times diluted in assay diluant) and incubated at room temperature in dark for further 1 hour. After incubation was over each well was washed 7 times with wash buffer and 100 μ l of TMB substrate solution (freshly prepared) was added and incubated for 20 to 30 min followed by addition of stop solution (2 M H₂SO₄) and absorbance was read at 450 nm within 10 min of stop

solution addition. CCL2 level in each sample was calculated using the equation of regression line generated with by plotting absorbance of different standards against their known concentrations.

3.5.10.2. CXCL12 measurement

CXCL12 levels in serum and cell culture supernatant samples were determined using Elisa. Animal group treated with anti-CXCL12 Spiegelmer were expected to have significantly elevated CXCL12 levels, samples from Spiegelmer treated group were diluted 1000 times with assay diluant. Capture antibody (Anti-mouse CXCL12, 8 µg/ml) was coated on polyethylene flat bottom 96 well plates (nunc plates) using carbonate-bicarbonate (pH 9.6) coating buffer. After overnight incubation of capture antibody at 4 °C, plate was washed 3 times with wash buffer (Tris NaCl with Tween 20) and blocked with blocking solution (Tris, NaCl with 1% BSA, pH 8) at room temperature for 1 hour. After blocking was over plate was washed 5 times with wash buffer and then diluted samples or standards were added in respective wells and further incubated for 2 hour. After incubation was over each well was washed 5 times with wash buffer and diluted detection antibody (biotinylated anti-mouse antibody) was added and the plate was incubated for further 1 hour. After incubation was over each well was washed 3 times with wash buffer and HRP (using the suggested dilution 1: 250) was added and plate was incubated in dark for further 30 min. After HRP incubation was over each well was washed 5 times with wash buffer and TMB reagent (freshly prepared by mixing equal volumes of two substrate reagents) was added and incubated in dark till colour reaction was completed followed by addition of stop solution (2 M H₂SO₄) and absorbance was read at 450 nm within 10 min. CXCL12 content in each sample was determined using the equation of regression line generated with by plotting absorbance of different standards against their known concentrations.

3.5.11. Glomerular filtration rate determination

Glomerular filtration rate in conscious mice was determined using Fluorescein Isothiocyanate-inulin (FITC-inulin) clearance from plasma after single bolus intravenous injection. In short, FITC-inulin was dissolved in 0.9% NaCl facilitated

by heating at 65 °C so as to get a 5 % solution. Animals were anesthetized using isoflurane for short duration, and FITC-inulin (5%) solution was rapidly injected retroorbitally (3.74 ul/gm body weight). Blood samples were drawn at different time point (3, 7, 10, 15, 35, 55 and 75 minutes post inulin injection). Blood samples were centrifuged at 8000 rpm for 5 min and plasma was separated. Each plasma sample was buffered to pH 7.4 by mixing 10 µl of plasma with 40 µl of 500 mM HEPES buffer (pH 7.4) in 96 well plate. Fluorescence was determined using excitation filter having wave length of 485 nm while read filter was set at wave length of 535 nm. For GFR calculation two-compartment clearance was employed. In two compartment model the initial, rapid decay phase represents redistribution of tracer from the intravascular compartment to extracellular fluid. Later, slower decay in concentration of the tracer due to systemic clearance from plasma predominates. At any given time (tx), the plasma concentration of the tracer (Y) can be calculated as

$$Y = Ae^{-\alpha tx} + Be^{-\beta tx} + \text{Plateau}$$

Where,

- Y is plasma concentration of tracer
- A is y-intercept of fast decay rate (SPAN1)
- B is y-intercept of slow decay rate (SAPN2)
- α is fast decay rate constant
- β is slow decay rate constant

These parameters were calculated using non-linear curve-fitting program (GraphPad Prism) followed by exponential two-phase decay with plateau set as zero.

GFR was calculated as:

$$\text{GFR} = I / (A/\alpha + B/\beta)$$

Calculated GFR was reported as ml/min and was expressed as mean \pm SEM for each group.

3.5.12. Fluorescence activated cell sorting

3.5.12.1. Kidney cells isolation for FACS

- Isolated kidneys were smashed in to small pieces using scalpel in a plate containing Paris-buffer (3ml) on ice and was transferred to 10 ml Falcon tube with ice cold Paris-buffer.
- Tube was then centrifuged at 1200 rcf for 5 minutes at 4 °C.
- Supernatant was discarded and pellet was re-suspended in 10 ml ice cold HBSS (with Ca, Mg)
- Centrifuged at 1200 rcf for 5 minutes at 4 °C
- Supernatant was discarded and pellet was digested with Collagenase/DNase solution (5 ml preheated Collagenase/DNase solution) and was incubated for 20 min at 37 °C with through mixing in between.
- Centrifuged at 1200 rcf for 5 minutes at room temperature.
- Supernatant was discarded and pellet was washed two times in 10 ml ice cold HBSS (with Ca, Mg) each time centrifuged at 1200 rcf for 5 minutes at 4 °C and supernatant was discarded.
- Pellet was re-suspended in 5ml of 2mM EDTA in HBSS (without Ca, Mg) and was incubated for 20 min at 37 °C.
- Centrifuged at 400 rcf (30g) for 5 minutes at 4 °C.
- Pipette the supernatant in new cooled Falcon tube kept on ice (preserve this supernatant) and process the remaining pellet.
- Re-digested the remaining pellet with Collagenase (5ml preheated Collagenase solution was added) and was incubated at 37 °C for 20 min with through mixing in between.
- Digested pellet was transferred to ice place, cooled down on ice, then whole suspension was pressed through 19G needle twice, followed by 26G and finally was pressed through 30G needle and was mixed with the supernatant in Falcon (stored previously).
- Centrifuged at 1200 rcf for 5 minutes at room temperature and supernatant was discarded.
- Pellet was re-suspended in 10 ml ice cold PBS (without Ca, Mg) and centrifuged at 1200 rpm for 5 min at 4 °C, supernatant was discarded.

- Pellet was dissolved in FACS-buffer (DPBS + 0.2 % BSA + 0.1 % Na Azide) and was passed through 70 um nylon filter (which was rinsed previously with 1ml PBS), filtrate was collected in new Falcon on ice, volume was made up to 10 ml with PBS.
- Centrifuged at 1500 rpm at 4 °C for 5 min and supernatant was discarded.
- Obtained pellet was re-suspended in 200 to 500 ul (depending on pellet size) of FACS- buffer and processed for staining with different antibodies.

3.5.12.2. Staining for FACS

Sufficient number of isolated kidney cells (suspended in FACS buffer) from each sample were transferred to FACS-tubes containing master mix serum (5 ul of rat serum and 5 ul of mouse serum) and incubated for 10 min. Required antibodies were prepared and added to the above mixture and incubated at room temperature for further 60 min in dark. After antibodies (cKit, Sca or CXCR4) incubation FACS buffer (2 ml) was added and vortexed thoroughly, centrifuged at 1200 rpm for 5 min at 4 °C, this procedure was repeated twice (two washes) and finally pellet was suspended in 300 µl of FACS buffer and was processed for FACS analysis.

3.5.12.3. Preparation of blood for FACS

Blood samples were collected in micro-centrifuge tubes containing EDTA (5 µl per 100 µl of blood). 100 µl of blood samples were transferred to FACS tubes containing serum master mix (5 µl of rat serum + 5 µl of mouse serum) and incubated for 10 min at room temperature. Different antibodies (cKit, Sca or CXCR4) were added to respective tubes (1.4 ul per AB) and were incubated in dark for further 60 min. After antibody incubation 2 ml of diluted lysis buffer (1:10 times) (BD FACS lysis solution, 349202) was added to each tube vortexed and incubated for further 10 min. Then tubes were centrifuged at 1200 rpm for 4 min at 4 °C. Supernatant was discarded and washed twice with FACS buffer followed by centrifugation at 1200 rpm for 4 min at 4 °C, finally supernatant was sucked so that last 300 µl of FACS buffer remains in the tube.

3.5.13. Immunostaining

For immunohistological studies middle part of kidney from each mouse were fixed in formalin (10 % in PBS or Saline) over night and processed using tissue processors (Leica) and paraffin blocks were prepared. 2 µm thick paraffin-embedded sections were cut. De-paraffinization was carried out using xylene (3 * 5 min) followed by re-hydration, which was carried out by incubating the sections in 100% absolute ethanol (3 * 3 min), 95% ethanol (2 * 3 min) and 70% ethanol (1 * 3 min) followed by washing with PBS (2 * 5 min). Blocking endogenous peroxidase was carried out by incubating sections in H₂O₂ and methanol mixture (20 ml of 30% H₂O₂ in 180ml of methanol) for 20 min in dark followed by washing in PBS (2* 5min). For unmasking of antigen sections were dipped in antigen unmasking solution (3 ml of antigen unmasking solution + 300 ml of distilled water) and cooked in microwave for total of 10 min (4*2.5 min, every 2.5 min water level was checked and made up to the initial levels with distilled water every time). After microwave cooking sections were cooled to room temperature for 20 min and washed with PBS. Blocking endogenous biotin was carried out by incubating sections with one drop of Avidin (Vector) for 15 min followed by incubation with Biotin (Vector) for further 15 min. After the incubation was over sections were washed with PBS (2* 5 min).

Sections were incubated with different primary antibodies either for 1 hour at room temperature or over night at 4 °C in a wet chamber followed by wash with PBS (2* 5 min). After washing sections were incubated with biotinylated secondary antibodies (1:300, dilution in PBS) for 30 min followed by wash with PBS (2* 5 min). Substrate solution (ABC solution, Vector) was and sections were incubated for 30 min at room temperature in a wet chamber followed by wash with PBS (1* 5 min). Tris (1* 5 min) and sections were stained for DAB followed by counter staining with methyl green (Fluka). Then sections were washed with alcohol (96 %) to remove excess stain and xylene. Sections were dried and mounted with VectaMount (Vector).

The following rat and rabbit antibodies were used as primary antibodies: rat anti-Mac2 (glomerular macrophages, Cederlane, Ontario, Canada, 1:50), rat anti-F4/80 (macrophages, Serotec, Oxford, UK, 1:50), anti-Ki-67 (cell proliferation, Dianova, Hamburg, Germany, 1:25), anti-mMECA-32 (endothelial cells, Iowa Hybridoma

Bank, USA, 1:5), anti-m CXCL12 (R&D System, 1: 100) and anti-m SMA- α (1:50). For each immuno staining negative controls staining was performed by incubation with a respective isotype antibody instead of primary antibody.

3.5.14. Periodic acid Schiff staining

Formalin-fixed tissues were processed using tissue processors (Leica) and paraffin blocks were prepared. 2 μ m thick paraffin-embedded sections were cut. De-paraffinization was carried out using xylene (3 * 5 min) followed by re-hydration by incubating the sections in 100% absolute ethanol (3 * 3 min), 95% ethanol (2 * 3 min) and 70% ethanol (1 * 3 min) followed by washing with distilled water (2 * 5 min). Re-hydrated sections were incubated with Periodic acid (2 % in distilled water) for 5 min followed by washing with distilled water (1* 5 min). Then sections were incubated with Schiff solution for 20 min at room temperature followed by washing with tap water (1* 7 min) and counter staining with Hematoxylin solution (1* 2 min). This was followed by washing with tap water (1* 5 min) and finally sections were dipped in alcohol 90% and dried and closed with cover slips.

3.5.15. Silver staining

Formalin fixed tissue were processed using tissue processors (Leica) and paraffin blocks were prepared. 2 μ m thick paraffin-embedded sections were cut. De-paraffinization was carried out using xylene (3 * 5 min) followed by re-hydration, which was carried out by incubating the sections in 100% absolute ethanol (3 * 3 min), 95% ethanol (2 * 3 min) and 70% ethanol (1 * 3 min) followed by washing with distilled water (2 * 5 min). Re-hydrated sections were processed for silver staining using tissue section staining kit from Bio-Optica (Milano, Italy). In short the principle involves initial oxidation of sections with potassium permanganate followed by treatment with trivalent iron. The bound iron is then replaced by silver using ammonical silver solution.

3.5.16. Histopathological evaluations

3.5.16.1. PAS staining: For quantitative analysis 2 μm sections were stained with periodic acid-Schiff reagent. Glomerular sclerotic lesions were assessed using a semi quantitative score by a blinded observer as follows:

0 = no lesion,

1 = <25% sclerotic

2 = 25-49% sclerotic

3 = 50-74% sclerotic

4 = 75-100% sclerotic

From each section 15 glomeruli were analyzed. All sections were quantified in each group and were expressed as percentage of glomeruli with each score (mean \pm SEM).

3.5.16.2. Silver staining: Silver staining was performed on 2 μm sections following manufacturer's instructions (Bio-Optica, Milano, Italy). The indices for interstitial volume, interstitial collagen deposition, tubular cell damage, and tubular dilatation were evaluated manually by superposing a grid containing 100 (10 x 10) sampling points on photographs of 10 non-overlapping cortical high power fields of silver-stained tissue (200 X) of each kidney.

3.5.16.3. Mac2 staining: Number of infiltrated macrophages in glomeruli as well as in interstitium were counted in sections stained with Mac2 (pan marker for macrophage) antibodies. Mac2 positive cells were counted manually in 15 glomeruli or 15 non-overlapping high power fields interstitium for each section and were presented as mean \pm standard error of mean for respective groups.

3.5.16.4. Ki67 staining: Number of proliferating cells within glomeruli were evaluated using Ki 67 staining. For quantification Ki67 positive cells were counted manually in 15 glomeruli in each section and presented as mean \pm standard error of mean for respective groups.

3.5.16.5. SMA- α staining: For tissue fibrosis assessment sections were stained with SMA- α anti-body. For quantification a semi-quantitative method was employed, in short each glomerulus was scored from 0 (least positive) to 4 (most positive cells) by

a blinded observer. For each section 20 glomeruli were scored and finally presented as mean \pm standard error of mean for respective groups.

3.5.16.6. Meca32 staining: Number of Meca32 positive endothelial cells were calculated manually in 10 non-overlapping high power fields (200X). Positive cells were counted manually using Adobe photo shop software after capturing images from all sections (10 images per section). Results are presented as \pm minus standard error of mean for respective groups.

3.5.17. RNA analysis

3.5.17.1. RNA isolation: When animals were sacrificed on termination of the study, small parts of kidney from each mouse were preserved in RNA-later and stored at -20 °C until processed for RNA isolation. RNA isolation was carried out using RNA isolation kit from Qiagen (Germany). In short, tissues (30 mg) preserved in RNA-later were homogenized using blade homogenizer for 30 seconds at 14500 rpm in lysis buffer (600 μ l) containing β -mercaptoethanol (10 μ l/ml). The homogenate was centrifuged at 15000 rpm for 3 min. and 350 μ l of supernatant was transferred to fresh DEPC-treated tube to this equal amount (350 μ l) of 70 % ethanol was added and whole mixture was loaded on RNA column and processed for RNA isolation as per the manufacturer's instruction. Isolated RNA was stored at -80 °C until further used.

3.5.17.2. RNA quantification and purity check: For quantification isolated RNA samples were diluted in DEPC water (2 μ l of RNA + 98 μ l of DEPC water, 50 times dilution) and absorbance was measured at two wavelengths as 260 nm and 280 nm.

$$\text{Amount of RNA } (\mu\text{g}/\mu\text{l}) = \text{O.D. at 260 nm} * 40 * 50 (\text{dilution factor}) / 1000$$

The ratio of optical densities at 260 nm and 280 nm is an indicator for RNA purity (indicative of protein contamination in the RNA samples). Only samples with a ratio of 1.8 or more were considered to be of acceptable quality.

3.5.17.3. RNA integrity check: Further quality check (if necessary) was performed using a denaturing RNA gel. In short 2 % Agarose gel with Ethidium-bromide was casted, RNA samples were mixed with RNA loading buffer (4:1 ratio) (Sigma) and were loaded on the gel. Electrophoresis was carried out at constant volt (70-100 V) using MOBS running buffer for 1 hour and the gel was read on a gel documentation apparatus under UV lamp. RNA samples showing a single bright band were considered to be of good quality. Loss of RNA integrity could be detected as smear formation in the agarose gel (Figure 9).

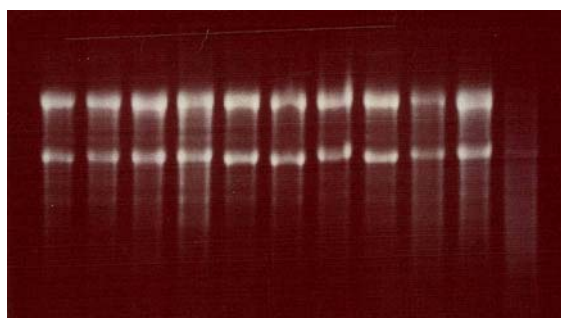


Figure 9: Representative agarose gel for RNA integrity check.

3.5.17.4. cDNA synthesis and real-time RT-PCR (SYBR Green)

The isolated RNA samples were quantified and processed for cDNA conversion using reverse transcriptase II (Invitrogen). RNA samples were diluted in DEPC treated tubes with water to get final concentration of 2 μg / 30 μl , to this diluted RNA samples 13.9 μl of master mix* was added, all tubes were incubated at 42 $^{\circ}\text{C}$ for 1 hour and 30 min on thermal shaker. Upon completion of incubation cDNA samples were stored at -20 $^{\circ}\text{C}$ until used for RT-PCR analysis using SYBR green.

*The master mix was prepared by mixing 9 μl of 5x buffer (Invitrogen, Karlsruhe, Germany), 1 μl of 25 mM dNTP mixture (Amersham Pharmacia Biotech, Freiburg, Germany), 2 μl of 0.1 M DTT (Invitrogen, Karlsruhe, Germany), 1 μl of 40U/ μl RNasin (Promega, Mannheim, Germany), 0.5 μl of Hexanucleotide (Roche, Mannheim, Germany), 1 μl of Superscript (Invitrogen, Karlsruhe, Germany) or ddH₂O in the case of the control cDNA (RT minus).

The cDNA samples prepared as described above were diluted 1:10 a dilution for the real-time RT-PCR. 2 μl of diluted cDNA samples were mixed with SYBR green

master mix (10 µl), forward primer, specific for gene of interest (0.6 µl), reverse primer specific for gene of interest (0.6 µl), Taq polymerase (0.16 µl) and distilled water (6.64 µl). The real-time RT-PCR was performed using Light Cycler480.

For RT-PCR following protocol was used

Pre-incubation was carried out for 5 minutes at 95 °C so as to activate the polymerase and complete de-naturation of cDNA samples. Followed by amplification for 40 cycles, each comprising of 15 seconds incubation at 95 °C and 45 seconds incubation at 60 °C. For melting curve initial 95 °C for 5 seconds followed by 65 °C for 1 min with continuous heating was used. The RT-PCR for the reference genes (18S rRNA) was carried out under similar conditions. The CT values were calculated using the Light Cycler480 and the results were normalized with respective reference gene expression for each sample. In all cases controls consisting of ddH₂O were negative for target or reference genes. All designed SYBR green primers for all genes evaluated were obtained from Metabion (Martinsried, Germany).

3.5.17.5. Oligonucleotide primers used for SYBR-Green RT-PCR

18S	Forward primer: 5'-GCAATTATTCCCCATGAACG-3' Reverse primer: 5'-AGGGCCTCACTAAACCATCC-3'
Ccl2	Forward primer: 5'-ATTGGGATCATCTTGCTGGT-3' Reverse primer: 5'-CCTGCTGTTCACAGTTGCC-3'
iNos	Forward primer: 5'-TGAAGAAAACCCCTTGTGCT-3' Reverse primer: 5'-TTCTGTGCTGTCCCAGTGAG-3'
Cxcl12	Forward primer: 5'-GCGCTCTGCATCAGTGAC-3' Reverse primer: 5'-TTTCAGATGCTTGACGTTGG-3'
Arg I	Forward primer: 5'-AGAGATTATCGGAGCGCCTT-3' Reverse primer: 5'-TTTTTCCAGCAGACCAGCTT-3'
Mcr1	Forward primer: 5'-ATATATAACAAGAATGGTGGGCAGT-3' Reverse primer: 5'-TCCATCCAAATGAATTTCTTATCC-3'
Mcr2	Forward primer: 5'-GCAAAACCTGCAGAAGCTGT-3' Reverse primer: 5'-ACCATCTGTCCACCTGAAGC-3'
Ym1	Forward primer: 5'-TCTGGGTACAAGATCCCTGAA-3' Reverse primer: 5'-TTTCTCCAGTGTAGCCATCCTT-3'

Il10 Forward primer: 5'-ATCGATTTCTCCCCTGTGAA-3'
Reverse primer: 5'-TGTCAAATTCATTCATGGCCT-3'

Fizz1(Retnla) Forward primer: 5'-CCCTTCTCATCTGCATCTCC-3'
Reverse primer: 5'-CTGGATTGGCAAGAAGTTCC-3'

All primers were procured at concentrations 100 pmol/ul and were used at 10 pmol/ul concentrations after dilution with distilled water before use in RT-PCR mixture.

3.5.18. In vitro methods

3.5.18.1. Culture of murine cells

The murine macrophage cell line *J774* (American Type Culture Collection, Rockville, MD, USA) or murine glomerular endothelial cell lines were grown in RPMI 1640 medium containing 10% heat-inactivated fetal calf serum, penicillin 100 U/ml and streptomycin 100µg/ml (complete RPMI medium) under standard culture conditions (in an incubator set at 37 °C supplied with 5 % CO₂/air). A proximal tubular epithelial cell line was maintained in DMEM medium (GIBCO/Invitrogen, Carlsbad, CA, USA) containing 10% FCS and 1% penicillin-streptomycin under standard culture conditions as described above. Once culture plates were confluent with *J774* mouse macrophages or proximal tubular epithelial cells (every 24-36 hrs.) were normally split into 6 /12 well plate or subcultured according to the following procedure: After removing the old medium, cells were washed twice with PBS. Subsequently, the appropriate volume of EDTA-trypsin solution was added to the culture flasks and the cells were incubated at RT for 5 min. Trypsinization was stopped by adding complete medium and cells were re-suspended and transferred to new sterile Falcon tube. Cells were centrifuged at 1000 RPM for 3 min at RT, supernatant was discarded and the pellet was re-suspended in 5 ml of fresh RPMI or DMEM medium (depending on the cell line). For subculturing relatively less number of cells were transferred to new culture plates containing fresh media. Before splitting into 6 /12 well plates number of cells were counted using Neubauers' chamber and desired number of cells were transferred to each well of 6 /12 well plates containing fresh media and incubated at 37 °C for 24 h under standard culture conditions before stimulation with different ligands.

3.5.18.2. Culture of immortalized murine podocytes

In order to propagate, podocytes were cultivated at lower temperature (33 °C) in RPMI 1640 supplemented with 10 % FCS, 100 U/ml penicillin, 0.1 mg/ml streptomycin and 10 U/ml of mouse recombinant γ -interferon in 5 % CO₂ atmosphere. For differentiation, podocytes were maintained at higher temperatures (38 °C) without recombinant γ -interferon for at least 2 weeks. Differentiated podocyte phenotype were assessed by morphology (large and well spread cells) and from time to time by WT1 and nephrin immunofluorescence.

3.5.18.3. Cell freezing and thawing

At earlier passages large amounts of cells were grown under standard culture conditions and were frozen for future use. Cells to be frozen were detached from the culture plates and were spun down under sterile conditions for 3 min at 1000 RPM. The cell pellet was maintained on ice and carefully re-suspended in cold freezing medium (90 % respective culture medium and 10 % DMSO) by pipetting the suspension repeatedly up and down. 1.5 ml aliquots were quickly dispensed into freezing vials (4 °C). The cells were slowly frozen at -20 °C for 1 h and then at -80 °C overnight. The next day, all aliquots were transferred to liquid nitrogen.

In order to thaw cells a frozen vial was removed from liquid nitrogen and put in a water bath at 37 °C. The cells were then dispensed in 5 ml of warm complete growth medium and spun down at 1000 RPM for 5-7 min. Then the old medium was removed and the cells were re-suspended in fresh medium and transferred to new culture plate. The medium was changed once more after 24 h.

3.5.18.4. Stimulation experiments

Before stimulation with any ligand all cells split in 6 /12 well plates for stimulation experiments (*J774*, *GENC*, *MTC* or *Podocytes*) were maintained in RPMI 1640 or DMEM supplemented with 1% penicillin-streptomycin and less (1 %) or no FCS for at least 24 hrs (serum starvation).

3.6. Computer programs

- CellQuest software
- ABI PRISM Sequence Detection software 1.0
- Light Cycler 480 Software
- SPSS for Windows 13.0
- Graph pad prism 5
- Endnote plus 9
- Office XP, 2003
- Photoshop 7.0, CS
- Windows 2003 Professional

3.7. Statistical analysis

Data are presented as mean \pm SEM. For multiple comparison of groups one way ANOVA was used followed by post-hoc Bonferroni's test, using SigmaStat (Jandel Scientific, Erkarath, Germany). Paired Student's t-test was used for the comparison of single groups. A value of $p < 0.05$ was considered to indicate statistical significance.

4. Results

4.1. Animal model validation

4.1.1. Glomerulosclerosis is aggravated upon uninephrectomy

There are several animal models that have been described for experimental diabetic nephropathy. The most widely accepted animal model for experimental type 2 diabetic nephropathy is db/db mice. We performed uninephrectomy at early age (6 weeks of age) which aggravated the development of diabetic nephropathy in db/db mice. To validate the development of diabetic nephropathy animals were sacrificed at the age of 24 weeks and kidney sections were analysed histochemically.

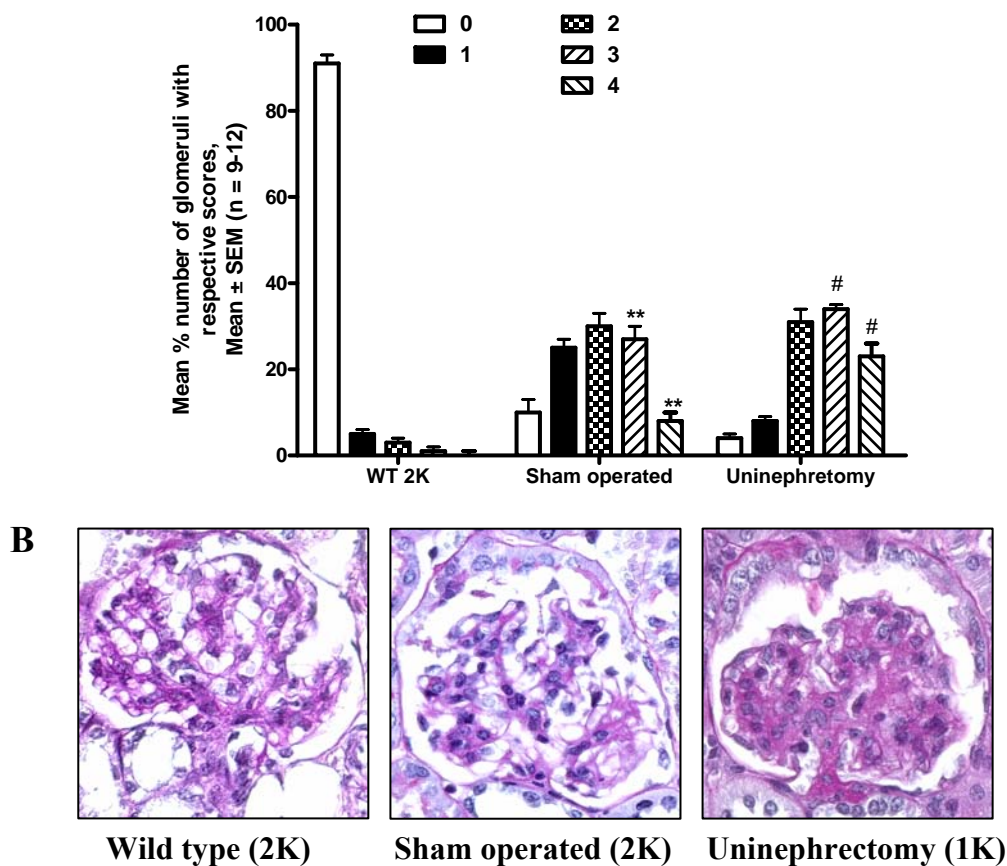


Figure 10 : PAS stains for renal sections. A: PAS stains were scored for the extent of glomerulosclerosis from 0-4 as described in methods. From each mouse 15 glomeruli from each renal section were graded by that score. The graph illustrates the mean percentage of each score \pm SEM from all mice in each group (n=9-12). Sham operated mice showed development of mild glomerulosclerosis compared to wild type mice. Uninephrectomy was associated with a shift towards higher scores of glomerulosclerosis. ** $p < 0.01$ versus wild type mice and # $p < 0.05$ versus sham operated db/db mice. B: Representative renal sections from 24 weeks old wild type and db/db mice stained for periodic acid Schiff (PAS) (magnification 630X).

Glomeruli from PAS staining of kidney sections were scored manually as described in materials. Uninephrectomy in db/db mice resulted in a significant increase in the percentage of glomeruli with higher scores, indicative of glomerulosclerosis (Figure 10).

4.1.2. Glomerulosclerosis was associated with macrophage infiltration in kidney

In order to evaluate contribution of different inflammatory pathways in development of diabetic nephropathy. We evaluated kidney sections for number of infiltrating macrophages in different compartments. Kidney sections were stained for Mac2 (marker for macrophages) and sections were quantified manually as described in methods section.

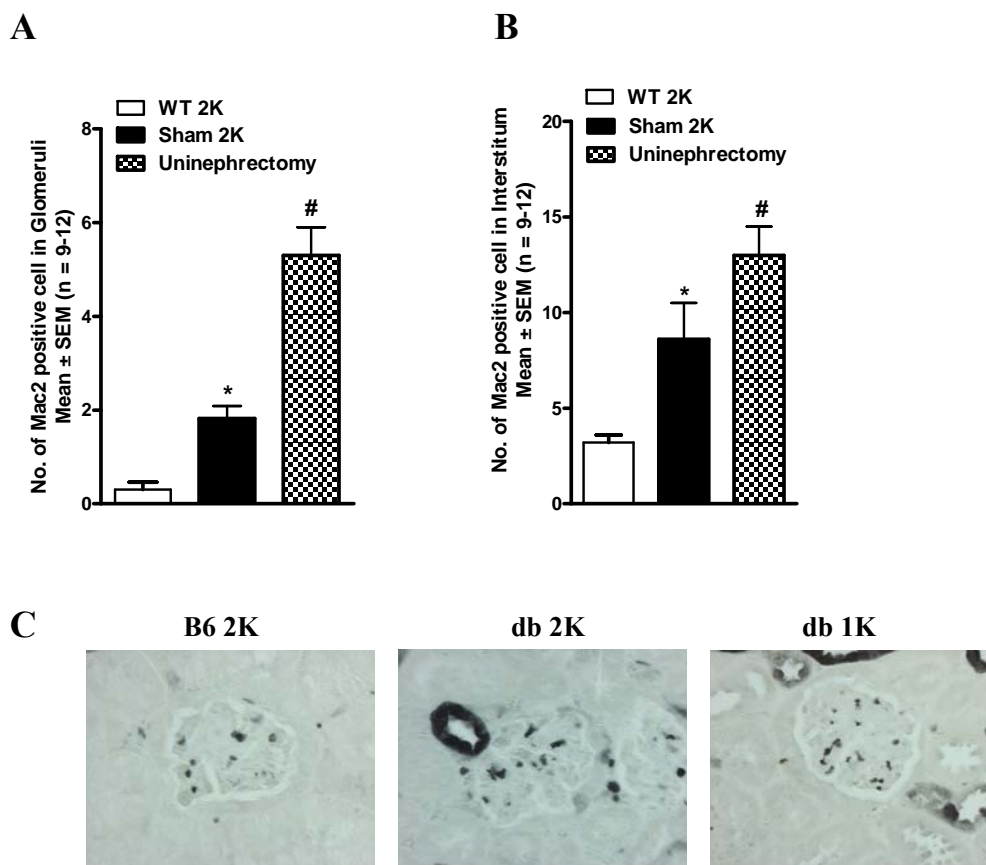


Figure 11 : Renal sections from 24 week old mice with or without uninephrectomy were stained for Mac2. Graphs show the numbers of positive cells in 15 glomeruli (A) or interstitium (B) in wild type, sham-operated (2K) and uninephrectomized (1K) db/db mice at 6 months of age. * $p < 0.05$ versus wild type mice and # $p < 0.05$ versus sham operated db/db mice. C: Representative renal sections from 24 weeks old wild type and db/db mice stained for Mac2 (magnification 400X).

Aggravated glomerulosclerosis in db/db mice upon uninephrectomy was associated with increased numbers of infiltrating macrophages in glomeruli (Figure 11).

4.1.3. Uninephrectomy in db/db mice resulted in increased albuminuria and decreased glomerular filtration rate

Development of diabetic nephropathy has been characterized with increased albuminuria in different animal models as well as in humans, with associated impairment of glomerular filtration rate. Uninephrectomy at early age (6 week) in db/db mice resulted in significant increased albuminuria and was associated with decreased GFR compared to sham operated mice at the age of 24 week, indicative of the development of diabetic nephropathy (Table 3).

Table 3: Effect of uninephrectomy on albuminuria and glomerular filtration rate

	WT (2K)	db/db (2K)	db/db (1K)
Urinary albumin to creatinine ratio (mg/dl)	0.08 ± 0.02	0.24 ± 0.05	0.32 ± 0.13*
GFR (ml/min)	385 ± 103	293 ± 74	116 ± 22**
Body weight (g)	27 ± 0.58	58 ± 2.46	56 ± 2.55
Plasma glucose (mg/dl)	142 ± 3.5	414 ± 22	399 ± 25

WT; wild type, 2K; sham operated, 1K; uninephrectomised, GFR; glomerular filtration rate, * p < 0.05, ** p < 0.01 compared to sham operated db/db (2K) mice.

4.2. Role of pro-inflammatory chemokines in diabetic nephropathy

4.2.1. CCL2/MCP-1 blockade at different stages of disease progression

4.2.1.1. CCL2 levels in serum

To assess the efficiency of employed Spiegelmer for its biological activity we estimated CCL2 levels in serum from all groups. Serum levels of CCL2 were significantly (p < 0.05) increased in all groups of mice treated with mNOX-E36 compared to vehicle of Poc treated mice at 6 months of age, indicating that CCL2-specific Spiegelmers retain CCL2 in the intravascular compartment (Figure 12).

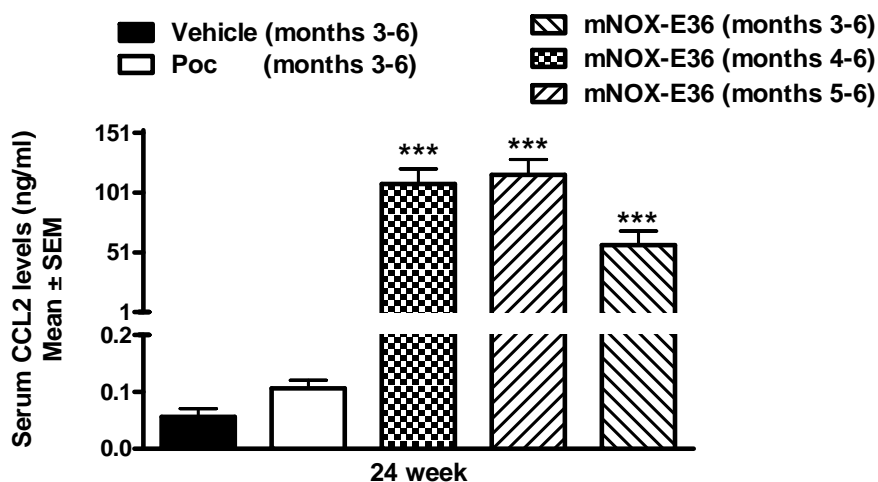


Figure 12: Serum CCL2 levels. CCL2 serum levels were estimated in the serum samples collected at the age of 24 weeks from mice of all groups using ELISA. *** $p < 0.001$ versus vehicle treated mice.

4.2.1.2. CCL2 blockade prevented further increase in urinary albumin to creatinine ratio

Albumin / creatinine ratio is an important clinical parameter for assessment of renal disease progression. In diabetic nephritis urinary albumin to creatinine ratio has been reported to increase with the progression of kidney inflammation. In our animal model of diabetic nephropathy we observed a trend in increase of urinary albumin to creatinine ratio over the time. To assess the effect of CCL2 blockade on progression of disease we estimated urinary albumin to creatinine ratio at different time points of the study. Treatment with a CCL2 antagonist (mNOX-E36) was expected to inhibit the progression of renal disease in db/db mice, which can be indicated by the reduction of albumin / creatinine ratio, when compared to vehicle or Poc-treated groups.

A subcutaneous administration of CCL2 antagonist mNOX-E36 (50 mg/kg, three times per week) for different time lengths [3 to 6 months, 4 to 6 months and 5 to 6 months] to uninephrectomized db/db mice inhibited further increase in urinary albumin/ creatinine ratio compared to Poc-treated group (Figure 13).

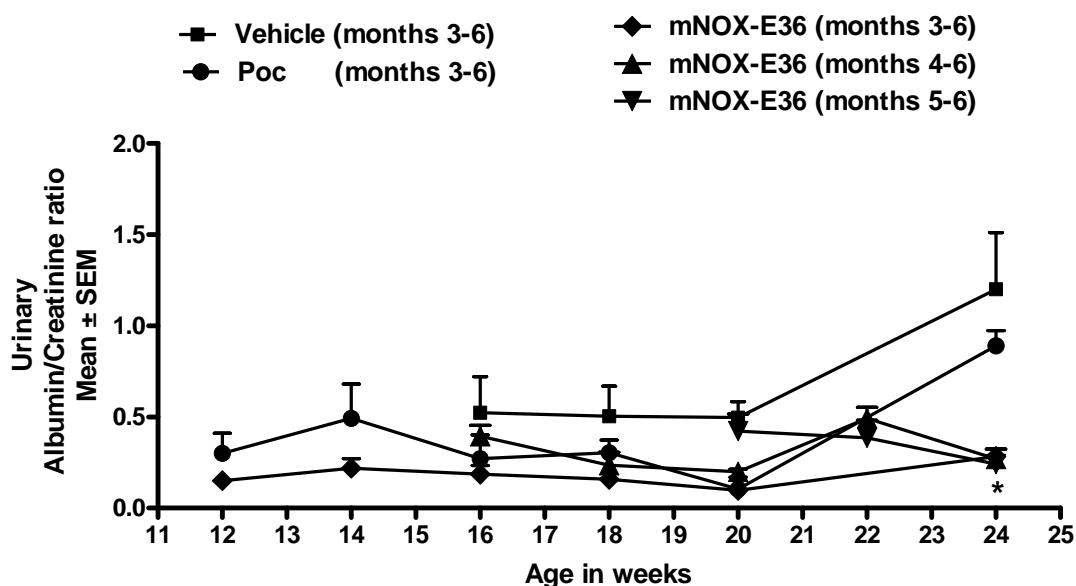


Figure 13: Urinary albumin to creatinine ratio. Proteinuria was determined after every 2 weeks of Spiegelmer injections in uninephrectomized db/db mice treated as indicated. Data represent means of urinary albumin/creatinine ratio \pm SEM. * $p < 0.05$ mNOX-E36 versus vehicle treated 1K db/db mice.

4.2.1.3. CCL2 blockade inhibited mesangial cell proliferation

Glomerulosclerosis in diabetic nephropathy is well correlated with mesangial cells hyper proliferation and matrix expansion. To assess the effect of CCL2 blockade on renal cell proliferation we performed Ki 67 immuno staining of kidney sections from all groups as described in materials and methods. Upon treatment with mNOX-E36 numbers of Ki 67 positive cells in glomeruli were significantly reduced compared to vehicle or Poc-treated mice indicative of less proliferation within glomeruli, which was consistent with our earlier report⁶¹ (Figure 14).

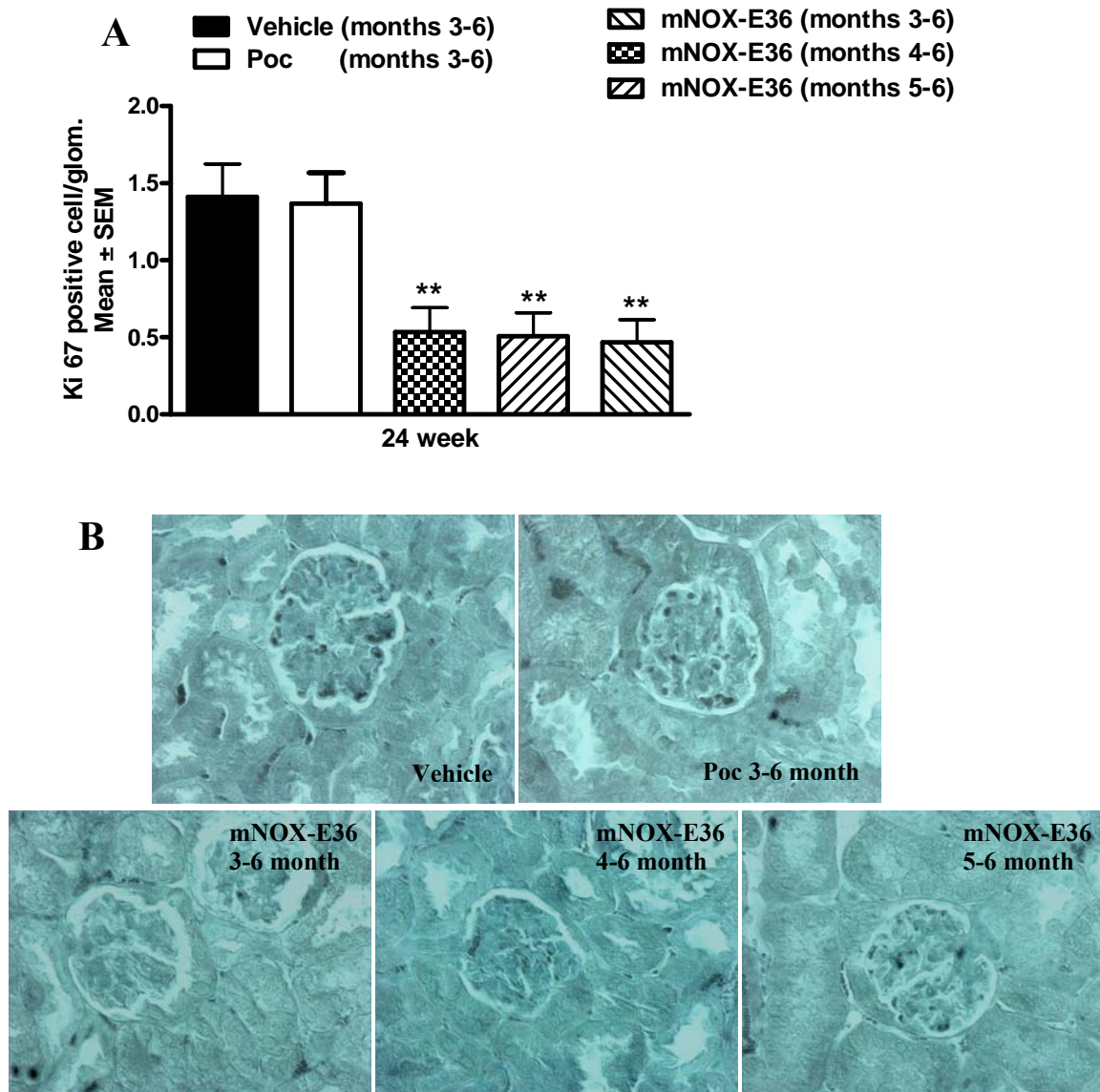


Figure 14: Ki 67 staining of kidney sections. A: Immunohistochemical evaluation of Ki-67 stained renal sections from different group of mice as indicated. Data is represented as mean \pm SEM ** $p < 0.01$ mNOX-E36 versus Poc treated 1K db/db mice. B: Representative renal sections stained for Ki-67 in uninephrectomized (1K) db/db, vehicle treated mice, Poc treated, active spiegelmer (mNOX-E36) treatment started at different stages of disease progression, month 3-6, month 4-5 or month 5-6 (magnification 400X).

4.2.1.4. Macrophage infiltration was inhibited upon CCL2 blockade

Infiltration of macrophages to renal compartment is considered to be hallmark of diabetic nephropathy progression. We tried to inhibit the recruitment of macrophages to the kidney by blocking CCL2. Mac2 being a marker for macrophages in order to assess number of infiltrated macrophages in different compartments of kidney we employed Mac2 staining of paraffin-embedded kidney

sections. The numbers of Mac2-positive cells were counted manually. We observed a significant reduction in the number of Mac2-positive cells in glomeruli as well as in the interstitium in mNOX-E36-treated group as compared to vehicle of Poc-treated group, which is consistent with our earlier report⁶¹. Interestingly, we did not observe any difference in percentage reduction of macrophage infiltration in groups of mice treated for different time lengths (Figure 15).

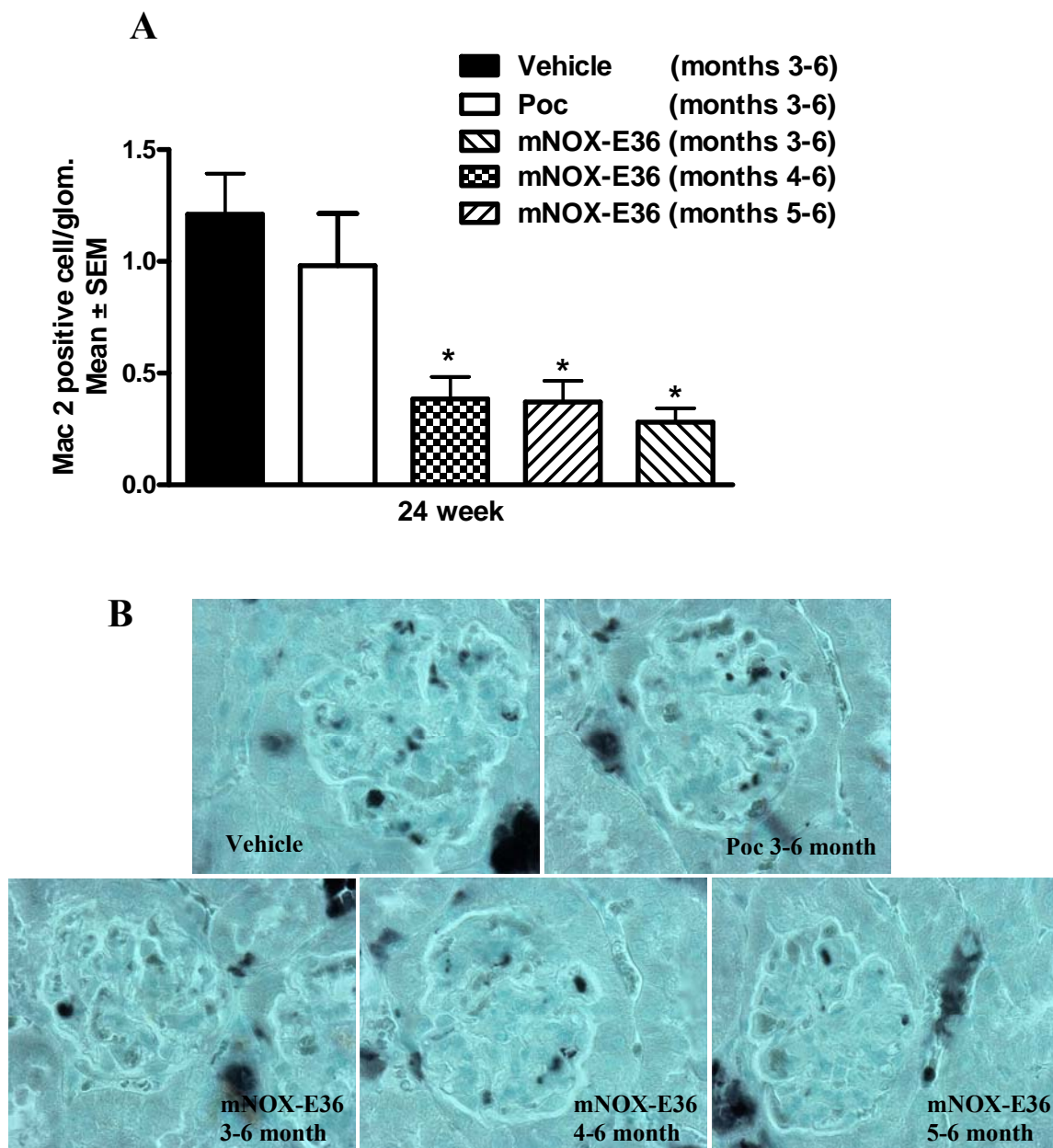


Figure 15: Renal sections from mice of all groups were stained for Mac2. Graphs shows the numbers of positive cells in 15 glomeruli in uninephrectomized (1K) db/db (A) Date is represented as mean \pm sem * $p < 0.05$ compared to vehicle treated mice. Representative images from renal sections (magnification 630X) (B).

4.2.1.5. Improvement of glomerular pathology upon CCL2 blockade

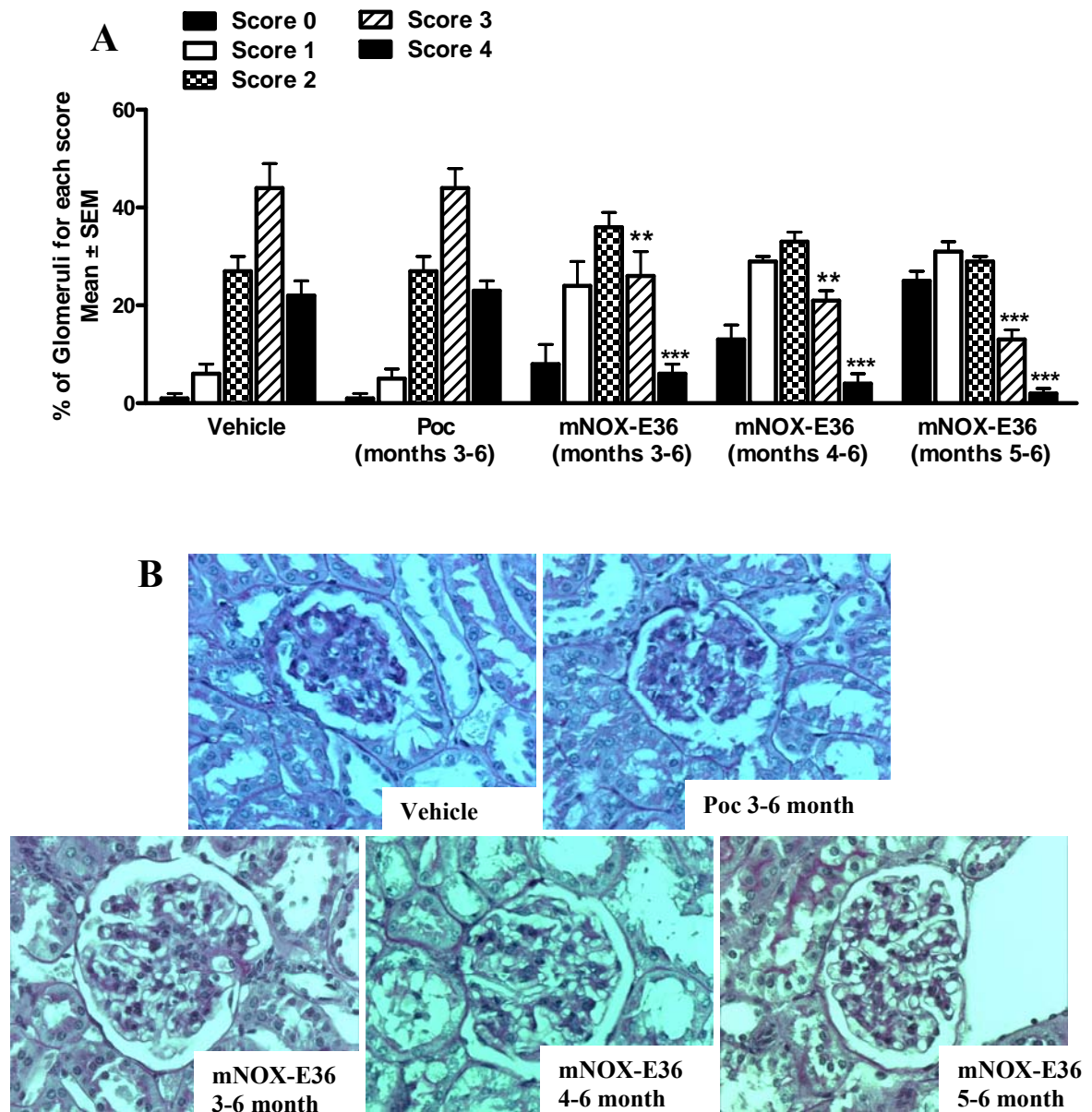


Figure 16: PAS staining of renal sections. Renal sections from mice of all groups treated for different time lengths as indicated were stained with PAS and scored for the extent of glomerulosclerosis (as described in methods). A: The graph illustrates mean percentage of each score \pm SEM from all mice in each group (n=10) *p<0.05 versus Poc treated mice. B: Representative images from different groups at the age of 24 weeks stained for PAS (magnification 400X).

Treatment with mNOX-E36 was associated with a significant ($p < 0.05$) improvement of global diabetic glomerulosclerosis in 1K db/db mice compared to vehicle or Poc-treated mice. In fact, mNOX-E36 treatment reduced glomerulosclerosis in 1K db/db mice to the extent of glomerulosclerosis present in

age-matched 2K db/db mice, which is again consistent with our earlier publication⁶¹. The improvement of glomerulosclerosis in mice treated with mNOX-E36 was found to be independent of length of the treatment periods tested (Figure 16).

4.2.1.6. Renal CCL2 mRNA expression

In order to study whether treatment with mNOX-E36 affects intrarenal inflammation in db/db mice, real-time RT-PCR (SYBR green) was performed for the proinflammatory chemokine CCL2. We found CCL2 mRNA expression was progressively up regulated in kidneys of db/db mice during the progression of renal disease. Kidneys of 6-months-old 2K db/db mice showed low CCL2 mRNA expression level while early uninephrectomy was associated with a marked increase in renal CCL2 mRNA expression in db/db mice at 6 months of age (Figure 17A).

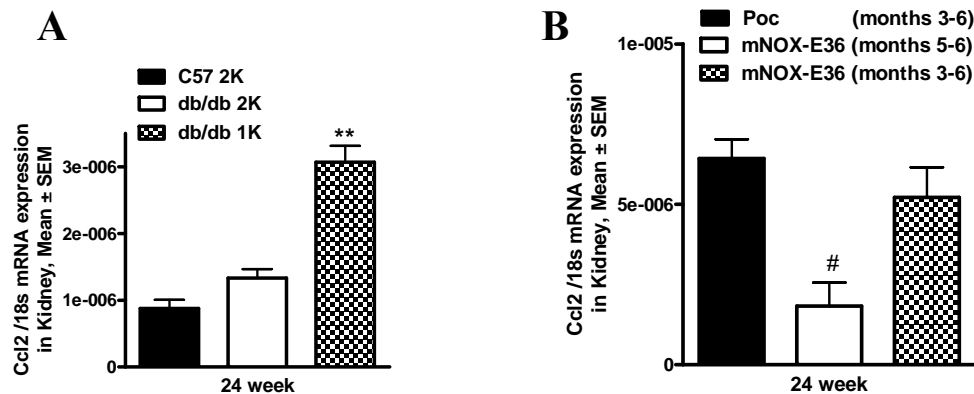


Figure 17: The mRNA expression levels of CCL2. The mRNA expression levels of CCL2 were quantified by real-time RT-PCR and corrected for respective 18s rRNA expression levels. The data represented as means \pm SEM (n = 3 pooled samples). ** p < 0.01 versus wild type 2K mice, # p < 0.05 versus Poc-treated 1K mice.

Treatment with mNOX-E36, from month 5 to month 6 of age reduced total renal expression of CCL2 mRNA significantly compared to Poc-treated group. But reduction upon mNOX-E36 treatment from month 3 to month 6 of age (the longest treated group) was not statistically significant compared to Poc-treated mice (Figure 17B).

4.2.1.7. Effect of CCL2 blockade on glomerular filtration rate

In this study, the GFR was determined by the ability of db/db mice to excrete FITC-labelled inulin. Progressing inflammation of the kidneys results in a loss of filtering ability and results in decreased glomerular filtration rate (GFR) in diabetic mice. In db/db mice, the GFR decreases with age. We observed reduced GFR in db/db mice at the age of 24 weeks as compared to age matched wild type mice. Uninephrectomy in db/db mice aggravates this process, as we observed significantly reduced GFR in uninephrectomised db/db mice compared to age-matched wild type or sham operated mice (Figure 18A). All 1K db/db mice groups treated with mNOX-E36 [3 to 6 months, 4 to 6 months and 5 to 6 months] showed a statistically significant ($p < 0.01$) improvement of GFR compared to the Poc-treated 1K db/db mice (Figure 18B).

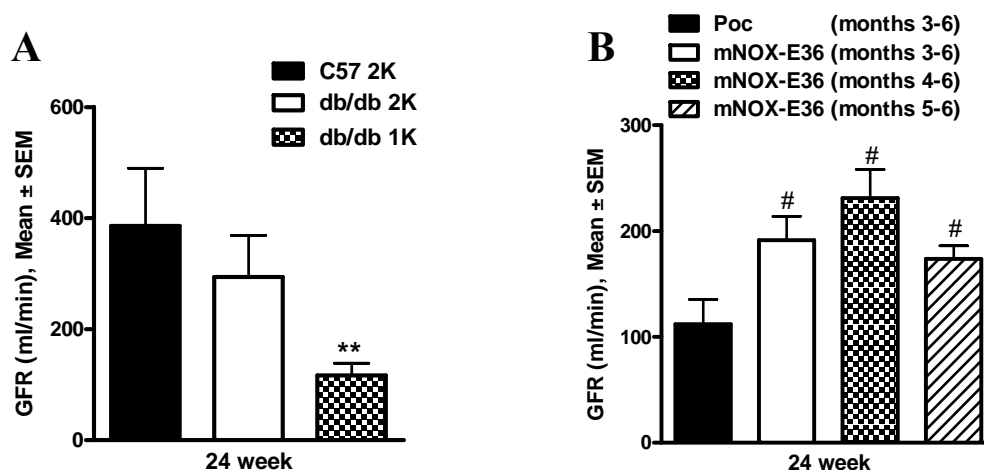


Figure 18: Glomerular filtration rate. Glomerular filtration rate (GFR) was measured by FITC-inulin clearance kinetics in 6 months old C57BL/6 wild-type mice, sham-operated db/db mice (2K) and in uninephrectomized db/db mice (1K) (A) data represent means \pm SEM from 4-7 mice, ** $p < 0.01$ versus wild type 2K mice. At the end of study glomerular filtration rate (GFR) was measured in all groups treated with Poc or mNOX-E36 for different time periods as indicated in uninephrectomized db/db mice (B) data represent means \pm SEM from 5-7 mice, # $p < 0.05$ compared to Poc-treated mice.

4.2.1.8. Effect of CCL2 blockade on body weight and blood glucose

Treatment with mNOX-E36 for different time lengths in uninephrectomized db/db mice did not show and significant changes in body weight compared to the vehicle-treated mice, which is an indirect indication of any changes in body physiology and food intake in treated mice. Some studies have shown a reduction in blood glucose

levels upon treatment with CCL2 antagonists, which was associated with increased insulin sensitivity in treated mice ¹⁷⁴ (Figure 19).

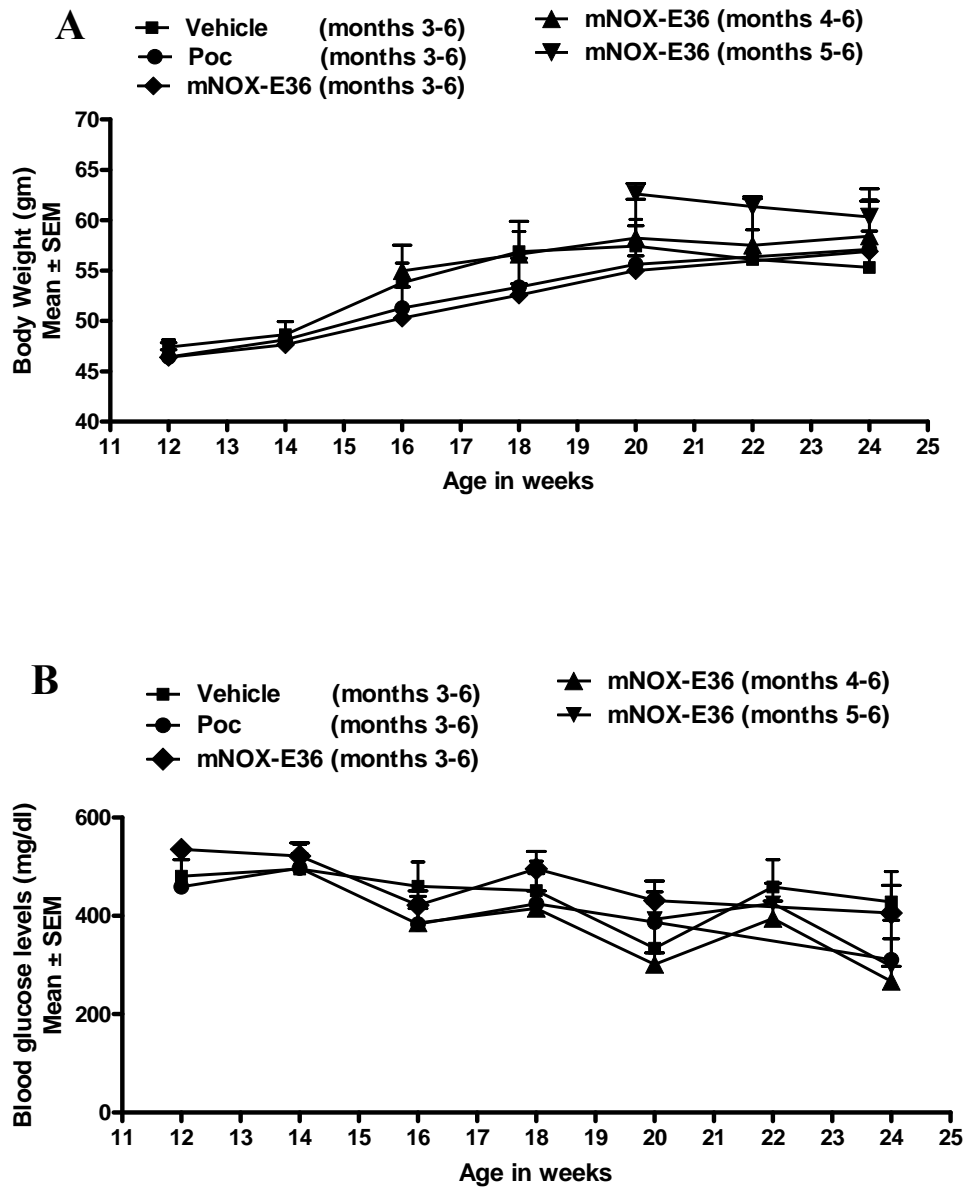


Figure 19: Body weight and blood glucose levels. All animals were monitored through out the study period for any change in body weight (A) or blood glucose levels (B). Data is represented mean ± SEM (n = 9-12).

4.2.2. Effect of CCR2 and CCR5 dual antagonists in diabetic nephropathy

4.2.2.1. Improvement of urinary albumin to creatinine ratio upon CCR2 and CCR5 antagonism

Albumin / creatinine ratio is an important clinical parameter for assessment of renal disease progression. In diabetic nephritis urinary albumin to creatinine ratio has been reported to increase with the progression of kidney inflammation. In our animal model of diabetic nephropathy we observed a trend in increase of urinary albumin to creatinine ratio over the time. To assess the effect of dual CCR2 and CCR5 blockade on the progression of disease we estimated urinary albumin to a creatinine ratio at different time points of the study.

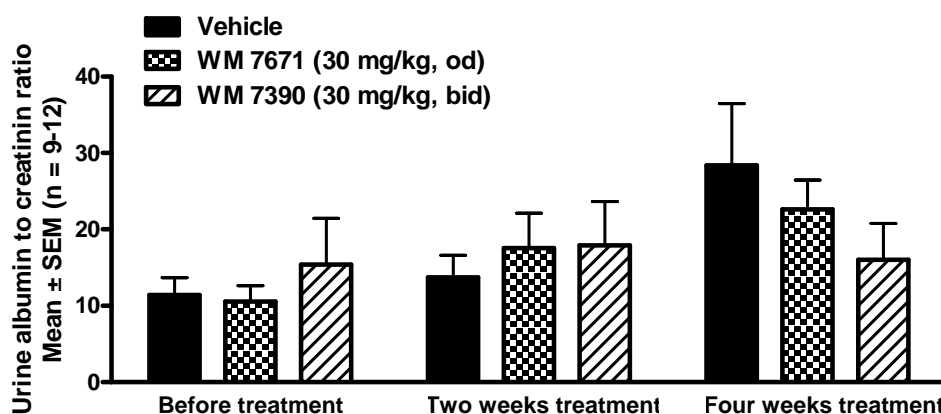


Figure 20: Urinary albumin to creatinine ratio. Proteinuria was determined after every 2 weeks of CCR2 and CCR5 dual antagonists in uninephrectomized db/db mice treated as indicated. Data represent means of urinary albumin/creatinine ratio \pm SEM (n = 9-12).

Vehicle treated mice showed progressive increase in urinary albumin to creatinine ratio over the time. Treatment with orally active CCR2 and CCR5 dual antagonist WM 7671 and WM 7390 inhibited further increase in ratio over the duration of treatment. WM 7390 was found to be more potent to inhibit further increase. Although this was not statistically significant the trend in further growth was inhibited (Figure 20).

4.2.2.2. Effect of CCR2 and CCR5 dual antagonists on the macrophages

Mac2 being a pan marker for macrophages in order to assess number of infiltrated macrophages in different compartments of kidney we employed Mac2 staining of paraffin-embedded kidney sections. Numbers of Mac2-positive cells were counted manually as described in materials and methods.

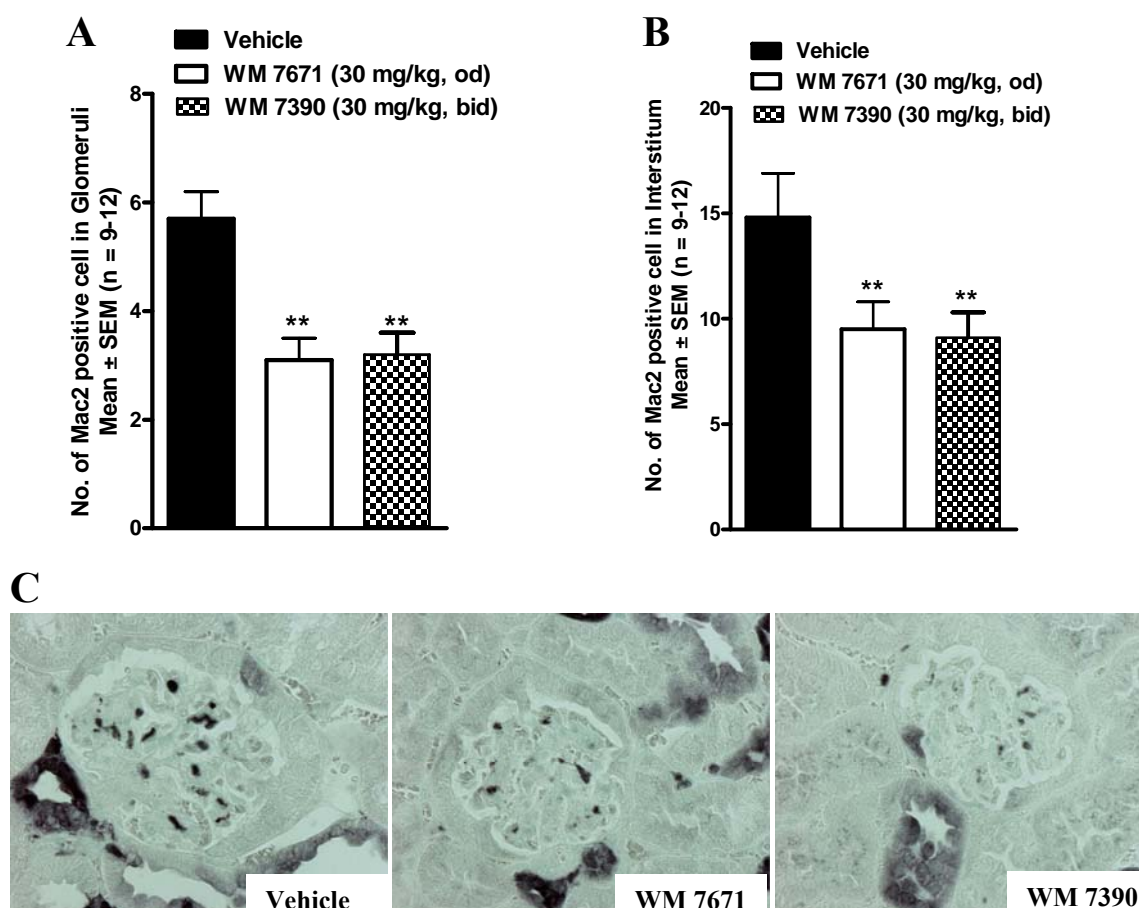


Figure 21: Mac2 staining of renal sections. Renal sections from 24 week old mice with or without uninephrectomy were stained for Mac2. A: Graphs show the numbers of Mac2 positive cells in 15 glomeruli of different groups treated with vehicle of dual antagonists as indicated. B: Graph shows the number of Mac2 positive cells in interstitium (in 10 non overlapping high power fields) animal treated with vehicle or either of the dual antagonists as indicated at 6 months of age. ** $p < 0.01$ verses vehicle treated 1K db/db mice. C: Representative renal sections from 24 weeks old 1K db/db mice stained for Mac2 (magnification 400X).

We observed a significant reduction in number of Mac2-positive cells in glomeruli as well as in the interstitium in mice groups treated with WM 7671 and WM 7390 as compared to vehicle treated group. The percentage reduction of macrophage infiltration in glomeruli and interstitium upon treated with either of the two dual

antagonists (WM 7671 or WM 7390) was not more than 50 %, which was observed on blocking CCL2 alone (Figure 21).

4.2.2.3. Effect of CCR2 and CCR5 dual antagonists on glomerulosclerosis

Glomerulosclerosis was assessed in kidney sections from all groups using PAS stain as described. Glomeruli were scored manually in each sections and percentage of glomeruli with respective scores in each group are presented. Mean percentage of glomeruli with higher scores were significantly reduced upon treatment with WM 7671 or WM 7390 in uninephrectomized db/db mice as compared to vehicle treated mice. Both antagonists significantly improved glomerulosclerosis (Figure 22).

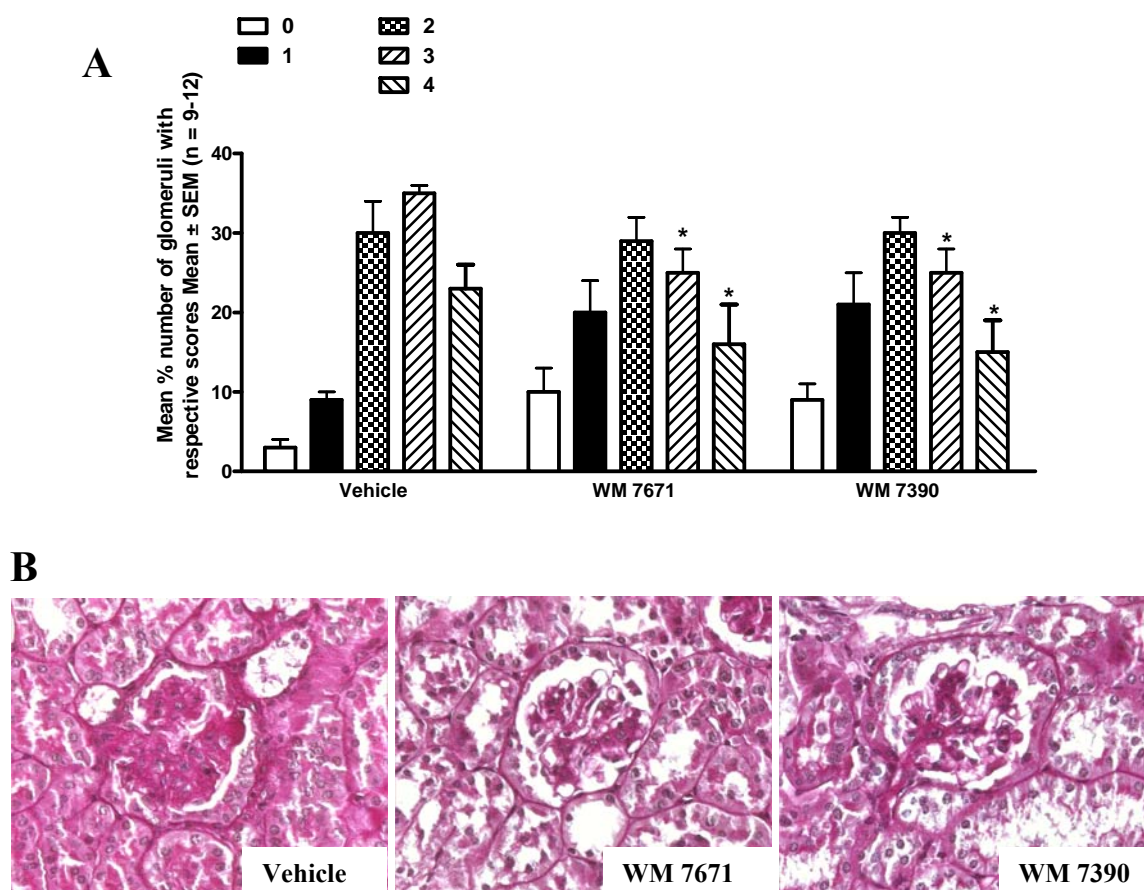


Figure 22: PAS staining for renal sections. Renal sections from mice of all groups treated with either of the dual CCR2 CCR5 dual antagonists as indicated were stained with PAS and scored for evaluation of glomerulosclerosis (as described in methods). A: The graph illustrates the mean percentage of each score \pm SEM from all mice in each group (n=10) *p<0.05 versus vehicle treated mice. B: Representative images from different groups at the age of 24 weeks stained for PAS (magnification 400X).

4.2.2.4. Effect of CCR2 and CCR5 dual antagonists on tubular pathology

Improvement of tubular damage was assessed in treated db/db mice, by morphometry analysis of silver stains from paraffin-embedded kidney sections. Morphometry was performed using a 100 grid point assessment of each section. Numbers of cells beneath each grid point were classified in one of the four classes as: tubular cell damage, tubular dilatation, interstitial volume or collagen deposition. Mean percentage of cells for each of the four classes were counted and presented as mean \pm sem. We did not observe any significant effect upon on treatment (with either of the antagonists tested) on tubular cell damage in compared to vehicle treated group (Figure 23).

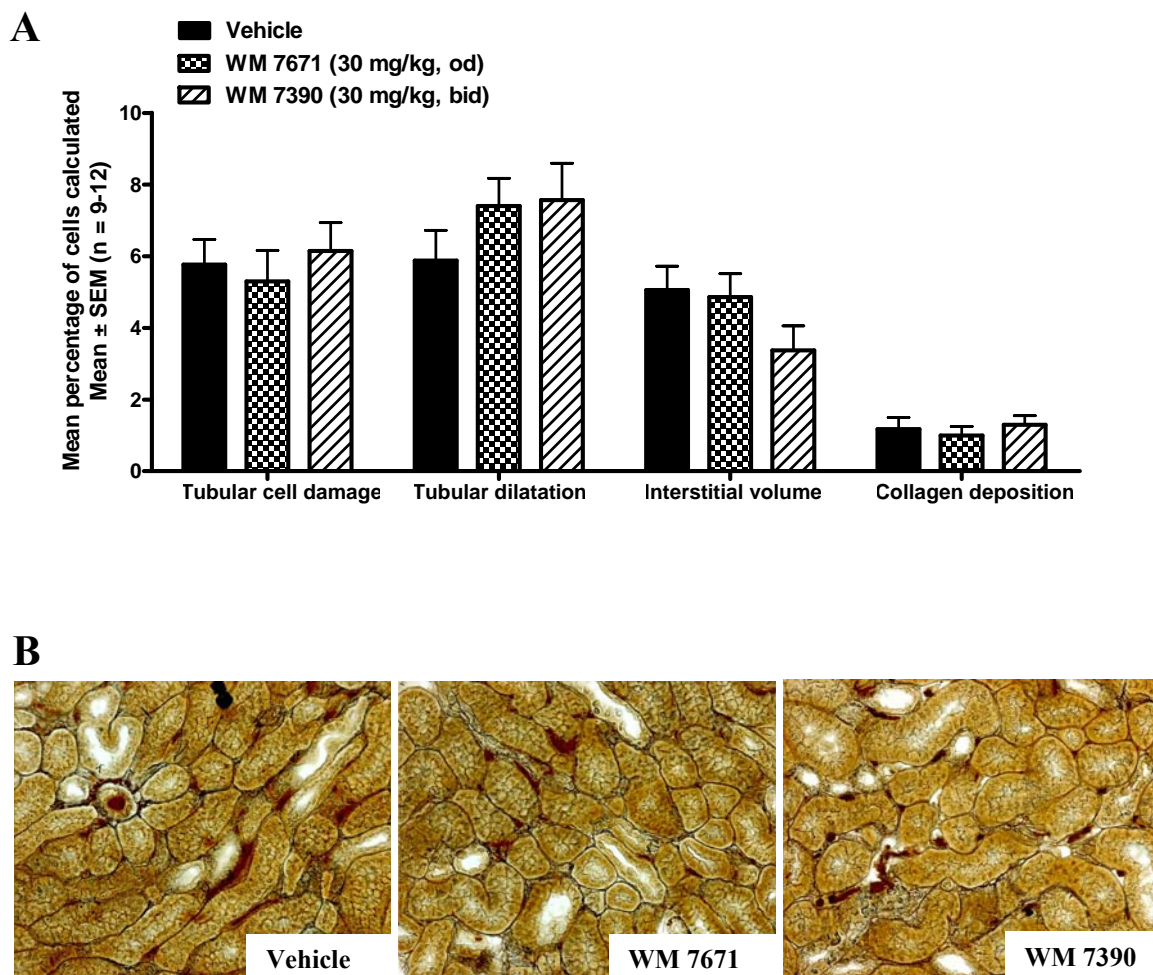


Figure 23: Silver staining of renal sections. Silver staining of all renal sections from all groups was performed. Tubular pathological changes were evaluated using morphometric analysis of these renal sections as described in methods. A: Graph represents percentage means of cells for respective pathological index as indicated in graph. B: Representative images of renal sections from different animal groups. The data represent means \pm SEM of the respective index from 9-12 mice in uninephrectomized (1K) db/db mice.

4.2.2.5. Effect on body weight and blood glucose

Treatment with CCR2 and CCR5 dual antagonists (WM 7671 and WM 7390) in uninephrectomized db/db mice for four weeks did not show any significant changes in body weight and blood glucose levels compared to the vehicle treated mice (Figure 24).

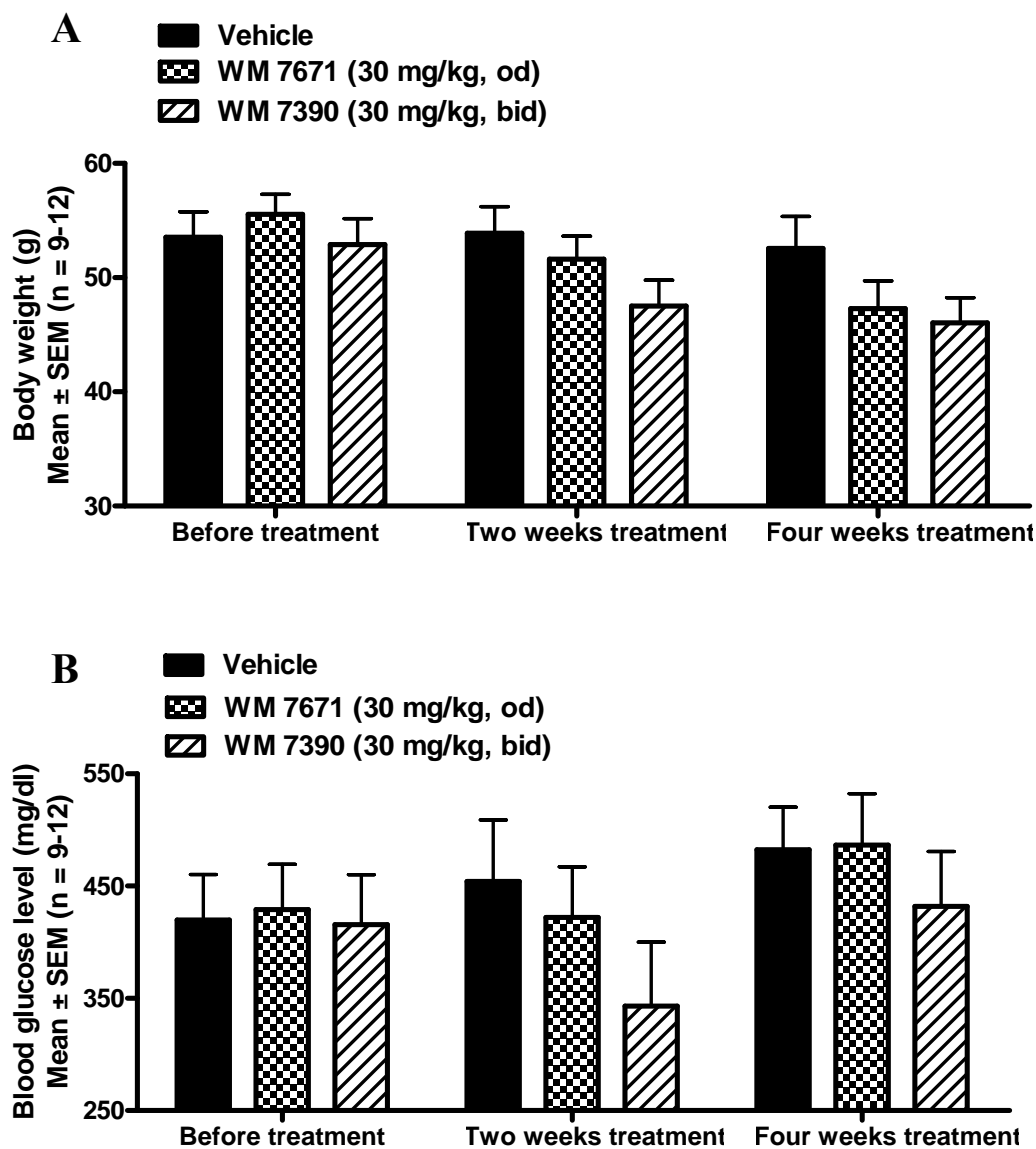


Figure 24: Body weight and blood glucose levels. All animals were monitored through out the study period for any change in body weight (A) or blood glucose levels (B). Data is represented as mean \pm SEM (n = 9-12).

4.3. Inhibition of the homeostatic chemokine CXCL12 in diabetic nephropathy

4.3.1. Plasma levels of CXCL12

To achieve CXCL12 antagonism we used a RNA-aptamer (Spiegelmer mNOX-A12), developed by NOXXON Pharma (Berlin). This RNA-aptamer binds to the active site of CXCL12 and makes its biologically non-functional CXCL12 bound to Spiegelmer remains in circulation. To assess the efficiency of the employed Spiegelmer for its biological activity we estimated CXCL12 levels in serum from all groups using Elisa. Serum levels of CXCL12 were significantly ($p < 0.05$) increased in mice treated with mNOX-A12 compared to vehicle of revmNOX-A12 treated mice at 6 months of age, indicating that CXCL12 specific Spiegelmers retain CXCL12 in the intravascular compartment (Figure 25). This finding is consistent with our previous observations with other Spiegelmers and indicates that the CXCL12 antagonist retains CXCL12 in the circulation⁶¹.

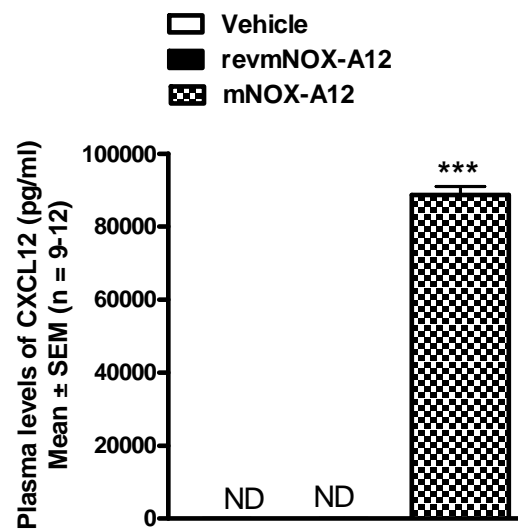


Figure 25: Serum CXCL12 levels. Serum CXCL12 levels were determined by Elisa in 6 months uninephrectomized (1K) db/db mice upon treatment with active spiegelmer of control spiegelmer (n=10-12 in each group). Data are means \pm SEM, *** $p < 0.001$ versus revmNOX-A12. ND; not detected.

4.3.2. CXCL12 blockade prevents proteinuria in db/db mice

In diabetic nephropathy glomerular pathology is usually associated with increasing levels of proteinuria indicative of progressive structural damage at the glomerular filtration barrier ⁶. Thus, the beneficial effect of CXCL12 blockade on glomerular structure should be associated with less proteinuria. To evaluate any effect of CXCL12 on improvement of progression of diabetic nephropathy albumin/creatinine ratio was determined at different time points of the study. mNOX-A12 but not the revmNOX-A12 Spiegelmer or vehicle prevented the progressive increase of urinary albumin/creatinine ratio in db/db mice (Figure 26). Thus, CXCL12 inhibition improves glomerular pathology and proteinuria in db/db mice.

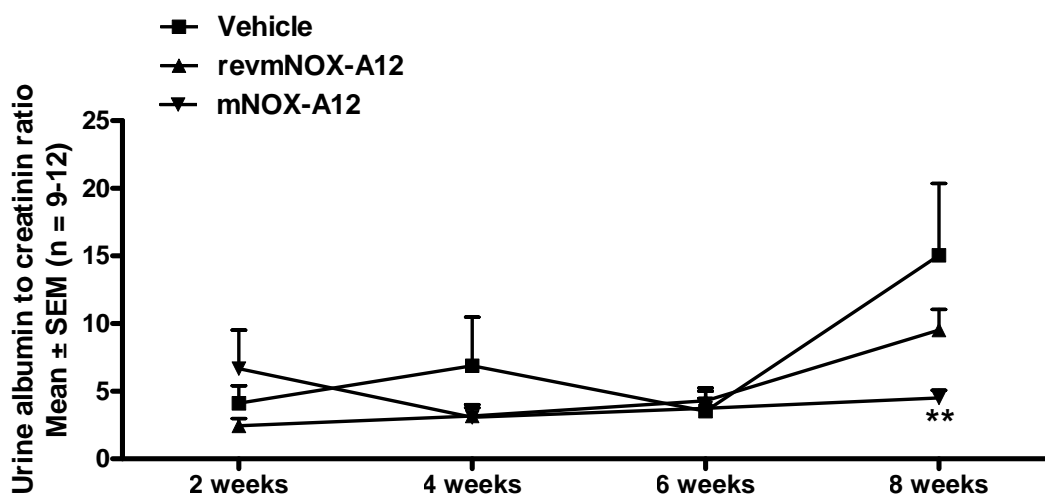


Figure 26: Urinary albumin to creatinine ratio. Proteinuria was determined after every 2 weeks of CXCL12 antagonist administration in uninephrectomized db/db mice treated as indicated. Data represent means of urinary albumin/creatinine ratio \pm SEM, * $p < 0.01$ versus vehicle treated 1K db/db mice (n = 9-12).

4.3.3. Effect of CXCL12 blockade on glomerulosclerosis in db/db mice

To test if CXCL12 blockade affects glomerular pathology in db/db mice, we initiated subcutaneous injections with anti-CXCL12 or control Spiegelmer (50 mg/kg, every alternate day) at an age of 4 months in uninephrectomized db/db mice. Injections were continued for 8 weeks. Renal histomorphology in 6 months old db/db mice showed moderate glomerulosclerosis as compared to age-matched wild-

type mice which was aggravated to diffuse glomerulosclerosis by early uninephrectomy of db/db mice (Figure 27). CXCL12 inhibition reduced the extent of glomerulosclerosis in uninephrectomized db/db mice to the level of age-matched sham-operated db/db mice (Figure 27). The control Spiegelmer had no effect. Thus, CXCL12 blockade started at 4 months of age reduces diffuse glomerulosclerosis in uninephrectomized db/db mice at 6 months of age.

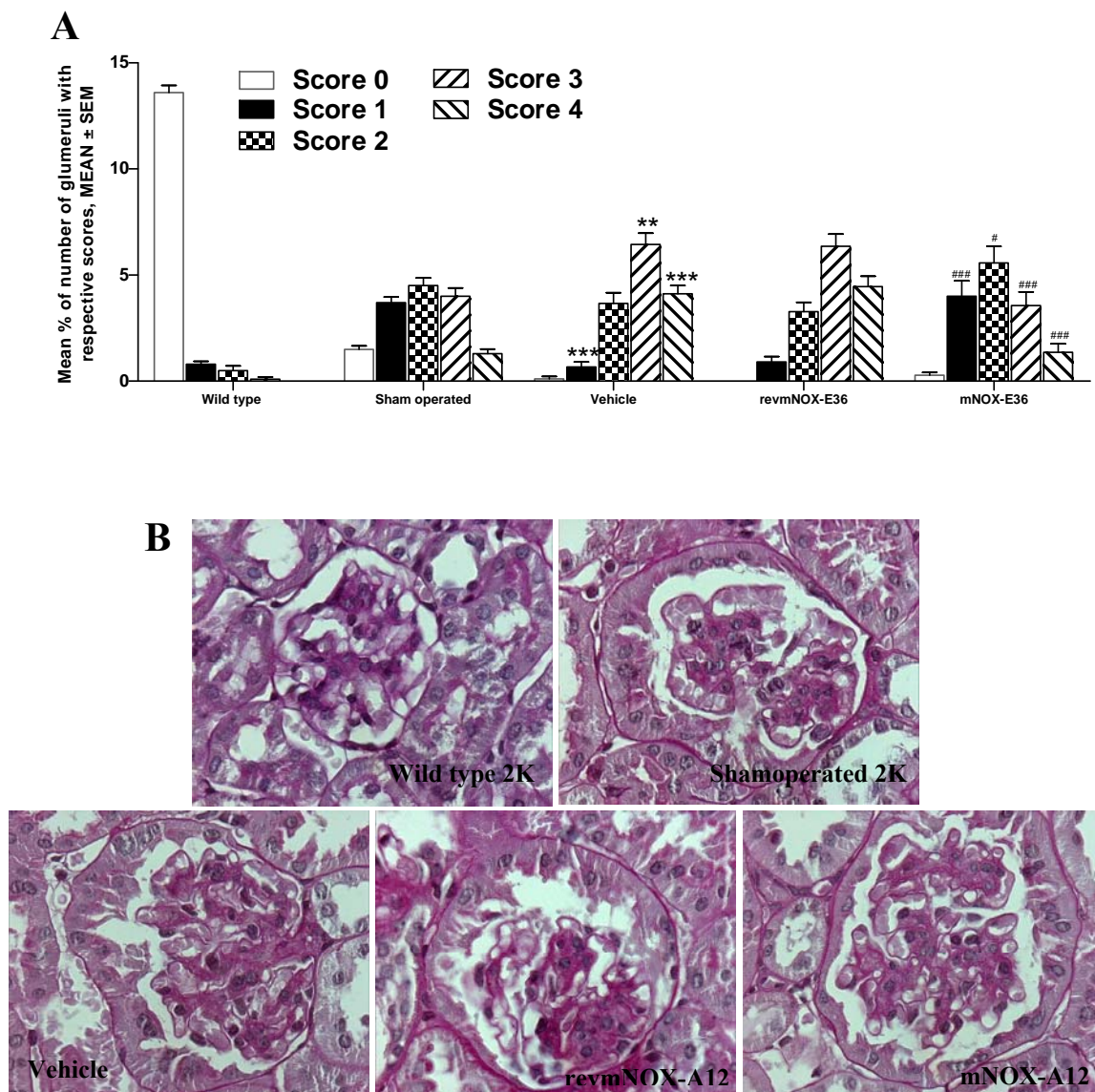


Figure 27: PAS staining for renal sections. Renal sections from mice of all groups treated with Cxcl12 antagonist as indicated were stained with PAS and scored for evaluation of glomerulosclerosis (as described in methods). A: The graph illustrates the mean percentage of each score \pm SEM from all mice in each group (n=10) ** p < 0.01, *** p < 0.01 compared to sham operated mice, # p < 0.05, ### p < 0.001 versus vehicle treated mice. B: Representative images from different groups at the age of 24 weeks stained for PAS (magnification 630X).

4.3.4. CXCL12 blockade and tubulointerstitial pathology in db/db mice

Advanced diabetic nephropathy is also associated with progressive tubulointerstitial injury. We quantified tubular dilatation, tubular cell damage, and interstitial volume as markers of tubulointerstitial damage by blinded morphometry and the numbers of Ki-67 proliferative tubular cells and Meca32 positive peritubular capillary cross sections as markers of interstitial vascular pathology in db/db mice at 6 months of age. 1K db/db mice revealed significant changes in the numbers of Ki-67 proliferative tubular cells and Meca32 positive peritubular capillary cross sections but not of tubular dilatation, tubular cell damage, and interstitial volume (Figures 28 and 29). As such the histomorphological abnormalities of the tubulointerstitial compartment were rather mild in 1K db/db mice. However, CXCL12 blockade significantly increased the numbers of peritubular cross sections and improved the tubular cell damage score but not up to the level of 2K wild-type mice (Figures 28 and 30). Control Spiegelmer was ineffective in this regard. CXCL12 blockade, however, did not significantly affect any of the other histomorphological parameters of tubulointerstitial damage (Figure 28). Thus, CXCL12 blockade significantly improves tubular cell damage and the peritubular vasculature density in db/db mice.

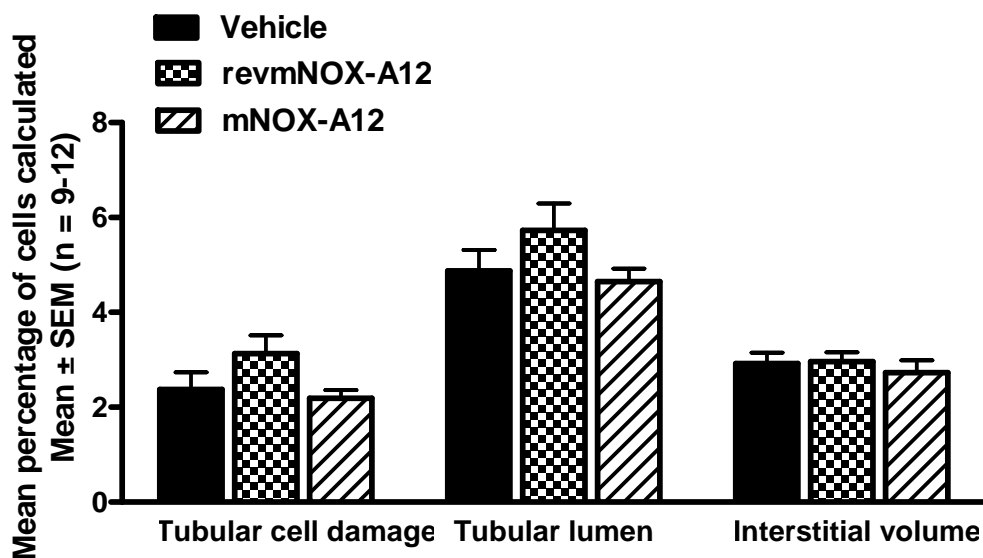


Figure 28: Silver staining for renal sections. Silver staining of all renal sections from all groups treated with either vehicle or Cxcl12 antagonist was performed. Tubular pathological changes were evaluated using morphometric analysis of these renal sections as described in methods. A: Graph represents percentage means of cells for respective pathological index as indicated in graph. The data represent means \pm SEM of the respective index from 9-12 mice in group.

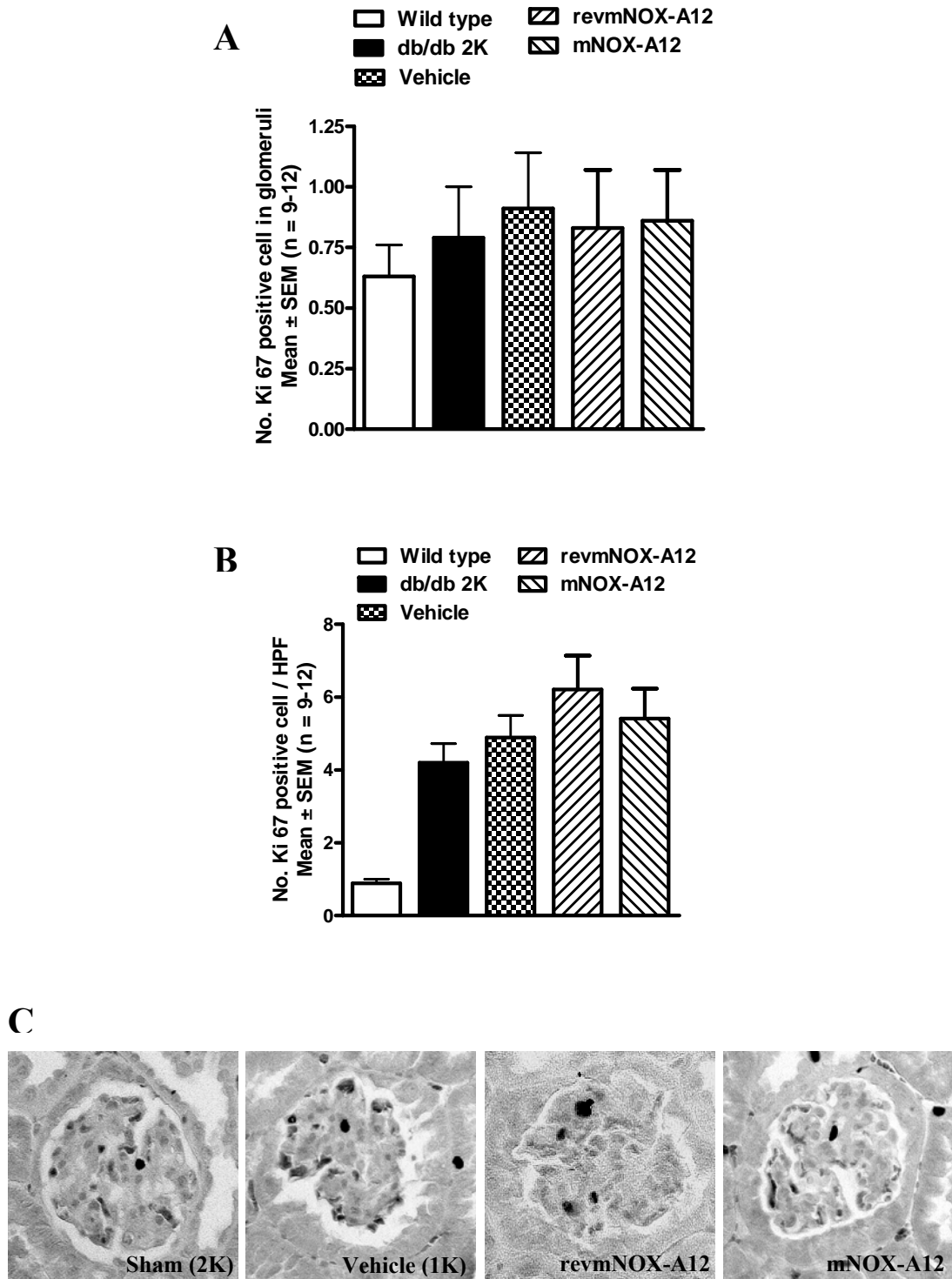


Figure 29: Ki 67 staining of renal sections. Ki 67 staining of all renal sections from all groups treated with either vehicle or Cxcl12 antagonist was performed. Proliferating glomerular and interstitial cells were counted manually by in renal sections as described in methods. A: Graph represents mean number of Ki67 positive cells in glomeruli (A) and interstitium (B) as indicated in graph. The data represent means \pm SEM of the respective index from 9-12 mice in group. C: Representative images of renal sections from different animal groups (magnification 400X).

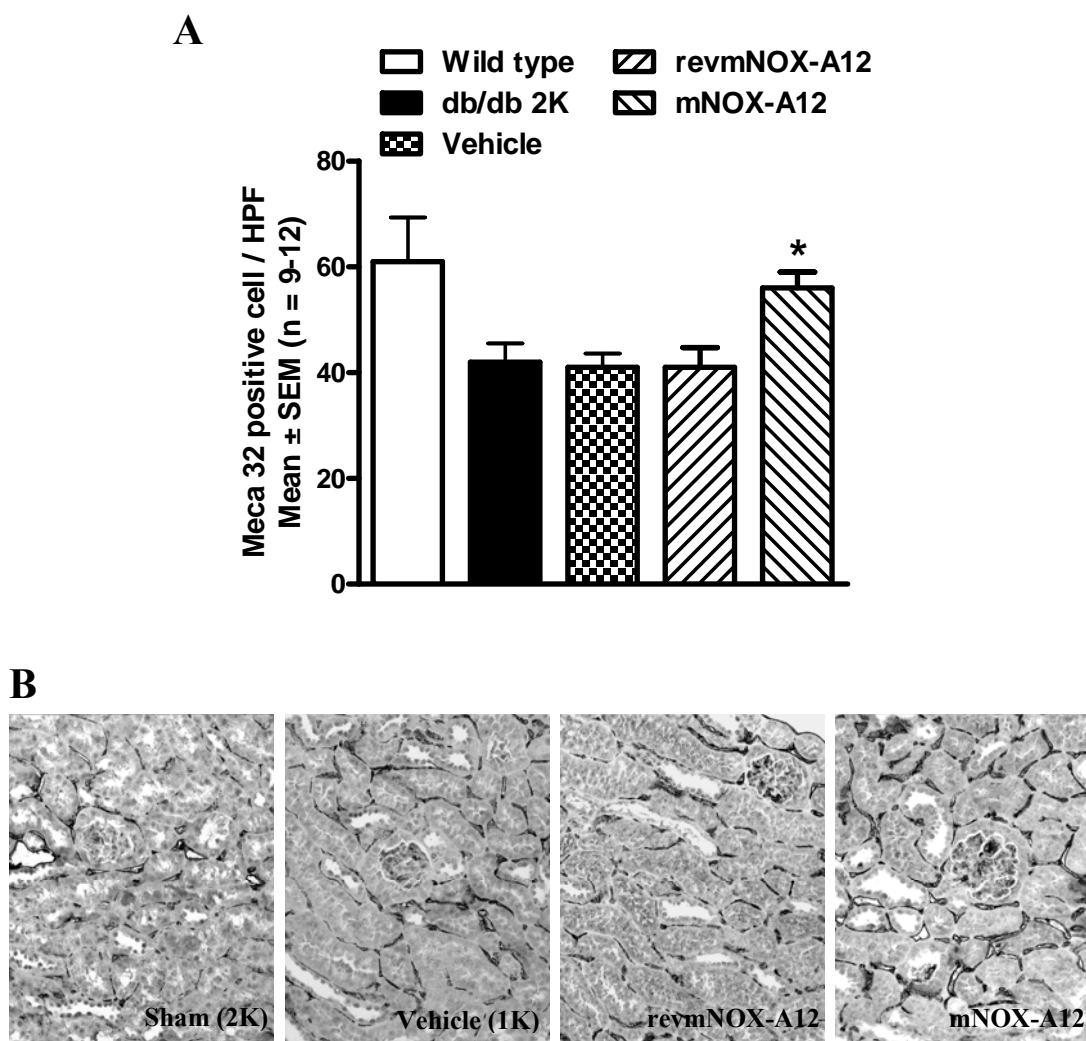


Figure 30: Meca32 staining of renal sections. Meca32 staining of all renal sections from all groups treated with either vehicle or CXCL12 antagonist was performed. Number of Meca32 positive capillaries in each renal section was counted as described in methods. A: Graph represents percentage means of Meca 32 positive capillaries in respective groups as indicated in graph. The data represent means \pm SEM of the respective index from 9-12 mice in group. B: Representative images of renal sections from different animal groups (Magnification 400X).

4.3.5. Effect of CXCL12 blockade on infiltrating macrophages in 1K db/db mice

Chemokine-mediated glomerular pathology in db/db mice can be mediated by macrophage recruitment^{61, 96}. To evaluate whether beneficial effect on renal physiology and histomorphological changes in kidney upon CXCL12 inhibition was associated with macrophage infiltration? we therefore evaluated the number of glomerular macrophages by immunostaining for Mac2. Mac2-positive cells were virtually absent in glomeruli of 2K wild-type mice but were increased in vehicle-treated 1K db/db mice (Figure 31). Neither revmNOX-A12 nor mNOX-A12

Spiegelmer injections affected the number of Mac2 positive cells in glomeruli of 1K db/db mice (Figure 31). Thus, CXCL12 blockade prevents glomerular pathology and dysfunction in db/db mice independent of infiltrating glomerular macrophages.

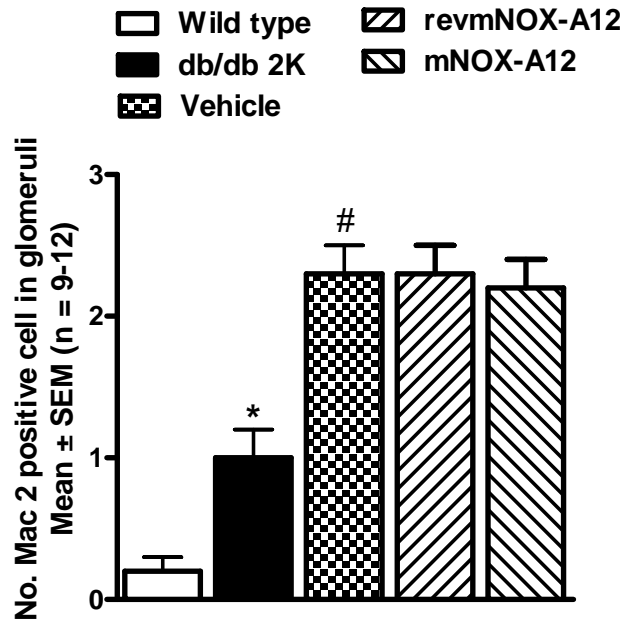


Figure 31: Mac2 staining for renal sections. Renal sections from 24 week old mice with or without uninephrectomy were stained for Mac2. Graphs show the number of Mac2 positive cells in 15 glomeruli of different groups treated with vehicle or CXCL12 antagonist as indicated at 6 months of age. * $p < 0.05$ compared to wild type 2K mice, # $p < 0.05$ compared to sham operated mice.

4.3.6. Effect of CXCL12 blockade on stem cell mobilization

CXCL12 has been reported to be involved in homing and migration of stem cells to different compartments in the body. Its role in migration of CXCR4 positive stem cells after acute kidney injury is well documented. We tried to evaluate if the beneficial effect observed upon treatment with CXCL12 antagonist are associated with stem cell mobilisation and tissue repair. We performed FACS analysis for cKit and Sca double positive cells in bone marrow, peripheral blood and kidneys isolated from all groups at the end of treatment. Similarly numbers of CXCR4 positive cells were analyzed.

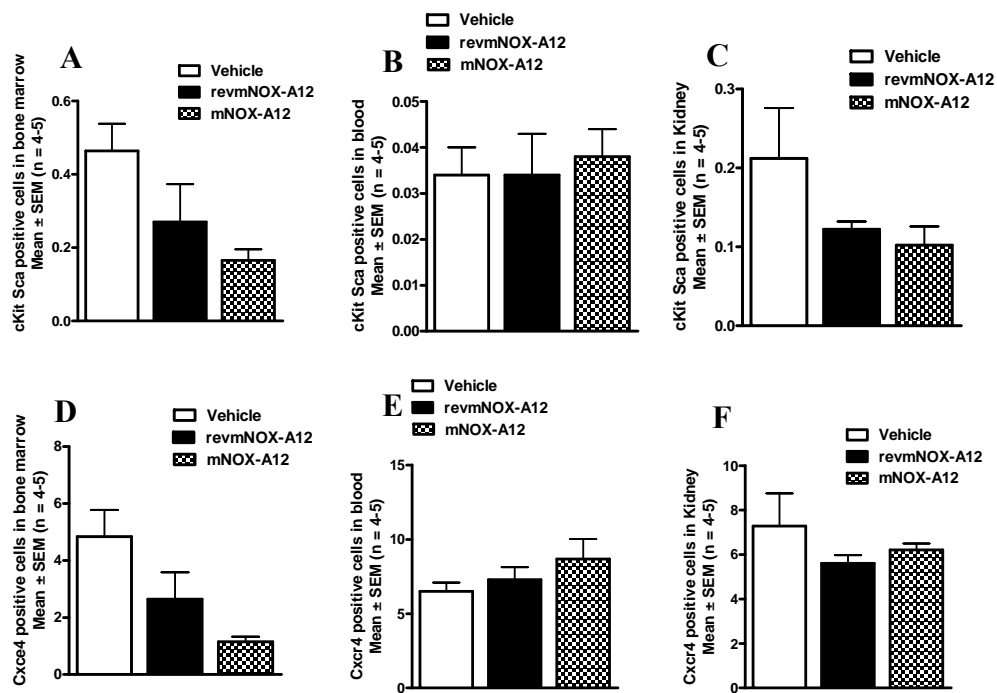


Figure 32: FACS analysis of bone marrow, blood and kidney cell preparations. FACS analysis for cKit and Sca double positive stem cells and CXCR4 positive cells in bone marrow, circulating blood and kidney performed 3hr post last administration of CXCL12 antagonist. For each sample 50,000 events were counted. Graphs represent the mean percentage of events for each group (A) cKit and Sca double positive cells in bone marrow, (B) cKit and Sca double positive cells in circulating blood, (C) cKit and Sca double positive cells in kidney, (D) CXCR4 positive cells in bone marrow, (E) CXCR4 positive cells in circulating blood and (F) Cxcr4 positive cells in kidney. Data represented as mean \pm SEM (n = 5-7), * $p < 0.05$ compared to vehicle treated group.

We found ckit and sca double positive cells in bone marrow were significantly less in mice treated with CXCL12 antagonist compared to vehicle treated, at the same time there was not much significant difference in the number of ckit and Sca double positive cells in peripheral blood and kidney in all groups. Similarly, the number of CXCR4 positive cells in bone marrow was significantly lower in mice treated with CXCL12 antagonists compared to vehicle treated group. At the same time we did not observe any change in the number of CXCR4 positive cells in kidney samples. Thus, the observed beneficial effects of CXCL12 antagonist are independent of stem cell recruitment into kidney (Figure 32).

4.3.7. Effect of CXCL12 blockade on macrophage polarization in kidney

Beneficial effects observed upon CXCL12 antagonist administration in db/db mice were independent of number of infiltrating macrophages in kidney. Macrophage activation and polarization is now being extensively studied. Macrophage polarization as classically activated (class I) macrophages which mainly contributes to inflammatory processes on the other hand alternatively activated macrophages (class II) are mainly responsible for tissue repair. Thus, to evaluate the effects of CXCL12 antagonism modulation on macrophage polarisation we performed RT-PCR from RNA isolated from whole kidney, for different macrophage phase markers including Arg1, MRC1 and MRC2, YM1 and iNos. Our results show over-expression of class I markers like iNOS at the same time markers for alternative (Class II) activation were also up-regulated upon treatment. Thus, CXCL12 blockade induced mixed population of renal macrophages characterised by class I as well as class II markers (Figure 33).

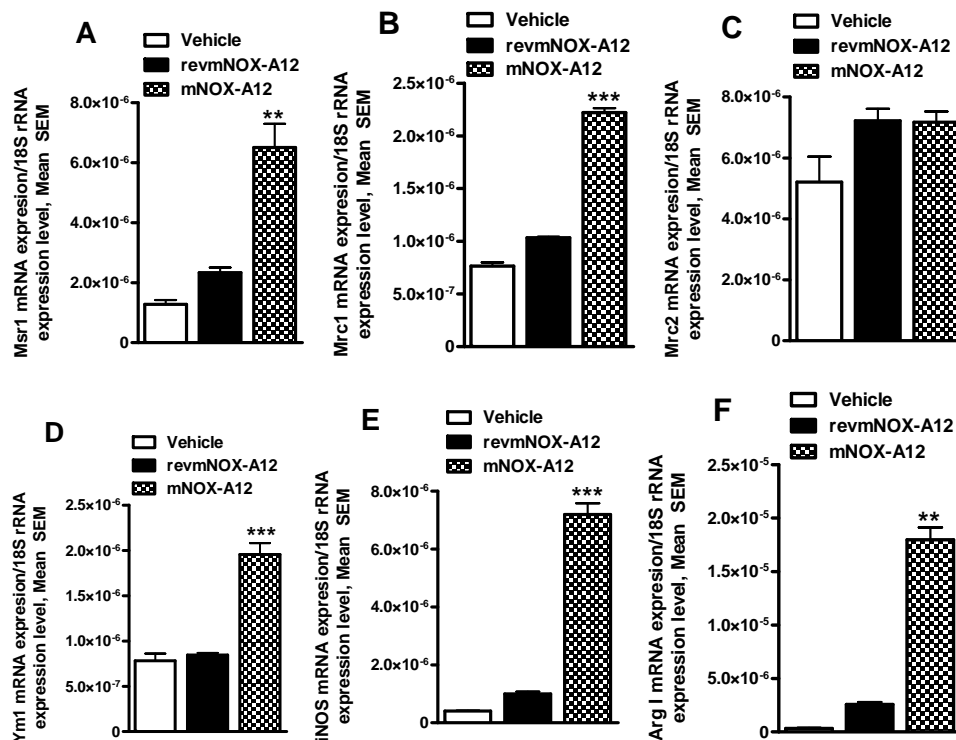


Figure 33: Macrophage marker expression profile in kidney. mRNA expression for different classically activated macrophage (Class I) and alternatively activated macrophage (Class II) markers, Msr1(A); Mrc1 (B); Mrc2 (C); Ym1 (D); iNOS (E) and Arg1 (F) were evaluated in whole renal RNA preparations from all mice groups treated either with vehicle or CXCL12 antagonist. Expression level for each gene was normalized with 18S rRNA expression level of the respective sample. Data represented as mean \pm SEM (n = 3-5), ** p<0.01, ***p<0.001 compared to vehicle treated group.

4.3.8. CXCL12 is mainly produced by podocytes in db/db mice

We questioned whether CXCL12 is expressed in kidneys of db/db mice and first analyzed CXCL12 mRNA expression using RT-PCR in db/db mice kidney. CXCL12 mRNA was detectable in renal cortex preparations from 6 week old db/db mice (Figure 34). The renal CXCL12 mRNA levels did not significantly differ from those of sham-operated or uninephrectomized 6 months old db/db mice (Figure 34). CXCL12 immunostaining was positive in collecting ducts at the renal papilla, the uroepithelium along the renal pelvis, and in endothelial and smooth muscle cells of intrarenal vessels (Figure 35). In the renal cortex CXCL12 staining was also detected in glomeruli of 6 week old db/db mice. At higher magnification the glomerular staining originated from the cells on the outside of the glomerular capillaries, i.e. the visceral epithelial cells or podocytes (Figure 35). Co-staining with fluoro-chrome-labelled antibodies against CXCL12 and WT1 confirmed podocyte-specific CXCL12 expression in glomeruli and excluded that CXCL12 expression in mesangial cells (Figure 36). Six months old uninephrectomized db/db mice with type2 diabetes revealed the identical CXCL12 staining pattern and staining intensity as compared to 6 week old 2K db/db mice (Figure 35). Thus, podocytes are the major source of CXCL12 expression in glomeruli of db/db mice.

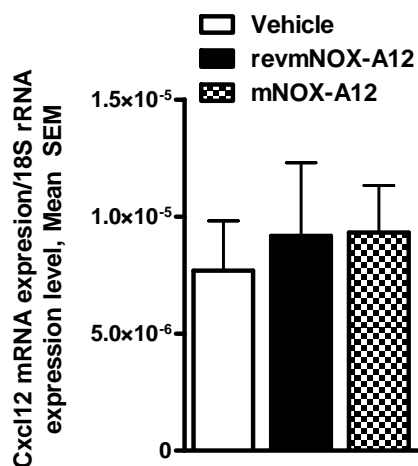


Figure 34: The mRNA expression levels of CXCL12. The mRNA expression levels of CXCL12 were quantified by real-time RT-PCR and corrected for respective 18s rRNA levels. The data shown are means \pm SEM (n = 3-5).

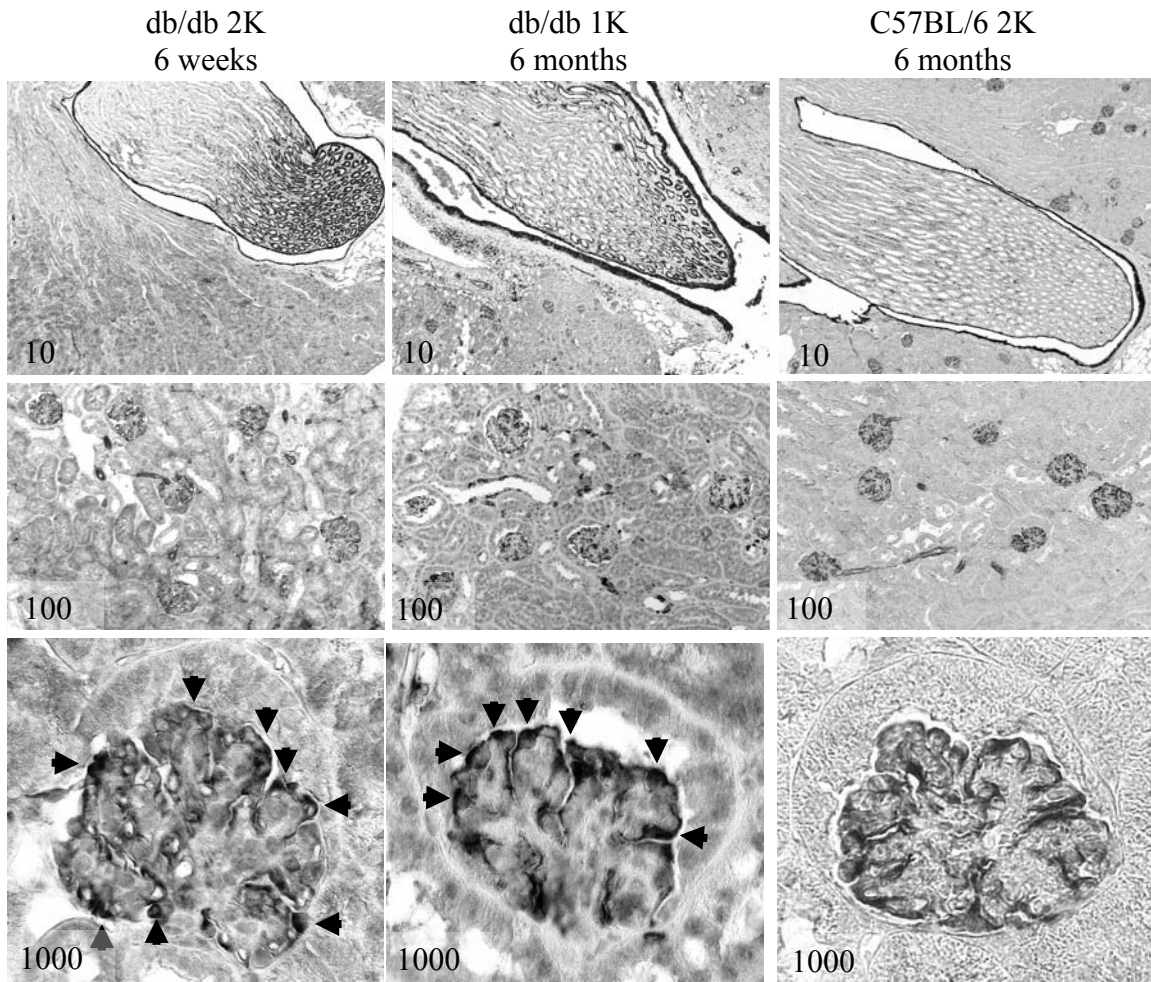


Figure 35: CXCL12 stains of renal sections at different age. Paraffin-embedded renal sections from kidneys of 6 week old 2K db/db mice and 6 months old 1K db/db mice were stained for CXCL12 and shown at three different magnifications. 10x/upper panel: renal medulla, papilla, and pelvis. 100x/middle panel: renal cortex, 1000x/lower panel: single glomeruli. Arrows indicate positive staining signals in visceral glomerular epithelia, i.e. podocytes. The images are representative for 8-12 mice in each group.

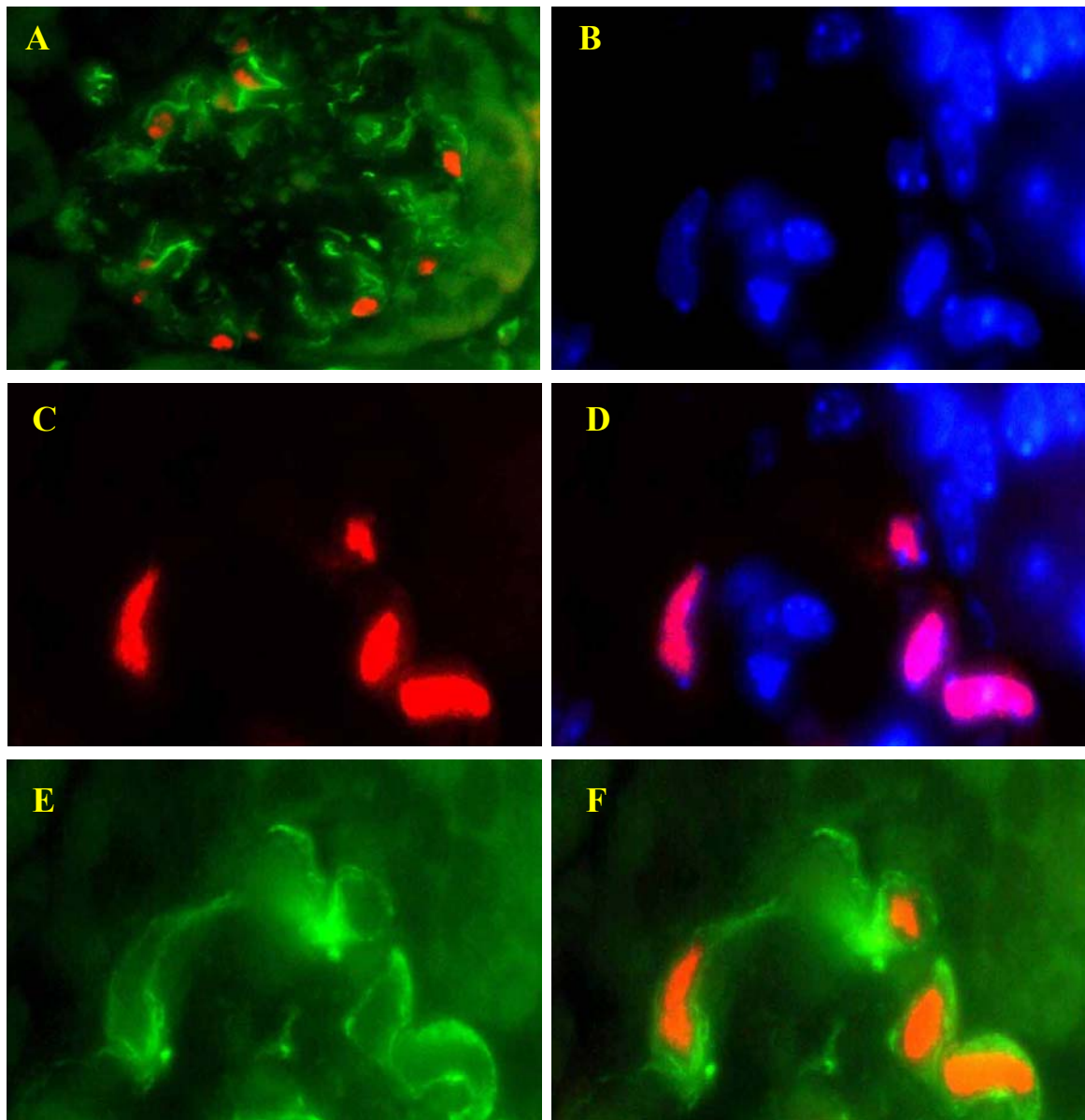


Figure 36: Fluorescence microscopy on renal sections. Fluorescence microscopy on renal sections of 6 months old db/db mice using a PE-labeled antibody for WT1 identified podocytes by red nuclear staining and using a FITC-labeled anti-CXCL12 antibody identified CXCL12 expression by green cytoplasmic staining (A, x400). At higher magnification (x1000) DAPI stains nuclei in blue (B) of which only few represent WT1 positive podocytes (C and D). Co-staining for CXCL12 (E) demonstrates that CXCL12 is present in the cytoplasm of podocytes with WT1 positive nuclei (F).

4.3.9. Effect of CXCL12 blockade on podocytes in glomeruli

Implication of podocyte loss in development of diabetic nephropathy is well established and is correlated to the proteinuria. We quantified WT1 positive cells in glomeruli of each group. Number of WT1 (specific protein markers for podocytes) positive cells were significantly increased in group of mice treated with mNOX-A12 compared to vehicle of control spiegelmer treated animals (Figure 37).

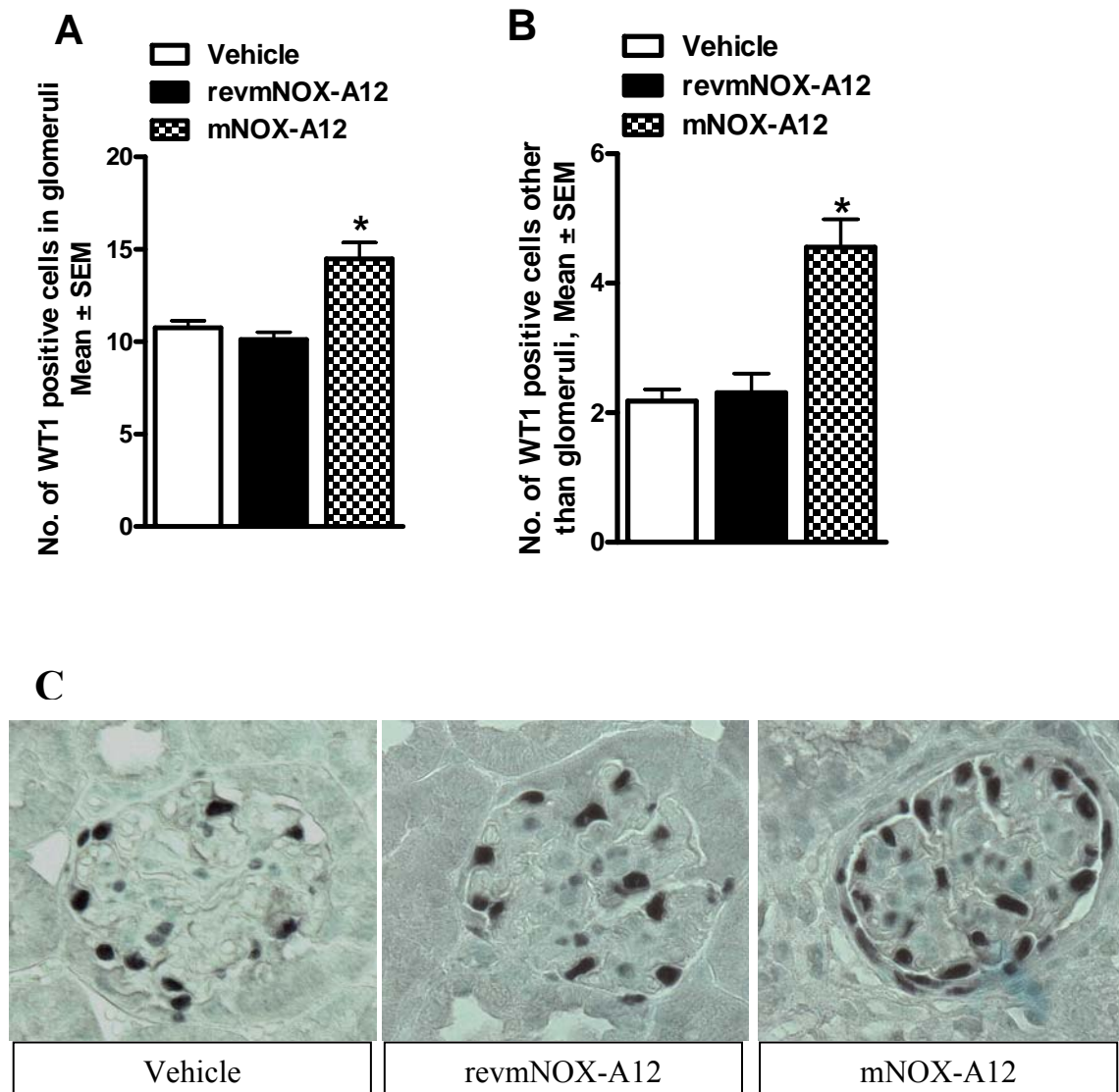


Figure 37: WT1 positive cells on glomerular tuft and in periphery. A: Graph showing mean number of WT1 positive cells on glomerular tuft. B: Graph showing mean number of WT1 positive cells in kidney present on cells other than glomerular tuft including parietal epithelial cells (PEC) and on vascular pole (VP). C: representative images of kidney sections stained for WT1. Images are representative of 8-10 mice from each group (400x). * $p < 0.05$ compared to vehicle treated mice.

4.3.10. Effect of CXCL12 blockade on body weight and blood glucose

Treatment with CXCL12 antagonists (mNOX-A12) in uninephrectomized db/db mice for eight weeks did not show any significant changes in body weight and blood glucose levels compared to vehicle or revmNOX-A12 treated mice (Figure 38).

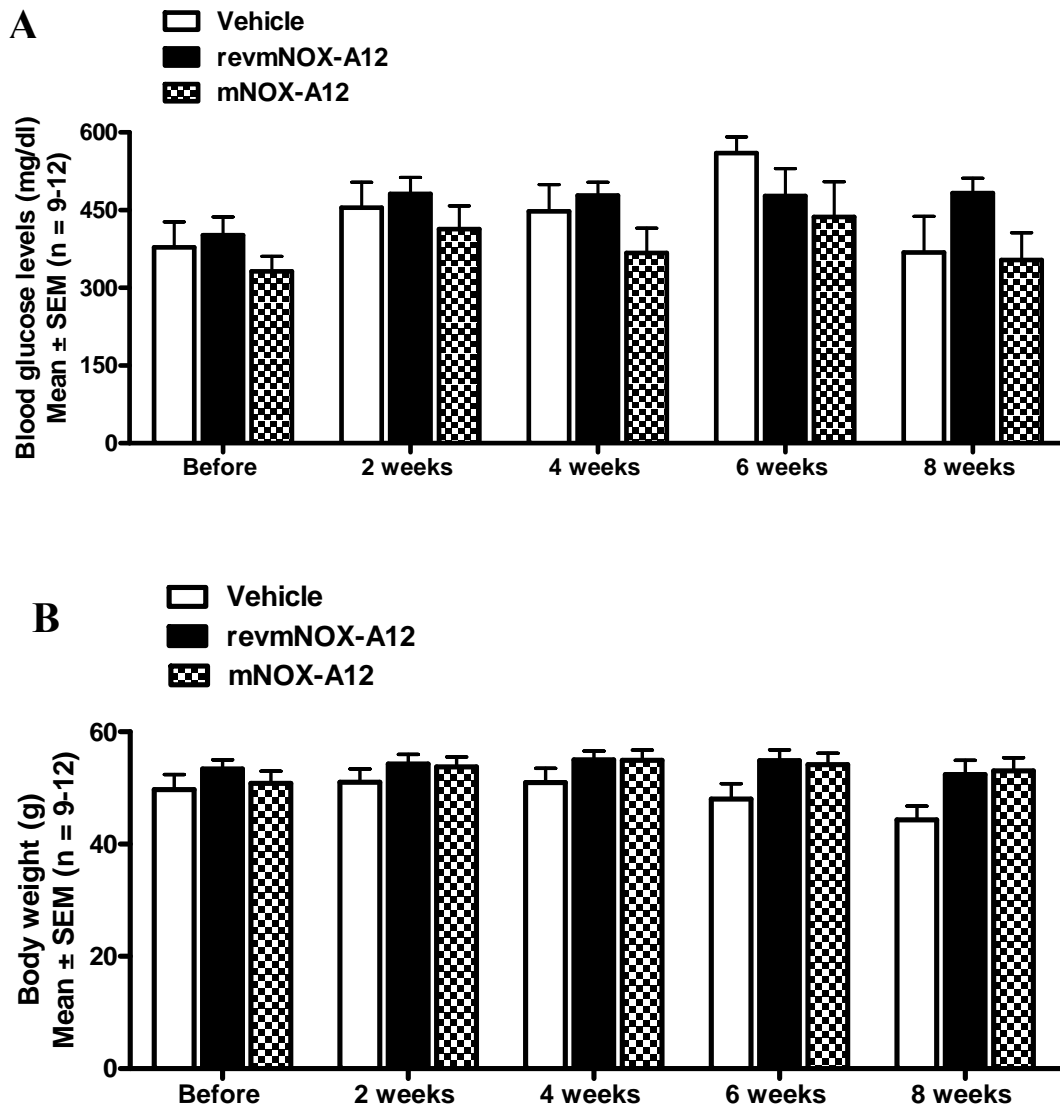


Figure 38: Body weight and blood glucose levels. All animals were monitored through out the study period for any change in body weight (A) or blood glucose levels (B). Data is represented as mean \pm SEM (n = 9-12).

5. Discussion

Several experimental animal models have been proposed for diabetic nephropathy, but none of these animal models represent chronicity which can mimic the advanced stage of human DN. In the current study we used genetically-induced type 2 diabetic (db/db) mice as mouse model of diabetic nephropathy. We performed uninephrectomy in these mice at early age (6 weeks) to aggravate the progression of diabetic nephropathy. All animal studies were terminated at 6 months of age of mice, which is relatively most chronic amongst the all animal models being used for diabetic nephropathy research. The histomorphological changes observed in uninephrectomised db/db mice were similar to the Kimmelstiel-Wilson lesions observed in human renal biopsies from patients with diabetic nephropathy. In addition increased mesangial cell proliferation and GBM expansion was observed in db/db mice and was aggravated upon uninephrectomy in these mice.

Diabetic nephropathy in humans is characterized by microalbuminuria and progressive decline in GFR which was also observed in our animal model and was associated with increased infiltration of macrophage in glomeruli and interstitium. Thus, uninephrectomised db/db mice represent an acceptable animal model for diabetic nephropathy.

5.1. Role of pro-inflammatory chemokines in diabetic nephropathy

The development and progression of diabetic nephropathy is considered to be multifactorial. Many pathomechanisms have been postulated to contribute to the development and progression of diabetic nephropathy, but the involvement of inflammation in diabetic nephropathy is relatively new and an emerging field of research. Macrophage and monocyte (M/M) infiltration is hallmark of renal inflammation and is a major factor contributing towards the development and progression of diabetic nephropathy. CCL2 is a chemoattractant chemokine which is mainly responsible for M/M recruitment into different renal compartments in animal models of diabetic nephropathy as well as in humans^{61, 91, 106, 175}. One of the studies with CCL2 deficient mice has reported protection of glomerular pathology upon streptozotocin induced diabetes in these mice⁹⁵. A similar study has reported development of diabetic nephropathy to be significantly inhibited in CCL2 deficient db/db type II diabetic mice⁹⁶. In a previous studies from our lab we observed a

significant reduction in the number of glomerular macrophages with associated protection from glomerulosclerosis and proteinuria in db/db mice upon late onset of CCL2 blockade, which was started at 4 month till 6 month of age. In this particular study we observed up to 40 % reduction in glomerular and interstitial macrophages⁶¹. We hypothesized that earlier CCL2 blockade, may further reduce macrophage infiltration and may show more beneficial effects in improving diabetic glomerulosclerosis. In the present study we evaluated the effects of CCL2 blockade started at different stages of disease progression using a Spiegelmer (mNOX-E36) in db/db mice. Animals underwent uninephrectomy at early age (6 weeks) which aggravates disease progression in db/db mice. To evaluate effect of CCL2 blockade at different stages of diabetic nephropathy, treatment with CCL2 antagonist, mNOX-E36 (50 mg/kg, s.c.) was started at 3 months, 4 months or 5 months of age and was continued till 6 months of age. Starting CCL2 blockade at different stages of disease progression resulted in reduced numbers of infiltrating macrophages in glomeruli as well as interstitium, which was consistent with our earlier report⁶¹. Reduced macrophage infiltration was associated with improved glomerulosclerosis compared to vehicle-treated group. In addition treatment with the CCL2 antagonist resulted in significant improvement of glomerular filtration rate and albuminuria. The numbers of glomerular proliferating cells in glomeruli were also reduced upon CCL2 antagonist administration which can be attributed to reduced macrophage- dependent mesangial cell proliferation and glomerular inflammation⁷³. Observed improvement of glomerular pathology and GFR in mice treated with CCL2 antagonist was consistent with our previous report and is further supported by earlier studies^{95, 96}. Interestingly, infiltration of glomerular and interstitial macrophages was inhibited to a similar extent in all treatment groups, and was independent of the treatment duration. Similarly, improvement of GFR and inhibition of albuminuria and glomerular cell proliferation was observed to be independent of the treatment duration. We did not observe any changes in blood glucose levels of mice treated with CCL2 antagonist compared to vehicle treated mice, which does not support the published study¹⁷⁴ the possible justification can be the age at which mice are treated with CCL2 antagonist. The results of this study have confirmed the involvement of CCL2-mediated macrophages recruitment in development and progression of diabetic nephropathy. CCL2 blockade initiated at an early stage of disease progression failed to show any further reduction in infiltrating macrophages over the

late onset of blockade which does not support our hypothesis of further reduction of infiltrating macrophages upon CCL2 blockade at earlier stage of diabetic nephropathy. The results of the study suggest involvement of other chemokine-chemokine receptor in addition to CCL2-mediated macrophages recruitment.

Thus, we further hypothesized that targeting more than one chemokine or chemokine receptors simultaneously may show some additive or synergistic effects in ameliorating the disease progression compared to single chemokine antagonism. There are several more chemokine-chemokine receptors that have been reported to be altered in experimental diabetic nephropathy as well as in clinical kidney biopsies from diabetic patients. CCR2 acts as receptor for many chemokines including CCL2, CCL13, CCL7 and CCL8 and is mainly expressed on monocytes, basophils, memory T-cells and pDCs. Improvement of renal fibrosis¹²⁷, inhibition of macrophage trafficking¹²⁸ and improvement of glomerulonephritis¹³² has been documented upon CCR2 antagonism. CCR5 acts as common receptor for CCL8, CCL4, CCL3 and CCL5. Antagonism of CCR5 was associated with decreased macrophage infiltration in glomerular compartment in addition to reduction in collagen IV deposition¹²³. A simultaneous involvement of CCR2 and CCR5 in progression of diabetic nephropathy has not been explored yet. In one of the studies CCR5 deficiency was found to be associated with counter upregulation of CCL3, CCL5 and CCR1 expression, unfortunately, this study did not report CCR2 expression levels in these mice. Thus, CCR2 and CCR5 being most attractive targets for diabetic nephropathy we hypothesized simultaneous blockade of CCR2 and CCR5 may show additive beneficial effects in ameliorating diabetic nephropathy. To test this hypothesis we evaluated effects of two different CCR2 and CCR5 dual antagonists in diabetic nephropathy using the same mouse model of diabetic nephropathy.

Db/db mice underwent uninephrectomy at early age (6 weeks of age), and were treated with orally active CCR2 and CCR5 dual antagonists for a duration of 4 weeks starting from 20 weeks of age. Animal groups treated with dual antagonists showed inhibition of further increase in urinary albumin to creatinine ratio as compared to vehicle treated animals. This was associated with improved glomerulosclerosis. There was no significant improvement of tubular pathology,

treatment with CCR2 and CCR5 dual antagonists failed to show any improvement of tubular cell damage, tubular dilatation, interstitial volume or collagen deposition. The improvement of glomerulosclerosis and improvement of albuminuria was associated with reduced number of macrophage infiltration in glomeruli as well as in interstitium. Improvement of glomerular pathology and albuminuria can be attributed to inhibition of macrophage infiltration to the glomerular and interstitial compartments. Surprisingly observed reduction in macrophage infiltration upon treatment with dual antagonists was up to 40 %, which was similar to CCL2 blockade alone. These results suggested that targeting CCR2 and CCR5 simultaneously in diabetic nephropathy had no additive effect over single CCL2 blockade. CCL2 being ligand for CCR2 can mediate migration leucocytes expressing CCR2 receptor which is mainly expressed by monocytes, memory T cells and pDCs ¹¹¹. Basophils and memory T cells express CCR2 but not CCR5 on the other hand immature DC, Th 1 and T regulatory cells express CCR5 but not CCR2 ¹¹¹. Thus, blocking CCR2 and CCR5 simultaneously can further inhibit the migration of Th 1 and T regulatory cells in addition compared to CCL2 blockade alone. The results suggest development and progression of diabetic nephropathy is not affected significantly by Th 1 and T regulatory cells. Since the type II diabetic animal model used in the current study does not support the role of Th 1 and T regulatory cells in development of DN, further studies with type I animal models are required to support this finding. Th 1 and T regulatory cells have not been looked at is a lacuna in the current study. Based on our results we can conclude that the similar set of population was affected upon either CCL2 blockade alone or CCR2 and CCR5 dual blockade. Another possibility can be counter up regulation of some other chemokine or chemokine receptor *in vivo* upon simultaneous blockade of CCR2 and CCR5, which was not looked into at present. Further studies in this regard will be helpful in understanding the complex *in vivo* situation. Results of the study does not support our hypothesis of targeting more than one chemokine receptor being more beneficial in improving the disease, but the hypothesis can not be ruled out completely, as inhibition of some other pair or chemokine-chemokine receptors may still show more beneficial effects in ameliorating diabetic nephropathy.

5.2. Role of homeostatic chemokines in diabetic nephropathy

CXCL12 is a crucial mediator in tissue repair in acute kidney injuries, cell survival and supports tissue reoxygenation and regeneration. On the other hand in chronic diseases like retinal angiogenesis or pulmonary tissue fibrosis CXCL12 is responsible for progression of disease. The available studies make us believe that CXCL12 mediated effects are tissue specific and are varied depending on the chronicity. Thus, known functions of CXCL12 do not allow to reliably predict its potential role in chronic glomerulopathies such as diabetic nephropathy. We hypothesised CXCL12 plays role in development and progression of diabetic nephropathy either beneficial or pathological. To evaluate possible involvement of CXCL12 in DN, db/db mice uninephrectomised at early age (6 weeks) received subcutaneous injections with either control spiegelmer (revmNOX-A12) or CXCL12 antagonist (mNOX-A12) every alternate day, started at 16 weeks of age till 24 weeks of age. At the end of the study consistent exposure of CXCL12 antagonist was confirmed by significantly increased serum levels of CXCL12 in mice group treated with antagonist. In the present study, we observed that transient blockade of CXCL12 prevented the progression of glomerulosclerosis and proteinuria in type 2 diabetes. Tubular cell damage was prevented upon CXCL12 blockade in uninephrectomized db/db mice, while we did not observe any significant changes in interstitial volume and tubular lumen. Since db/db mice model do not exhibit severe tubulopathy, we can not conclude about effect of CXCL12 antagonism in tubular pathology. Since glomerular proliferating Ki 67 positive cells were not affected upon CXCL12 blockade, improvement of glomerular pathology and albumin urea can not be attributed to effect of CXCL12 on mesangial cell proliferation.

In the present study we did not observe any changes in ckit and sca double positive stem cell population in kidney upon CXCL12 blockade. At the same time CXCR4 positive cell population was also not altered in kidney. The total ckit and sca double positive stem cell population observed in kidney was very less (< 0.5 % of total cell population) which makes it difficult to relate any changes with stem cells contributing towards improvement of glomerulosclerosis. Although stem cell population was reduced in bone marrow we did not observed any changes in kidney. Thus we exclude possibility of observed beneficial effects as a consequence of stem cell mobilisation to kidney, which is further supported by recent study describing

haematopoietic stem cell mobilization is independent of CXCL12-CXCR4 axis in kidney¹⁷⁶.

To explore other possible mechanisms involved in the glomerulosclerosis we looked at Mac2 staining from kidney sections from all groups. There were no significant differences between the groups for Mac2-positive cells within glomeruli, hence the observed beneficial effects upon CXCL12 blockade were independent of macrophage infiltration. As in recent past several studies have reported significance of macrophage polarisation in inflammation and disease progression. Classically activated macrophage (M1), have been reported to be pro-inflammatory and contributes towards inflammation on the other hand alternatively activated macrophages (M2) are reported to be anti-inflammatory, which has been confirmed recently in a in vivo study with SCID mice¹⁷⁷. To assess the effect of CXCL12 blockade on infiltrated and resident macrophages in glomeruli, expression levels of different phenotype markers of class M1 and M2 were analysed using RT-PCR. In the present study we observed some of M2 class markers were significantly up-regulated upon CXCL12 blockade at the same time expression levels of iNOS, which is class M1 marker was also enhanced. Since we looked into the whole kidney RNA preparations making it difficult to interpret whether this altered macrophage function affected disease progression. Further studies on isolated system with advanced experimental tools may be helpful in understanding the role of CXCL12 in macrophage polarisation.

The immunohistochemical analysis revealed constitutive expression of CXCL12 in podocytes of adult db/db mice, which was confirmed upon co-staining with WT1 (a specific podocyte marker). Our finding that adult C57BL/6 and db/db mouse kidneys express CXCL12 selectively in podocytes and not in any of the other glomerular cell types is consistent with a previous report that described glomerular CXCL12 expression in autoimmune-nephritic NZB/NZW F1 mice¹⁵⁴. However podocytes did not stain positive for CXCL12 in another study using female SCID mice¹⁷¹. Podocyte CXCL12 staining was also absent in human renal biopsies from children with various inflammatory disease entities¹⁴⁵. Glomerular CXCL12 staining was reported to localize to mesangial cells in healthy human kidneys¹⁷⁸. However, in this study the histomorphological illustrations are more consistent with

CXCL12 expression in podocytes rather than in mesangial cells. Furthermore, CXCL12 staining in adult human kidney shows prominent CXCL12 expression in podocytes only (S. Segerer personal communication). In db/db mice the podocyte-specific expression of CXCL12 corresponds to the glomerular expression pattern of VEGF, another hypoxia-inducible factor-1 regulated pro-angiogenic factor with similar functional roles in angiogenesis and hypoxia control ¹⁷⁹. Podocyte-derived CXCL12 and VEGF both regulates glomerular capillary formation during renal development ¹⁸⁰, further suggesting a role for CXCL12 in regulating glomerular structure by glomerular cell-cell interactions. These data confirm the functional importance of podocytes in the progression of (diabetic) glomerular disease ⁹⁶ and for the first time, demonstrate a pathogenic role of podocyte-derived CXCL12 in (diabetic) glomerulosclerosis.

Outside the kidney CXCL12 produced by distinct cells create appropriate microenvironments for other cell-types. For example, in the bone marrow stromal or endothelial cell-derived CXCL12 creates a niche for haematopoietic stem cells ¹⁸¹⁻¹⁸³. The CXCL12-dependent mechanism creates the necessary microenvironment for tumor metastasis engraftment ^{184, 185}, the homing of memory T cells to lymph nodes ¹⁸⁶ or the specific recruitment of bone marrow cells that orchestrate angiogenesis ¹⁸⁷. Accordingly we found that the progression of kidney disease in db/db mice did not increase renal *Cxcl12* mRNA expression levels. Renal CXCL12 immunostaining, although not being a reliable quantitative assessment of protein expression, did also not increase from young to older db/db mice. These expression data might suggest that glomerular CXCL12 is needed to maintain the glomerular structure in db/db mice and that blocking CXCL12 might have detrimental effects. However, it was recently shown that adding an anti-CXCL12-specific antibody to low cyclosporin-treatment significantly reduced renal allograft glomerulosclerosis, as compared to cyclosporin mono-therapy in a Fischer 344 to Lewis rat chronic renal allograft nephropathy model ¹⁶⁴. Unfortunately, glomerular CXCL12 immunostaining was not reported in this study but the authors referred to the CXCL12-mediated improvement of allograft glomerulosclerosis to reduce arteriolar intimal thickening. Balabanian, et al. documented podocyte CXCL12 expression in autoimmune-nephritic NZB/NZW F1 mice and also reported less glomerular pathology and proteinuria upon CXCL12 blockade with a neutralizing antibody ¹⁵⁴. This was

mainly attributed to the effects of CXCL12 blockade on systemic autoimmunity and immune complex disease, which does not reliably allow us to conclude on the local role of CXCL12 expression on glomerular pathology in this model. The type 2 diabetic nephropathy model of db/db mice used in the current study is independent of systemic allo- or autoimmunity and is thought to represent tissue remodelling as a consequence of hyperglycemia and glomerular hyperfiltration¹⁸⁸. Hence, the preventive effect of CXCL12 blockade on glomerulosclerosis in db/db mice should largely relate to the effects of blocking CXCL12 at the glomerular level. This would argue for a novel pathogenic role of podocyte-derived CXCL12 in (diabetic) glomerulosclerosis. This, again, would be consistent with the role of VEGF in rodent diabetic nephropathy, as VEGF is also produced by podocytes, acts locally on the glomerular vasculature, and blocking VEGF reduces glomerular pathology and proteinuria in experimental diabetic nephropathy²³.

Our study does not yet define the underlying maladaptive function of CXCL12 but we found that CXCL12 blockade was associated with higher podocyte numbers. The possible reasons for this observation might be increased regeneration of podocytes or decreased podocyte loss. This could either relate to less podocyte death or increased podocyte regeneration. We observed increased number of WT1 positive parietal epithelial cells in peripheral as well as on the vascular pole upon CXCL12 blockade, in addition to increased number of podocytes on glomerular tuft. This observation is further supported by recent study from Appel et al. in which authors have reported parietal epithelial cell differentiation to podocytes¹⁸⁹. Hence, CXCL12 may either regulate podocyte cell cycle or podocyte regeneration from parietal epithelial cells^{189, 190}. This will require a podocyte-specific knock-out of CXCL12 in diabetic mice and given the role of podocyte CXCL12 on renal development, this knock-out will need to be conditional.

6. Summary and conclusions

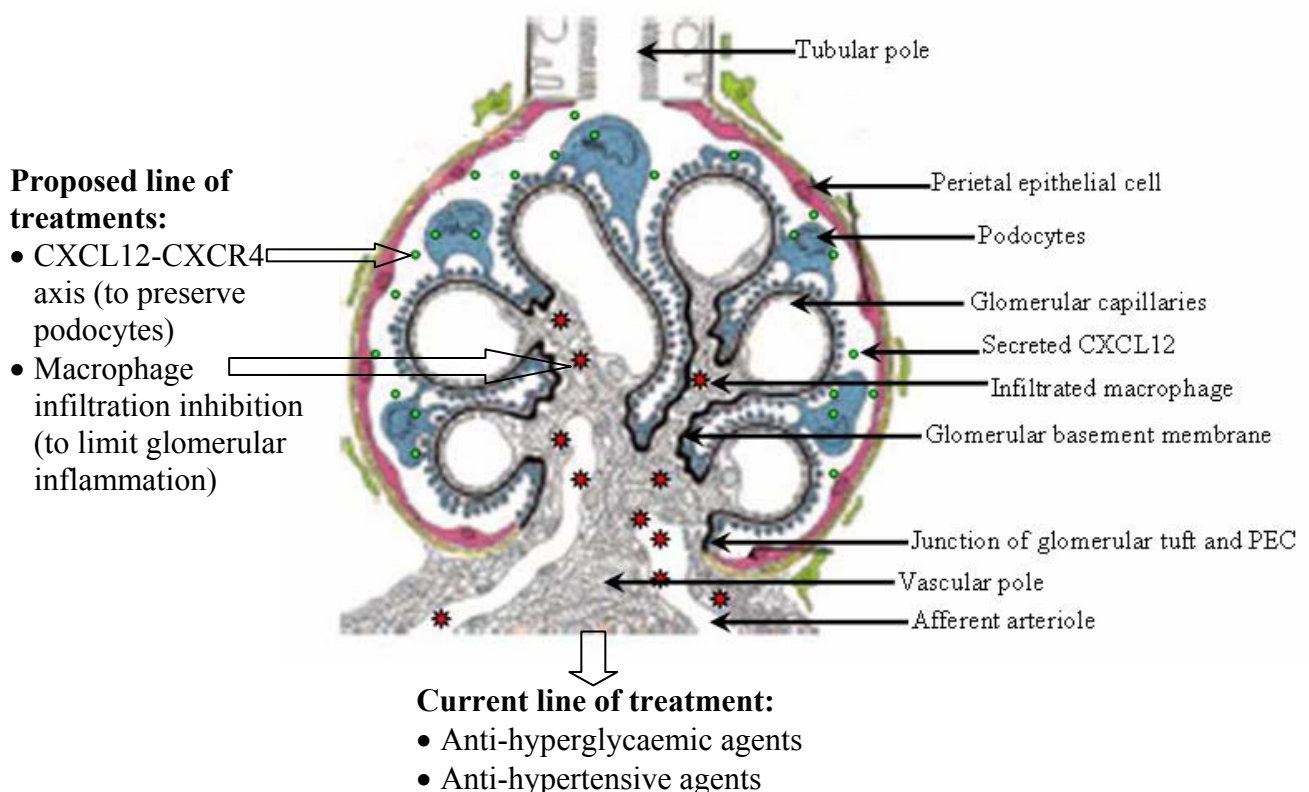
The role of inflammation in development and progression of diabetic nephropathy was evident from macrophage infiltration and CCL2 up regulation in kidney. The progression of diabetic nephropathy can be inhibited with CCL2 antagonists like mNOX-E36. CCL2 inhibition started at different stages of the disease progression showed no additive effects. The maximum percentage reduction of infiltrating macrophages into kidneys of diabetic mice achieved was independent of the duration of blockade with CCL2 antagonist. Thus, from results of the current study an involvement of other chemokine-chemokine receptor systems in the progression of disease is evident.

When two different chemokine receptors CCR2 and CCR5 were blocked simultaneously using dual antagonists (WM 7671 and WM 7390), we did not observe any further reduction in macrophage infiltration and improvement of glomerulosclerosis as compared to CCL2 chemokine blockade alone. Thus, targeting CCR2 and CCR5 simultaneously showed no additive advantage in improving diabetic nephropathy over CCL2 blockade.

Blocking the homeostatic chemokine CXCL12 improved glomerular pathology and proteinuria in diabetic mice independent of macrophage infiltration. There was no significant change observed on tissue fibrosis upon treatment with CXCL12 antagonist, which rules out the inhibition of bone marrow derived fibroblasts to the kidney. The analysis of different macrophage phenotype markers showed up regulation of M1 as well as M2 macrophages markers, making it difficult to interpret if the observed effects are result of macrophage polarisation. Immunohistochemistry showed consistent expression of CXCL12 in kidney, mainly by podocytes. CXCL12 blockade resulted in increased number of WT1 positive podocytes which can be attributed either to less podocyte loss or regeneration of podocytes. These data for the first time demonstrate a pathogenic role of CXCL12 in (diabetic) glomerulosclerosis and we postulate that glomerular podocytes are an important source of this chemokine.

In the current studies with different chemokine antagonists we found inhibition of the pro-inflammatory chemokine CCL2 could inhibit progression of glomerulosclerosis and was associated with decreased infiltration of macrophages to the glomerular and interstitial compartments. Similar effects were observed upon simultaneous antagonism of CCR2 and CCR5. Beneficial effects upon simultaneous blockade of CCR2 and CCR5 were similar to that of CCL2 blockade and were associated with decreased number of infiltrating macrophages. On the other hand beneficial effects observed upon CXCL12 blockade were independent of macrophage infiltration and were associated with increased number of podocytes.

Diabetic nephropathy is multifactorial and inflammation and podocyte injury are well established in its development and progression. Based on results of our study we may envision that targeting a pro-inflammatory chemokine (CCL2) and a homeostatic chemokine (CXCL12) simultaneously can be a better approach for treating diabetic nephropathy. To test this hypothesis will be one of our future goals.



7. Zusammenfassung

Die Rolle und Bedeutung der Entzündungsreaktion bei der Entwicklung und Progression der Diabetischen Nephropathie wurde in dieser Arbeit an Hand der Makrophageninfiltration und CCL2-Genhochregulierung in der Niere dargestellt.

Die Progression der Diabetischen Nephropathie kann durch CCL2-Antagonisten wie mNOX-E36 aufgehalten werden. Die CCL2-Antagonisierung in fortgeschrittenen Stadien der Erkrankung konnte keinen additiven Effekt des Pharmakons nachweisen. Die maximal erreichte Reduktion infiltrierender Makrophagen in Nieren diabetischer Mäuse war zudem unabhängig von der Dauer der CCL2-Blockade. Somit kann aus den Ergebnissen dieser Arbeit geschlossen werden, dass eine Beteiligung anderer Chemokin-Chemokin-Rezeptor-Systeme bei der Progression der Diabetischen Nephropathie vorliegen muss.

Bei gleichzeitiger Blockade der Chemokien-Rezeptoren CCR2 und CCR5 durch Verwendung der zweifach-Antagonisten WM 7671 und WM 7390 konnte keine vermehrte Reduktion der Makrophageninfiltration und auch keine Verbesserung des Grades der Glomerulosklerose im Vergleich zu der alleinigen CCL2-Blockade festgestellt werden. Somit erbrachte die gleichzeitige Blockade von CCR2 und CCR5 keinen zusätzlichen Vorteil zur Behandlung der Diabetischen Nephropathie durch CCL2-Antagonisierung.

Die Blockade des Chemokins CXCL12 zeigte eine Verbesserung der glomerulären Pathologie sowie eine Reduktion der Proteinurie bei diabetischen Mäusen unabhängig der Makrophageninfiltration. Es konnte keine signifikante Veränderung der Gewebsfibrose durch die Behandlung mit einem CXCL12-Antagonisten nachgewiesen werden, was die Inhibierung von Fibroblasten, die aus dem Knochenmark stammen, ausschließt. Die Analyse verschiedener Makrophagen-Phänotypen zeigte eine Hochregulierung von sowohl M1- als auch M2-Makrophagen-Marker, was es somit schwierig macht, die gezeigten Effekte als Makrophagen-Polarisierung zu interpretieren. In der Immunhistochemie konnte eine konsistente Expression von CXCL12 in der Niere und vor allem in Podozyten nachgewiesen werden. Die Blockade von CXCL12 führte zu einer Vermehrung WT1-positiver Podozyten, was einerseits auf einen verringerten Verlust oder

andererseits auf eine verstärkte Regeneration der Podozyten zurückgeführt werden kann. Diese Daten demonstrieren erstmals die Bedeutung von CXCL12 in der Pathogenese der diabetischen Nephropathie und man kann postulieren, dass glomeruläre Podozyten eine wichtige Herkunftsquelle dieses Chemokins darstellen.

In der aktuellen Studie mit verschiedenen Chemokin-Antagonisten konnte durch Inhibierung des proinflammatorischen Chemokins CCL2 die Progression der Glomerulosklerose verhindert werden, die mit verminderter Makrophageninfiltration im Glomerulus und Interstitium einherging. Ähnliche Effekte konnten mit der simultanen Blockade von CCR2 und CCR5 gezeigt werden. Positive Effekte der gleichzeitigen Antagonisierung von CCR2 und CCR5 waren gleich denen der CCL2-Blockade und waren mit einer verringerten Anzahl infiltrierender Makrophagen assoziiert. Andererseits konnten positive Effekte durch die CXCL12-Blockade nachgewiesen werden, welche unabhängig von der Makrophageninfiltration war und mit einer vermehrten Anzahl von Podozyten einherging.

Die Pathogenese der Diabetischen Nephropathie ist multifaktoriell und Inflammation sowie Podozyten-Schaden tragen sehr zum Verständnis der Entwicklung und Progression der Erkrankung bei. Basierend auf den Ergebnissen dieser Arbeit kann man sich vorstellen, dass die gezielte Pharmakotherapie durch gleichzeitige Antagonisierung des proinflammatorischen Chemokins CCL2 und des homeostatischen Chemokins CXCL12 eine bessere Lösung zur Behandlung der diabetischen Nephropathie bedeuten könne. Um diese Hypothese zu verifizieren bedarf es weitere Studien.

8. References

1. Wild S, Roglic G, Green A, Sicree R, King H. Global prevalence of diabetes: estimates for the year 2000 and projections for 2030. *Diabetes Care* 2004;27(5):1047-53.
2. Wolfgang P. Prevalence of nephropathy in the German diabetes population—Is early referral to nephrological care a realistic demand today? *NDT Plus* 2008; Supplement 4, Volume 1: iv2-iv5.
3. Effect of intensive therapy on the development and progression of diabetic nephropathy in the Diabetes Control and Complications Trial. The Diabetes Control and Complications (DCCT) Research Group. *Kidney Int* 1995;47(6):1703-20.
4. Ritz E, Rychlik I, Locatelli F, Halimi S. End-stage renal failure in type 2 diabetes: A medical catastrophe of worldwide dimensions. *Am J Kidney Dis* 1999;34(5):795-808.
5. K/DOQI clinical practice guidelines for chronic kidney disease: evaluation, classification, and stratification. *Am J Kidney Dis* 2002;39(2 Suppl 1):S1-266.
6. Adler AI, Stratton IM, Neil HA, et al. Association of systolic blood pressure with macrovascular and microvascular complications of type 2 diabetes (UKPDS 36): prospective observational study. *Bmj* 2000;321(7258):412-9.
7. Kelly DJ, Zhang Y, Hepper C, et al. Protein kinase C beta inhibition attenuates the progression of experimental diabetic nephropathy in the presence of continued hypertension. *Diabetes* 2003;52(2):512-8.
8. Hsieh TJ, Zhang SL, Filep JG, Tang SS, Ingelfinger JR, Chan JS. High glucose stimulates angiotensinogen gene expression via reactive oxygen species generation in rat kidney proximal tubular cells. *Endocrinology* 2002;143(8):2975-85.
9. Nishikawa T, Edelstein D, Du XL, et al. Normalizing mitochondrial superoxide production blocks three pathways of hyperglycaemic damage. *Nature* 2000;404(6779):787-90.
10. Kersten S, Desvergne B, Wahli W. Roles of PPARs in health and disease. *Nature* 2000;405(6785):421-4.

11. Semple RK, Chatterjee VK, O'Rahilly S. PPAR gamma and human metabolic disease. *J Clin Invest* 2006;116(3):581-9.
12. Dobrian AD. The complex role of PPARgamma in renal dysfunction in obesity: managing a Janus-faced receptor. *Vascul Pharmacol* 2006;45(1):36-45.
13. Iglarz M, Touyz RM, Amiri F, Lavoie MF, Diep QN, Schiffrin EL. Effect of peroxisome proliferator-activated receptor-alpha and -gamma activators on vascular remodeling in endothelin-dependent hypertension. *Arterioscler Thromb Vasc Biol* 2003;23(1):45-51.
14. Bakris G, Viberti G, Weston WM, Heise M, Porter LE, Freed MI. Rosiglitazone reduces urinary albumin excretion in type II diabetes. *J Hum Hypertens* 2003;17(1):7-12.
15. Baylis C, Atzpodien EA, Freshour G, Engels K. Peroxisome proliferator-activated receptor [gamma] agonist provides superior renal protection versus angiotensin-converting enzyme inhibition in a rat model of type 2 diabetes with obesity. *J Pharmacol Exp Ther* 2003;307(3):854-60.
16. Calkin AC, Giunti S, Jandeleit-Dahm KA, Allen TJ, Cooper ME, Thomas MC. PPAR-alpha and -gamma agonists attenuate diabetic kidney disease in the apolipoprotein E knockout mouse. *Nephrol Dial Transplant* 2006;21(9):2399-405.
17. Panchapakesan U, Sumual S, Pollock CA, Chen X. PPARgamma agonists exert antifibrotic effects in renal tubular cells exposed to high glucose. *Am J Physiol Renal Physiol* 2005;289(5):F1153-8.
18. Fukami K, Yamagishi S, Ueda S, Okuda S. Novel therapeutic targets for diabetic nephropathy. *Endocr Metab Immune Disord Drug Targets* 2007;7(2):83-92.
19. Tang SC, Leung JC, Chan LY, Tsang AW, Lai KN. Activation of tubular epithelial cells in diabetic nephropathy and the role of the peroxisome proliferator-activated receptor-gamma agonist. *J Am Soc Nephrol* 2006;17(6):1633-43.
20. Gugliucci A, Bendayan M. Reaction of advanced glycation endproducts with renal tissue from normal and streptozotocin-induced diabetic rats: an ultrastructural study using colloidal gold cytochemistry. *J Histochem Cytochem* 1995;43(6):591-600.

21. Beisswenger PJ, Makita Z, Curphey TJ, et al. Formation of immunochemical advanced glycosylation end products precedes and correlates with early manifestations of renal and retinal disease in diabetes. *Diabetes* 1995;44(7):824-9.
22. Yamagishi S, Inagaki Y, Okamoto T, Amano S, Koga K, Takeuchi M. Advanced glycation end products inhibit de novo protein synthesis and induce TGF-beta overexpression in proximal tubular cells. *Kidney Int* 2003;63(2):464-73.
23. Bohlander JM, Franke S, Stein G, Wolf G. Advanced glycation end products and the kidney. *Am J Physiol Renal Physiol* 2005;289(4):F645-59.
24. Yamagishi S, Inagaki Y, Okamoto T, et al. Advanced glycation end product-induced apoptosis and overexpression of vascular endothelial growth factor and monocyte chemoattractant protein-1 in human-cultured mesangial cells. *J Biol Chem* 2002;277(23):20309-15.
25. Banba N, Nakamura T, Matsumura M, Kuroda H, Hattori Y, Kasai K. Possible relationship of monocyte chemoattractant protein-1 with diabetic nephropathy. *Kidney Int* 2000;58(2):684-90.
26. Fukami K, Ueda S, Yamagishi S, et al. AGEs activate mesangial TGF-beta-Smad signaling via an angiotensin II type I receptor interaction. *Kidney Int* 2004;66(6):2137-47.
27. Dunlop M. Aldose reductase and the role of the polyol pathway in diabetic nephropathy. *Kidney Int Suppl* 2000;77:S3-12.
28. Passariello N, Sepe J, Marrazzo G, et al. Effect of aldose reductase inhibitor (tolrestat) on urinary albumin excretion rate and glomerular filtration rate in IDDM subjects with nephropathy. *Diabetes Care* 1993;16(5):789-95.
29. Shah IM, Mackay SP, McKay GA. Therapeutic strategies in the treatment of diabetic nephropathy - a translational medicine approach. *Curr Med Chem* 2009;16(8):997-1016.
30. Ruiz-Ortega M, Bustos C, Hernandez-Presa MA, Lorenzo O, Plaza JJ, Egido J. Angiotensin II participates in mononuclear cell recruitment in experimental immune complex nephritis through nuclear factor-kappa B activation and monocyte chemoattractant protein-1 synthesis. *J Immunol* 1998;161(1):430-9.

31. Thomas MC, Tikellis C, Burns WM, et al. Interactions between renin angiotensin system and advanced glycation in the kidney. *J Am Soc Nephrol* 2005;16(10):2976-84.
32. Moreau P, d'Uscio LV, Shaw S, Takase H, Barton M, Luscher TF. Angiotensin II increases tissue endothelin and induces vascular hypertrophy: reversal by ET(A)-receptor antagonist. *Circulation* 1997;96(5):1593-7.
33. Mohacsi A, Magyar J, Tamas B, Nanasi PP. Effects of endothelins on cardiac and vascular cells: new therapeutic target for the future? *Curr Vasc Pharmacol* 2004;2(1):53-63.
34. Mildenerger E, Biesel B, Siegel G, Versmold HT. Nitric oxide and endothelin in oxygen-dependent regulation of vascular tone of human umbilical vein. *Am J Physiol Heart Circ Physiol* 2003;285(4):H1730-7.
35. Lip GY. Darusentan (Abbott Laboratories). *IDrugs* 2001;4(11):1284-92.
36. Hocher B, Schwarz A, Reinbacher D, et al. Effects of endothelin receptor antagonists on the progression of diabetic nephropathy. *Nephron* 2001;87(2):161-9.
37. Ziyadeh FN, Hoffman BB, Han DC, et al. Long-term prevention of renal insufficiency, excess matrix gene expression, and glomerular mesangial matrix expansion by treatment with monoclonal antitransforming growth factor-beta antibody in db/db diabetic mice. *Proc Natl Acad Sci U S A* 2000;97(14):8015-20.
38. Kagami S, Border WA, Miller DE, Noble NA. Angiotensin II stimulates extracellular matrix protein synthesis through induction of transforming growth factor-beta expression in rat glomerular mesangial cells. *J Clin Invest* 1994;93(6):2431-7.
39. Roestenberg P, van Nieuwenhoven FA, Wieten L, et al. Connective tissue growth factor is increased in plasma of type 1 diabetic patients with nephropathy. *Diabetes Care* 2004;27(5):1164-70.
40. Riser BL, Denichilo M, Cortes P, et al. Regulation of connective tissue growth factor activity in cultured rat mesangial cells and its expression in experimental diabetic glomerulosclerosis. *J Am Soc Nephrol* 2000;11(1):25-38.
41. Kohno K, Katayama T, Majima K, et al. A case of normotensive scleroderma renal crisis after high-dose methylprednisolone treatment. *Clin Nephrol* 2000;53(6):479-82.

42. Nakagawa H, Sasahara M, Haneda M, Koya D, Hazama F, Kikkawa R. Immunohistochemical characterization of glomerular PDGF B-chain and PDGF beta-receptor expression in diabetic rats. *Diabetes Res Clin Pract* 2000;48(2):87-98.
43. Savikko J, Taskinen E, Von Willebrand E. Chronic allograft nephropathy is prevented by inhibition of platelet-derived growth factor receptor: tyrosine kinase inhibitors as a potential therapy. *Transplantation* 2003;75(8):1147-53.
44. Abboud HE. Role of platelet-derived growth factor in renal injury. *Annu Rev Physiol* 1995;57:297-309.
45. Kelly DJ, Gilbert RE, Cox AJ, Soulis T, Jerums G, Cooper ME. Aminoguanidine ameliorates overexpression of pro-sclerotic growth factors and collagen deposition in experimental diabetic nephropathy. *J Am Soc Nephrol* 2001;12(10):2098-107.
46. Lassila M, Jandeleit-Dahm K, Seah KK, et al. Imatinib attenuates diabetic nephropathy in apolipoprotein E-knockout mice. *J Am Soc Nephrol* 2005;16(2):363-73.
47. Johnson RJ, Raines EW, Floege J, et al. Inhibition of mesangial cell proliferation and matrix expansion in glomerulonephritis in the rat by antibody to platelet-derived growth factor. *J Exp Med* 1992;175(5):1413-6.
48. Tsiani E, Lekas P, Fantus IG, Dlugosz J, Whiteside C. High glucose-enhanced activation of mesangial cell p38 MAPK by ET-1, ANG II, and platelet-derived growth factor. *Am J Physiol Endocrinol Metab* 2002;282(1):E161-9.
49. Cooper ME, Vranes D, Youssef S, et al. Increased renal expression of vascular endothelial growth factor (VEGF) and its receptor VEGFR-2 in experimental diabetes. *Diabetes* 1999;48(11):2229-39.
50. de Vriese AS, Tilton RG, Elger M, Stephan CC, Kriz W, Lameire NH. Antibodies against vascular endothelial growth factor improve early renal dysfunction in experimental diabetes. *J Am Soc Nephrol* 2001;12(5):993-1000.
51. Flyvbjerg A, Dagnaes-Hansen F, De Vriese AS, Schrijvers BF, Tilton RG, Rasch R. Amelioration of long-term renal changes in obese type 2 diabetic mice by a neutralizing vascular endothelial growth factor antibody. *Diabetes* 2002;51(10):3090-4.
52. Schrijvers BF, Flyvbjerg A, Tilton RG, Lameire NH, De Vriese AS. A neutralizing VEGF antibody prevents glomerular hypertrophy in a model of

- obese type 2 diabetes, the Zucker diabetic fatty rat. *Nephrol Dial Transplant* 2006;21(2):324-9.
53. Ruster C, Wolf G. The role of chemokines and chemokine receptors in diabetic nephropathy. *Front Biosci* 2008;13:944-55.
 54. Galkina E, Ley K. Leukocyte recruitment and vascular injury in diabetic nephropathy. *J Am Soc Nephrol* 2006;17(2):368-77.
 55. Sassy-Prigent C, Heudes D, Mandet C, et al. Early glomerular macrophage recruitment in streptozotocin-induced diabetic rats. *Diabetes* 2000;49(3):466-75.
 56. Chow F, Ozols E, Nikolic-Paterson DJ, Atkins RC, Tesch GH. Macrophages in mouse type 2 diabetic nephropathy: correlation with diabetic state and progressive renal injury. *Kidney Int* 2004;65(1):116-28.
 57. Ninichuk V, Khandoga AG, Segerer S, et al. The role of interstitial macrophages in nephropathy of type 2 diabetic db/db mice. *Am J Pathol* 2007;170(4):1267-76.
 58. Moriya R, Manivel JC, Mauer M. Juxtaglomerular apparatus T-cell infiltration affects glomerular structure in Type 1 diabetic patients. *Diabetologia* 2004;47(1):82-8.
 59. Fardon NJ, Wilkinson R, Thomas TH. Abnormalities in primary granule exocytosis in neutrophils from Type I diabetic patients with nephropathy. *Clin Sci (Lond)* 2002;102(1):69-75.
 60. Takahashi T, Hato F, Yamane T, et al. Increased spontaneous adherence of neutrophils from type 2 diabetic patients with overt proteinuria: possible role of the progression of diabetic nephropathy. *Diabetes Care* 2000;23(3):417-8.
 61. Ninichuk V, Clauss S, Kulkarni O, et al. Late onset of Ccl2 blockade with the Spiegelmer mNOX-E36-3'PEG prevents glomerulosclerosis and improves glomerular filtration rate in db/db mice. *Am J Pathol* 2008;172(3):628-37.
 62. Tuttle KR, Bakris GL, Toto RD, McGill JB, Hu K, Anderson PW. The effect of ruboxistaurin on nephropathy in type 2 diabetes. *Diabetes Care* 2005;28(11):2686-90.
 63. Kelly DJ, Chanty A, Gow RM, Zhang Y, Gilbert RE. Protein kinase C β inhibition attenuates osteopontin expression, macrophage recruitment, and tubulointerstitial injury in advanced experimental diabetic nephropathy. *J Am Soc Nephrol* 2005;16(6):1654-60.

64. Schmid H, Boucherot A, Yasuda Y, et al. Modular activation of nuclear factor- κ B transcriptional programs in human diabetic nephropathy. *Diabetes* 2006;55(11):2993-3003.
65. Sugimoto H, Shikata K, Hirata K, et al. Increased expression of intercellular adhesion molecule-1 (ICAM-1) in diabetic rat glomeruli: glomerular hyperfiltration is a potential mechanism of ICAM-1 upregulation. *Diabetes* 1997;46(12):2075-81.
66. Coimbra TM, Janssen U, Grone HJ, et al. Early events leading to renal injury in obese Zucker (fatty) rats with type II diabetes. *Kidney Int* 2000;57(1):167-82.
67. Chow FY, Nikolic-Paterson DJ, Ozols E, Atkins RC, Tesch GH. Intercellular adhesion molecule-1 deficiency is protective against nephropathy in type 2 diabetic db/db mice. *J Am Soc Nephrol* 2005;16(6):1711-22.
68. Imani F, Horii Y, Suthanthiran M, et al. Advanced glycosylation endproduct-specific receptors on human and rat T-lymphocytes mediate synthesis of interferon gamma: role in tissue remodeling. *J Exp Med* 1993;178(6):2165-72.
69. Castano L, Eisenbarth GS. Type-I diabetes: a chronic autoimmune disease of human, mouse, and rat. *Annu Rev Immunol* 1990;8:647-79.
70. Odobasic D, Kitching AR, Tipping PG, Holdsworth SR. CD80 and CD86 costimulatory molecules regulate crescentic glomerulonephritis by different mechanisms. *Kidney Int* 2005;68(2):584-94.
71. Hirata K, Shikata K, Matsuda M, et al. Increased expression of selectins in kidneys of patients with diabetic nephropathy. *Diabetologia* 1998;41(2):185-92.
72. Wolf G. New insights into the pathophysiology of diabetic nephropathy: from haemodynamics to molecular pathology. *Eur J Clin Invest* 2004;34(12):785-96.
73. Ikezumi Y, Hurst LA, Masaki T, Atkins RC, Nikolic-Paterson DJ. Adoptive transfer studies demonstrate that macrophages can induce proteinuria and mesangial cell proliferation. *Kidney Int* 2003;63(1):83-95.
74. Matsui H, Suzuki M, Tsukuda R, Iida K, Miyasaka M, Ikeda H. Expression of ICAM-1 on glomeruli is associated with progression of diabetic nephropathy in a genetically obese diabetic rat, Wistar fatty. *Diabetes Res Clin Pract* 1996;32(1-2):1-9.

75. Park CW, Kim JH, Lee JH, et al. High glucose-induced intercellular adhesion molecule-1 (ICAM-1) expression through an osmotic effect in rat mesangial cells is PKC-NF-kappa B-dependent. *Diabetologia* 2000;43(12):1544-53.
76. Basta G, Lazzarini G, Massaro M, et al. Advanced glycation end products activate endothelium through signal-transduction receptor RAGE: a mechanism for amplification of inflammatory responses. *Circulation* 2002;105(7):816-22.
77. Onozato ML, Tojo A, Goto A, Fujita T. Radical scavenging effect of gliclazide in diabetic rats fed with a high cholesterol diet. *Kidney Int* 2004;65(3):951-60.
78. Okouchi M, Okayama N, Shimizu M, Omi H, Fukutomi T, Itoh M. High insulin exacerbates neutrophil-endothelial cell adhesion through endothelial surface expression of intercellular adhesion molecule-1 via activation of protein kinase C and mitogen-activated protein kinase. *Diabetologia* 2002;45(4):556-9.
79. Okada S, Shikata K, Matsuda M, et al. Intercellular adhesion molecule-1-deficient mice are resistant against renal injury after induction of diabetes. *Diabetes* 2003;52(10):2586-93.
80. Luster AD. Chemokines--chemotactic cytokines that mediate inflammation. *N Engl J Med* 1998;338(7):436-45.
81. Zlotnik A, Yoshie O. Chemokines: a new classification system and their role in immunity. *Immunity* 2000;12(2):121-7.
82. Godessart N. Chemokine receptors: attractive targets for drug discovery. *Ann N Y Acad Sci* 2005;1051:647-57.
83. Murphy PM, Baggiolini M, Charo IF, et al. International union of pharmacology. XXII. Nomenclature for chemokine receptors. *Pharmacol Rev* 2000;52(1):145-76.
84. Onuffer JJ, Horuk R. Chemokines, chemokine receptors and small-molecule antagonists: recent developments. *Trends Pharmacol Sci* 2002;23(10):459-67.
85. Johnson Z, Power CA, Weiss C, et al. Chemokine inhibition--why, when, where, which and how? *Biochem Soc Trans* 2004;32(Pt 2):366-77.
86. Moser B, Wolf M, Walz A, Loetscher P. Chemokines: multiple levels of leukocyte migration control. *Trends Immunol* 2004;25(2):75-84.
87. Proudfoot AE, Power CA, Wells TN. The strategy of blocking the chemokine system to combat disease. *Immunol Rev* 2000;177:246-56.

88. Panzer U, Steinmetz OM, Stahl RA, Wolf G. Kidney diseases and chemokines. *Curr Drug Targets* 2006;7(1):65-80.
89. Ihm CG. Monocyte chemoattractant peptide-1 in diabetic nephropathy. *Kidney Int Suppl* 1997;60:S20-2.
90. Wada T, Yokoyama H, Furuichi K, et al. Intervention of crescentic glomerulonephritis by antibodies to monocyte chemoattractant and activating factor (MCAF/MCP-1). *Faseb J* 1996;10(12):1418-25.
91. Wada T, Furuichi K, Segawa-Takaeda C, et al. MIP-1 α and MCP-1 contribute to crescents and interstitial lesions in human crescentic glomerulonephritis. *Kidney Int* 1999;56(3):995-1003.
92. Furuichi K, Wada T, Sakai N, et al. Distinct expression of CCR1 and CCR5 in glomerular and interstitial lesions of human glomerular diseases. *Am J Nephrol* 2000;20(4):291-9.
93. Tashiro K, Koyanagi I, Saitoh A, et al. Urinary levels of monocyte chemoattractant protein-1 (MCP-1) and interleukin-8 (IL-8), and renal injuries in patients with type 2 diabetic nephropathy. *J Clin Lab Anal* 2002;16(1):1-4.
94. Morii T, Fujita H, Narita T, et al. Association of monocyte chemoattractant protein-1 with renal tubular damage in diabetic nephropathy. *J Diabetes Complications* 2003;17(1):11-5.
95. Chow FY, Nikolic-Paterson DJ, Ozols E, Atkins RC, Rollin BJ, Tesch GH. Monocyte chemoattractant protein-1 promotes the development of diabetic renal injury in streptozotocin-treated mice. *Kidney Int* 2006;69(1):73-80.
96. Chow FY, Nikolic-Paterson DJ, Ma FY, Ozols E, Rollins BJ, Tesch GH. Monocyte chemoattractant protein-1-induced tissue inflammation is critical for the development of renal injury but not type 2 diabetes in obese db/db mice. *Diabetologia* 2007;50(2):471-80.
97. Bierhaus A, Schiekofer S, Schwaninger M, et al. Diabetes-associated sustained activation of the transcription factor nuclear factor-kappaB. *Diabetes* 2001;50(12):2792-808.
98. Mezzano S, Aros C, Droguett A, et al. NF-kappaB activation and overexpression of regulated genes in human diabetic nephropathy. *Nephrol Dial Transplant* 2004;19(10):2505-12.

99. Mezzano S, Droguett A, Burgos ME, et al. Renin-angiotensin system activation and interstitial inflammation in human diabetic nephropathy. *Kidney Int Suppl* 2003(86):S64-70.
100. Gruden G, Setti G, Hayward A, et al. Mechanical stretch induces monocyte chemoattractant activity via an NF-kappaB-dependent monocyte chemoattractant protein-1-mediated pathway in human mesangial cells: inhibition by rosiglitazone. *J Am Soc Nephrol* 2005;16(3):688-96.
101. Kato S, Luyckx VA, Ots M, et al. Renin-angiotensin blockade lowers MCP-1 expression in diabetic rats. *Kidney Int* 1999;56(3):1037-48.
102. Mizuno M, Sada T, Kato M, Fukushima Y, Terashima H, Koike H. The effect of angiotensin II receptor blockade on an end-stage renal failure model of type 2 diabetes. *J Cardiovasc Pharmacol* 2006;48(4):135-42.
103. Amann B, Tinzmann R, Angelkort B. ACE inhibitors improve diabetic nephropathy through suppression of renal MCP-1. *Diabetes Care* 2003;26(8):2421-5.
104. Ogawa S, Mori T, Nako K, Kato T, Takeuchi K, Ito S. Angiotensin II type 1 receptor blockers reduce urinary oxidative stress markers in hypertensive diabetic nephropathy. *Hypertension* 2006;47(4):699-705.
105. Wang SN, LaPage J, Hirschberg R. Role of glomerular ultrafiltration of growth factors in progressive interstitial fibrosis in diabetic nephropathy. *Kidney Int* 2000;57(3):1002-14.
106. Schneider A, Panzer U, Zahner G, et al. Monocyte chemoattractant protein-1 mediates collagen deposition in experimental glomerulonephritis by transforming growth factor-beta. *Kidney Int* 1999;56(1):135-44.
107. Wolf G, Jocks T, Zahner G, Panzer U, Stahl RA. Existence of a regulatory loop between MCP-1 and TGF-beta in glomerular immune injury. *Am J Physiol Renal Physiol* 2002;283(5):F1075-84.
108. Bazan JF, Bacon KB, Hardiman G, et al. A new class of membrane-bound chemokine with a CX3C motif. *Nature* 1997;385(6617):640-4.
109. Kikuchi Y, Ikee R, Hemmi N, et al. Fractalkine and its receptor, CX3CR1, upregulation in streptozotocin-induced diabetic kidneys. *Nephron Exp Nephrol* 2004;97(1):e17-25.
110. Geissmann F, Jung S, Littman DR. Blood monocytes consist of two principal subsets with distinct migratory properties. *Immunity* 2003;19(1):71-82.

111. Viola A, Luster AD. Chemokines and their receptors: drug targets in immunity and inflammation. *Annu Rev Pharmacol Toxicol* 2008;48:171-97.
112. Donadelli R, Zanchi C, Morigi M, et al. Protein overload induces fractalkine upregulation in proximal tubular cells through nuclear factor kappaB- and p38 mitogen-activated protein kinase-dependent pathways. *J Am Soc Nephrol* 2003;14(10):2436-46.
113. Kikuchi Y, Imakiire T, Hyodo T, et al. Advanced glycation end-product induces fractalkine gene upregulation in normal rat glomeruli. *Nephrol Dial Transplant* 2005;20(12):2690-6.
114. Chen YM, Lin SL, Chen CW, Chiang WC, Tsai TJ, Hsieh BS. Tumor necrosis factor-alpha stimulates fractalkine production by mesangial cells and regulates monocyte transmigration: down-regulation by cAMP. *Kidney Int* 2003;63(2):474-86.
115. Ancuta P, Rao R, Moses A, et al. Fractalkine preferentially mediates arrest and migration of CD16+ monocytes. *J Exp Med* 2003;197(12):1701-7.
116. Heeger P, Wolf G, Meyers C, et al. Isolation and characterization of cDNA from renal tubular epithelium encoding murine Rantes. *Kidney Int* 1992;41(1):220-5.
117. Satriano JA, Banas B, Luckow B, Nelson P, Schlondorff DO. Regulation of RANTES and ICAM-1 expression in murine mesangial cells. *J Am Soc Nephrol* 1997;8(4):596-603.
118. Nelson PJ, Kim HT, Manning WC, Goralski TJ, Krensky AM. Genomic organization and transcriptional regulation of the RANTES chemokine gene. *J Immunol* 1993;151(5):2601-12.
119. Zoja C, Donadelli R, Colleoni S, et al. Protein overload stimulates RANTES production by proximal tubular cells depending on NF-kappa B activation. *Kidney Int* 1998;53(6):1608-15.
120. Wolf G, Ziyadeh FN, Thaïss F, et al. Angiotensin II stimulates expression of the chemokine RANTES in rat glomerular endothelial cells. Role of the angiotensin type 2 receptor. *J Clin Invest* 1997;100(5):1047-58.
121. Gong R, Rifai A, Tolbert EM, Biswas P, Centracchio JN, Dworkin LD. Hepatocyte growth factor ameliorates renal interstitial inflammation in rat remnant kidney by modulating tubular expression of macrophage

- chemoattractant protein-1 and RANTES. *J Am Soc Nephrol* 2004;15(11):2868-81.
122. Wolf G, Aberle S, Thaiss F, et al. TNF alpha induces expression of the chemoattractant cytokine RANTES in cultured mouse mesangial cells. *Kidney Int* 1993;44(4):795-804.
123. Panzer U, Schneider A, Wilken J, Thompson DA, Kent SB, Stahl RA. The chemokine receptor antagonist AOP-RANTES reduces monocyte infiltration in experimental glomerulonephritis. *Kidney Int* 1999;56(6):2107-15.
124. Panzer U, Steinmetz OM, Reinking RR, et al. Compartment-specific expression and function of the chemokine IP-10/CXCL10 in a model of renal endothelial microvascular injury. *J Am Soc Nephrol* 2006;17(2):454-64.
125. Segerer S, Alpers CE. Chemokines and chemokine receptors in renal pathology. *Curr Opin Nephrol Hypertens* 2003;12(3):243-9.
126. Segerer S, Cui Y, Hudkins KL, et al. Expression of the chemokine monocyte chemoattractant protein-1 and its receptor chemokine receptor 2 in human crescentic glomerulonephritis. *J Am Soc Nephrol* 2000;11(12):2231-42.
127. Kitagawa K, Wada T, Furuichi K, et al. Blockade of CCR2 ameliorates progressive fibrosis in kidney. *Am J Pathol* 2004;165(1):237-46.
128. Li L, Huang L, Sung SS, et al. The chemokine receptors CCR2 and CX3CR1 mediate monocyte/macrophage trafficking in kidney ischemia-reperfusion injury. *Kidney Int* 2008;74(12):1526-37.
129. Jia T, Serbina NV, Brandl K, et al. Additive roles for MCP-1 and MCP-3 in CCR2-mediated recruitment of inflammatory monocytes during *Listeria monocytogenes* infection. *J Immunol* 2008;180(10):6846-53.
130. Wada T, Furuichi K, Sakai N, et al. Gene therapy via blockade of monocyte chemoattractant protein-1 for renal fibrosis. *J Am Soc Nephrol* 2004;15(4):940-8.
131. Furuichi K, Wada T, Iwata Y, et al. CCR2 signaling contributes to ischemia-reperfusion injury in kidney. *J Am Soc Nephrol* 2003;14(10):2503-15.
132. McIntosh LM, Barnes JL, Barnes VL, McDonald JR. Selective CCR2-targeted macrophage depletion ameliorates experimental mesangioproliferative glomerulonephritis. *Clin Exp Immunol* 2009;155(2):295-303.

133. Manchanda PK, Singh R, Mittal RD. Cytokine (IL-10 -1082 and -819) and chemokine receptor (CCR2 and CCR5) gene polymorphism in North Indian patients with end-stage renal disease. *DNA Cell Biol* 2009;28(4):177-83.
134. Mokubo A, Tanaka Y, Nakajima K, et al. Chemotactic cytokine receptor 5 (CCR5) gene promoter polymorphism (59029A/G) is associated with diabetic nephropathy in Japanese patients with type 2 diabetes: a 10-year longitudinal study. *Diabetes Res Clin Pract* 2006;73(1):89-94.
135. Dytfeld J, Bogdanski P, Pupek-Musialik D, Jagodzinski PP, Bryl W, Kujawa A. [Expression of chemokine receptor CCR5 in patients with type 2 diabetes]. *Pol Merkur Lekarski* 2006;20(116):195-8.
136. Sakai N, Wada T, Furuichi K, et al. p38 MAPK phosphorylation and NF-kappa B activation in human crescentic glomerulonephritis. *Nephrol Dial Transplant* 2002;17(6):998-1004.
137. Abdi R, Smith RN, Makhlouf L, et al. The role of CC chemokine receptor 5 (CCR5) in islet allograft rejection. *Diabetes* 2002;51(8):2489-95.
138. Omrani MD, Mokhtari MR, Tagizadae A, Bagheri M, Ahmad-Poor P. Association of CCR5-59029 A/G and CCR2-V64I variants with renal allograft survival. *Iran J Immunol* 2008;5(4):201-6.
139. Turner JE, Paust HJ, Steinmetz OM, et al. CCR5 deficiency aggravates crescentic glomerulonephritis in mice. *J Immunol* 2008;181(9):6546-56.
140. Bickerstaff A, Nozaki T, Wang JJ, et al. Acute humoral rejection of renal allografts in CCR5(-/-) recipients. *Am J Transplant* 2008;8(3):557-66.
141. Bleul CC, Farzan M, Choe H, et al. The lymphocyte chemoattractant SDF-1 is a ligand for LESTR/fusin and blocks HIV-1 entry. *Nature* 1996;382(6594):829-33.
142. Burns JM, Summers BC, Wang Y, et al. A novel chemokine receptor for SDF-1 and I-TAC involved in cell survival, cell adhesion, and tumor development. *J Exp Med* 2006;203(9):2201-13.
143. Wang X, Li C, Chen Y, et al. Hypoxia enhances CXCR4 expression favoring microglia migration via HIF-1alpha activation. *Biochem Biophys Res Commun* 2008;371(2):283-8.
144. Schonemeier B, Schulz S, Hoell V, Stumm R. Enhanced expression of the CXCL12/SDF-1 chemokine receptor CXCR7 after cerebral ischemia in the rat brain. *J Neuroimmunol* 2008;198(1-2):39-45.

145. Lotan D, Sheinberg N, Kopolovic J, Dekel B. Expression of SDF-1/CXCR4 in injured human kidneys. *Pediatr Nephrol* 2008;23(1):71-7.
146. Butler JM, Guthrie SM, Koc M, et al. SDF-1 is both necessary and sufficient to promote proliferative retinopathy. *J Clin Invest* 2005;115(1):86-93.
147. Yano T, Liu Z, Donovan J, Thomas MK, Habener JF. Stromal cell derived factor-1 (SDF-1)/CXCL12 attenuates diabetes in mice and promotes pancreatic beta-cell survival by activation of the prosurvival kinase Akt. *Diabetes* 2007;56(12):2946-57.
148. Freeburg PB, Abrahamson DR. Hypoxia-inducible factors and kidney vascular development. *J Am Soc Nephrol* 2003;14(11):2723-30.
149. Ceradini DJ, Kulkarni AR, Callaghan MJ, et al. Progenitor cell trafficking is regulated by hypoxic gradients through HIF-1 induction of SDF-1. *Nat Med* 2004;10(8):858-64.
150. Schober A, Knarren S, Lietz M, Lin EA, Weber C. Crucial role of stromal cell-derived factor-1alpha in neointima formation after vascular injury in apolipoprotein E-deficient mice. *Circulation* 2003;108(20):2491-7.
151. Togel F, Isaac J, Hu Z, Weiss K, Westenfelder C. Renal SDF-1 signals mobilization and homing of CXCR4-positive cells to the kidney after ischemic injury. *Kidney Int* 2005;67(5):1772-84.
152. Hashimoto N, Jin H, Liu T, Chensue SW, Phan SH. Bone marrow-derived progenitor cells in pulmonary fibrosis. *J Clin Invest* 2004;113(2):243-52.
153. Takabatake Y, Sugiyama T, Kohara H, et al. The CXCL12 (SDF-1)/CXCR4 axis is essential for the development of renal vasculature. *J Am Soc Nephrol* 2009;20(8):1714-23.
154. Balabanian K, Couderc J, Bouchet-Delbos L, et al. Role of the chemokine stromal cell-derived factor 1 in autoantibody production and nephritis in murine lupus. *J Immunol* 2003;170(6):3392-400.
155. Wang A, Fairhurst AM, Tus K, et al. CXCR4/CXCL12 hyperexpression plays a pivotal role in the pathogenesis of lupus. *J Immunol* 2009;182(7):4448-58.
156. Lu DY, Tang CH, Yeh WL, et al. SDF-1alpha up-regulates interleukin-6 through CXCR4, PI3K/Akt, ERK, and NF-kappaB-dependent pathway in microglia. *Eur J Pharmacol* 2009;613(1-3):146-54.

157. De Klerck B, Geboes L, Hatse S, et al. Pro-inflammatory properties of stromal cell-derived factor-1 (CXCL12) in collagen-induced arthritis. *Arthritis Res Ther* 2005;7(6):R1208-20.
158. Phillips RJ, Burdick MD, Hong K, et al. Circulating fibrocytes traffic to the lungs in response to CXCL12 and mediate fibrosis. *J Clin Invest* 2004;114(3):438-46.
159. Xu J, Mora A, Shim H, Stecenko A, Brigham KL, Rojas M. Role of the SDF-1/CXCR4 axis in the pathogenesis of lung injury and fibrosis. *Am J Respir Cell Mol Biol* 2007;37(3):291-9.
160. Mehrad B, Burdick MD, Strieter RM. Fibrocyte CXCR4 regulation as a therapeutic target in pulmonary fibrosis. *Int J Biochem Cell Biol* 2009;41(8-9):1708-18.
161. Zagzag D, Krishnamachary B, Yee H, et al. Stromal cell-derived factor-1alpha and CXCR4 expression in hemangioblastoma and clear cell-renal cell carcinoma: von Hippel-Lindau loss-of-function induces expression of a ligand and its receptor. *Cancer Res* 2005;65(14):6178-88.
162. Burger JA, Kipps TJ. CXCR4: a key receptor in the crosstalk between tumor cells and their microenvironment. *Blood* 2006;107(5):1761-7.
163. Liang Z, Brooks J, Willard M, et al. CXCR4/CXCL12 axis promotes VEGF-mediated tumor angiogenesis through Akt signaling pathway. *Biochem Biophys Res Commun* 2007;359(3):716-22.
164. Gao C, Huan J. SDF-1 plays a key role in chronic allograft nephropathy in rats. *Transplant Proc* 2008;40(5):1674-8.
165. Palm F. Intrarenal oxygen in diabetes and a possible link to diabetic nephropathy. *Clin Exp Pharmacol Physiol* 2006;33(10):997-1001.
166. Salcedo R, Wasserman K, Young HA, et al. Vascular endothelial growth factor and basic fibroblast growth factor induce expression of CXCR4 on human endothelial cells: In vivo neovascularization induced by stromal-derived factor-1alpha. *Am J Pathol* 1999;154(4):1125-35.
167. Thelen M, Thelen S. CXCR7, CXCR4 and CXCL12: an eccentric trio? *J Neuroimmunol* 2008;198(1-2):9-13.
168. Thelen M. Dancing to the tune of chemokines. *Nat Immunol* 2001;2(2):129-34.

169. Infantino S, Moepps B, Thelen M. Expression and regulation of the orphan receptor RDC1 and its putative ligand in human dendritic and B cells. *J Immunol* 2006;176(4):2197-207.
170. Raggio C, Ruhl R, McAllister S, et al. Novel cellular genes essential for transformation of endothelial cells by Kaposi's sarcoma-associated herpesvirus. *Cancer Res* 2005;65(12):5084-95.
171. Mazzinghi B, Ronconi E, Lazzeri E, et al. Essential but differential role for CXCR4 and CXCR7 in the therapeutic homing of human renal progenitor cells. *J Exp Med* 2008;205(2):479-90.
172. Levoye A, Balabanian K, Baleux F, Bachelierie F, Lagane B. CXCR7 heterodimerizes with CXCR4 and regulates CXCL12-mediated G protein signaling. *Blood* 2009;113(24):6085-93.
173. Klussmann S, Nolte A, Bald R, Erdmann VA, Furste JP. Mirror-image RNA that binds D-adenosine. *Nat Biotechnol* 1996;14(9):1112-5.
174. Weisberg SP, Hunter D, Huber R, et al. CCR2 modulates inflammatory and metabolic effects of high-fat feeding. *J Clin Invest* 2006;116(1):115-24.
175. Ihm CG, Park JK, Hong SP, et al. A high glucose concentration stimulates the expression of monocyte chemoattractant protein 1 in human mesangial cells. *Nephron* 1998;79(1):33-7.
176. Stroo I, Stokman G, Teske GJ, Florquin S, Leemans JC. Haematopoietic stem cell migration to the ischemic damaged kidney is not altered by manipulating the SDF-1/CXCR4-axis. *Nephrol Dial Transplant* 2009;24(7):2082-8.
177. Wang Y, Wang YP, Zheng G, et al. Ex vivo programmed macrophages ameliorate experimental chronic inflammatory renal disease. *Kidney Int* 2007;72(3):290-9.
178. Hoffmann U, Banas B, Kruger B, et al. SDF-1 expression is elevated in chronic human renal allograft rejection. *Clin Transplant* 2006;20(6):712-8.
179. Hitchon C, Wong K, Ma G, Reed J, Lyttle D, El-Gabalawy H. Hypoxia-induced production of stromal cell-derived factor 1 (CXCL12) and vascular endothelial growth factor by synovial fibroblasts. *Arthritis Rheum* 2002;46(10):2587-97.
180. Eremina V, Quaggin SE. The role of VEGF-A in glomerular development and function. *Curr Opin Nephrol Hypertens* 2004;13(1):9-15.

181. Peled A, Petit I, Kollet O, et al. Dependence of human stem cell engraftment and repopulation of NOD/SCID mice on CXCR4. *Science* 1999;283(5403):845-8.
182. Avecilla ST, Hattori K, Heissig B, et al. Chemokine-mediated interaction of hematopoietic progenitors with the bone marrow vascular niche is required for thrombopoiesis. *Nat Med* 2004;10(1):64-71.
183. Sugiyama T, Kohara H, Noda M, Nagasawa T. Maintenance of the hematopoietic stem cell pool by CXCL12-CXCR4 chemokine signaling in bone marrow stromal cell niches. *Immunity* 2006;25(6):977-88.
184. Sipkins DA, Wei X, Wu JW, et al. In vivo imaging of specialized bone marrow endothelial microdomains for tumour engraftment. *Nature* 2005;435(7044):969-73.
185. Bartolome RA, Ferreira S, Miquilena-Colina ME, et al. The chemokine receptor CXCR4 and the metalloproteinase MT1-MMP are mutually required during melanoma metastasis to lungs. *Am J Pathol* 2009;174(2):602-12.
186. Scimone ML, Felbinger TW, Mazo IB, Stein JV, Von Andrian UH, Weninger W. CXCL12 mediates CCR7-independent homing of central memory cells, but not naive T cells, in peripheral lymph nodes. *J Exp Med* 2004;199(8):1113-20.
187. Grunewald M, Avraham I, Dor Y, et al. VEGF-induced adult neovascularization: recruitment, retention, and role of accessory cells. *Cell* 2006;124(1):175-89.
188. Breyer MD, Bottinger E, Brosius FC, 3rd, et al. Mouse models of diabetic nephropathy. *J Am Soc Nephrol* 2005;16(1):27-45.
189. Appel D, Kershaw DB, Smeets B, et al. Recruitment of podocytes from glomerular parietal epithelial cells. *J Am Soc Nephrol* 2009;20(2):333-43.
190. Ronconi E, Sagrinati C, Angelotti ML, et al. Regeneration of glomerular podocytes by human renal progenitors. *J Am Soc Nephrol* 2009;20(2):322-32.

9. Abbreviations

ACE	angiotensin converting enzyme
AGEs	advanced glycation end products
Ang II	angiotensin II
AOP-RANTES	RANTES receptor blocker
AR	aldose reductase
AT1R	angiotensin II type 1 receptor
AT2R	angiotensin II type 2 receptor
BM	basement membrane
BSA	bovine serum albumin
BUN	blood urea nitrogen
cDNA	complementary DNA
CCL2	chemokine C-C motif ligand 2
CCL5	chemokine C-C motif ligand 5
CCR1	chemokine C-C motif receptor 1
CCR2	chemokine C-C motif receptor 2
CCR3	chemokine C-C motif receptor 3
CCR5	chemokine C-C motif receptor 5
CCR7	chemokine C-C motif receptor 7
CX3CL1	chemokine C-X3-C motif ligand 3
CXCL10	chemokine C-X-C motif ligand 10
CXCL12	chemokine C-X-C motif ligand 12
CXCR2	chemokine C-X-C motif receptor 2
CXCR4	chemokine C-X-C motif receptor 4
CXCR7	chemokine C-X-C motif receptor 7
CX3CR1	chemokine C-X3-C motif receptor 1
CKD	chronic kidney disease
CML	N- ϵ -carboxymethyllysine
CT	cycle threshold
CTGF	connective tissue growth factor
DAG	diacylglycerol
3DG	3-deoxyglucosone

DARC	Duffy antigen receptor for chemokines
DCCT	Diabetes Control and Complication Trial
ddH ₂ O	double distilled water
DEPC	diethyl pyrocarbonate
DMEM	Dulbecco's modified Eagle's medium
DMSO	dimethyl sulfoxide
DN	diabetic nephropathy
et al.	et alii = and others
e.g.	exempli gratia = for instance
ECM	extracellular matrix
EDTA	ethylenediaminetetra acetic acid
ELISA	Enzyme-Linked Immunosorbent Assay
ESRD	end-stage renal disease
ET	endothelin
FACS	fluorescence activated cell sorting
FCS	fetal calf serum
FITC	fluorescein isothiocyanate
GBM	glomerular basement membrane
GENC	glomerular endothelial cell line
GFR	glomerular filtration rate
GPCR	G protein-coupled receptor
HE	Hematoxylin-Eosin
Hif	hypoxia inducible factor
HIV	human immunodeficiency virus
hpf	high-power-field
ICAM-1	intercellular adhesion molecule-1
sICAM-1	soluble intercellular adhesion molecule-1
i.e.	id est = in other words
IL	interleukin
IL-8	interleukin-8
IFN- γ	interferon- γ
IP-10	interferoninducible protein-10
J774	murine macrophage cell line

kDa	kilo dalton
K/DOQI	<u>K</u> idney <u>D</u> isease <u>O</u> utcomes <u>Q</u> uality <u>I</u> nitiative
MCP	monocyte chemoattractant protein
MCP-1	monocyte chemoattractant protein-1
MCP-2	monocyte chemoattractant protein-2
Met-RANTES	N-terminal with Methionin modified CCL5/RANTES
MG	methylglyoxal
min	minute/minutes
MIP	macrophage inflammatory protein
MIP-1	macrophage inflammatory protein-1
ml/min	milliliter/minute
M/M	monocytes / macrophages
mNOX-E36	anti-CCL2 Spiegelmer
mNOX-A12	anti-CXCL12 Spiegelmer
mRNA	messenger ribonucleic acid
MTC	murine tubular cell line
NADPH	nicotinamide adenine dinucleotide phosphate
n.d.	nondetectable
NF-κB	nuclear factor-κB
NO	nitric oxide
O.D.	optical density
PAS	Periodic acid Schiff
PBS	phosphate buffered saline
PCR	polymerase chain reaction
pDCs	plasma dendritic cells
PDGF	platelet derived growth factor
PGE2	prostaglandin E2
PKC	protein kinase C
Poc	scrambled sequence of RNA (Control Spiegelmer for mNOX-E36)
PPARs	peroxisome proliferator-activator receptors
PPAR-γ	peroxisome proliferator activator receptor gamma
RANTES	regulated on activation normal T cell expressed and secreted

RAS	renin angiotensin system
revmNOX-A12	Control Spiegelmer for mNOX-A12
RNA	ribonucleic acid
Rnase	ribonuclease
ROS	reactive oxygen species
RPM	revolutions per minute
RPMI Medium	cell culture medium
rRNA	ribosomal ribonucleic acid
RT	room temperature
RT-PCR	real-time reverse transcription-polymerase chain reaction
s	second
SDF-1	stromal cell-derived factor-1
SDH	sorbitol dehydrogenase
SMA	smooth muscle actin
STZ	streptozotocin
TGF- β	transforming growth factor- β
Th1	T helper cell type 1
TNF- α	tumor necrosis factor- α
TZDs	thiazolidinediones
U	units
UAE	urinary albumin excretion
UKPDS	UK Prospective Diabetes Study
UUO	unilateral uretral obstruction
VCAM-1	vascular cell adhesion molecule-1
VEGF	vascular endothelial growth factor
vs	versus
v/v	volume/volume
WM 7390	CCR2 and CCR5 dual atagonist
WM 7671	CCR2 and CCR5 dual atagonist
WT	wild type
WT1	Wilms tumor
1K	1 kidney
2K	2 kidneys

Appendix

1. FACS buffer :

Sterile DPBS	500 ml
Na Azide	500 mg (0.1 %)
BSA	1 g (0.2 %)

2. Paris Buffer:

20 mM Tris-HCL, 125 mM NaCl, 10 mM KCl, 10 mM Sodium acetate, 5 mM Glucose.

For 1000 ml:

Tris-HCL (MW 121.14)	2.4228 g
NaCl (MW 58.44)	7.31 g
KCl (MW 74.56)	0.74556 g
Sod. Acetate (MW 82.03)	0.8203 g
D-Glucose (MW 180.16)	0.9 g

3. 10X HBSS (Hank's Balanced Saline Solution) with Ca, Mg:

For 1000 ml

KCl	4 g	
KH ₂ PO ₄	0.6 g	
NaCl	80 g	
Na ₂ HPO ₄ .2H ₂ O	0.621 g	
NaHCO ₃	3.5 g	
CaCl ₂	1.4 g	(or CaCl ₂ .2H ₂ O 1.854 g)
MgCl ₂ .6H ₂ O	1 g	
MgSO ₄ .7H ₂ O	1 g	
D-Glucose	10 g	

Dissolve in 900 ml of distilled water and adjust to pH 7.4 with 1N HCl or 1N NaOH. Make up the volume with distilled water to 1000 ml.

4. 10X HBSS (Hank's Balanced Saline Solution) **without** Ca, Mg:

For 1000 ml

KCl	4 g
KH ₂ PO ₄	0.6 g

NaCl	80 g
Na ₂ HPO ₄ ·2H ₂ O	0.621 g

Dissolve in 1000 ml and autoclave.

5. DNase stock solution (1 mg/ml):

DNase (type III) 15000 U/6 mg (Sigma D5025)

To prepared 1 mg/ml solution: Add 6 ml of 50 % (w/v) Glycerol in 20 mM Tris-HCl (pH 7.5), 1 mM MgCl₂.

Can be kept at – 20 °C for several weeks.

Caution: Solution is stable only for 1 week at 4 °C.

6. 50 % Glycerol in 20 mM Tris-HCl (pH 7.5), 1 mM MgCl₂:

- a. 0.48 g of Tris-HCl in 100 ml of distilled water, adjust pH to 7.4 (= 40 mM)
- b. 50 ml of Glycerol 100 % + 50 ml of 40 mM Tris-HCl (20 mM)
- c. Add 100 ul of 1M MgCl₂ solution.

7. Collagenase / DNase solution:

1 mg/ml Collagenase, 0.1 mg/ml DNase in 1X HBSS (with Ca, Mg)

For 10 ml:

Collagenase (type I) (Sigma C0130)	10 mg
1 mg/ml DNase stock solution	1 ml
HBSS (with Ca, Mg)	9 ml

To be preheated in 37 °C water bath before use.

Caution: Prepare freshly every time (Stable only for few days)

8. Collagenase solution:

1 mg/ml Collagenase in 1X HBSS (with Ca, Mg)

For 10 ml:

Collagenase (type I)	10 mg
HBSS (with Ca, Mg)	10 ml

To be preheated in 37 °C water bath before use.

Caution: Prepare freshly every time (Stable only for few days)

9. EDTA 2 mM:

EDTA (MW) (Sigma)

EDTA 7.44 mg in 10 ml HBSS (**without** Ca, Mg)

To be preheated in 37 °C water bath before use.

10. Anesthesia mixture

10 ml Midazolam (1mg/ml)

2 ml Fentanyl (0.05 mg/ml)

1 ml Dormitor (1 mg/ml)

11. Antagonist mixture

5 ml Annexate (0.1mg/ml)

0.5 ml Antisedan (5 mg/ml)

3 ml Naloxon (0.4 mg/ml)

12. MACS Buffer

PBS pH 7.2

0.5% bovine serum albumin

2 mM EDTA

13. Citrate buffer 10X

110 mM Sodiumcitrate

in ddH₂O

with 2N NaOH to pH 6

14. PBS

2.74 M NaCl

54 mM KCl

30 mM KH₂PO₄

130 mM Na₂HPO₄

in ddH₂O

with HCl to pH 7.5

CURRICULUM VITAE

SAYYED SUFYAN ALI GHAZANFAR ALI

Medizinische Poliklinik der LMU München
Klinische Biochemie, Schillerstr 42
80336 München
Tel. +49(0)89/218075-856
Mobile: +49(0)17664213095
Email: sufyan.sayyed@med.uni-muenchen.de



ACADEMIC PROFILE

PhD. (2007 till date)

Ludwig-Maximilians Universität, München (Germany)

Thesis entitled:

- Role of pro-inflammatory and homeostatic chemokines in Diabetic nephropathy.

M.S. Pharmacology and Toxicology (2003 to 2005)

National Institute of Pharmaceutical Education and Research, Mohali (India)

Thesis entitled:

- Pharmacological Interventions Targeted at Oxidative Stress in Experimental Diabetic Neuropathy.

B. Pharm. Science (1999 - 2003)

Poona University, Pune (India)

Major subjects:

- Pharmacology, Pharmacognosy, Pharmaceutics and Medicinal Chemistry

ACADEMIC ACHIEVEMENTS

- Qualified GATE 2003 conducted by IIT, Madras with **94.13** percentile.
- Secured **19th** rank in the all India entrance exam for M.S. Pharm admission conducted by NIPER 2003.

INDUSTRIAL EXPERIENCE

Worked at Nicholas Piramal Research Center,(INDIA) as "Junior Research Scientist" from June 2005 to April 2007.

PUBLICATIONS from PhD

- **Sufyan G. Sayyed**, H. Hägele, O. P. Kulkarni, K. Endlich, S. Segerer, D. Eulberg, S. Klussmann, H.J. Anders; Podocytes express the homeostatic chemokine stromal cell-derived factor-1/CXCL12 which contributes to glomerulosclerosis, podocyte loss, and albuminuria in type 2 diabetes. *Diabetologia*, 2009, 52 (11), 2445-54.
- **Sufyan G. Sayyed**, Anil Bhanudas Gaikwad, Julia Lichtnekert, Onkar Kulkarni, Dirk Eulberg, Sven Klussmann, Kulbhushan Tikoo, Hans-Joachim Anders; Progressive glomerulosclerosis in type 2 diabetes is associated with renal histone H3K9 and H3K23 acetylation, H3K4 dimethylation and phosphorylation at serine 10, (*Under revision in NDT*)
- Anil Bhanudas Gaikwad, **Sufyan G. Sayyed**, Julia Lichtnekert, Kulbhushan Tikoo, Hans-Joachim Anders; Renal failure increases cardiac histone H3K9 and H3K23 acetylation, H3K4 dimethylation, phosphorylation at serine 10 and reduces the H3K9 dimethylation in type 2 diabetes. (*Under revision in American Journal of Pathology*)

PUBLICATIONS

- **Sufyan G. Sayyed**, Ashutosh Kumar and Shyam S. Sharma; Effects of U83836E on nerve functions, hyperalgesia and oxidative stress in experimental diabetic neuropathy. *Life Sciences*, 2006, 79 (8), 777-783.
- Shyam S. Sharma and **Sufyan G. Sayyed**; Trolox ameliorates the nerve conduction velocity, nerve blood flow and nociception deficits in experimental diabetic neuropathy. *Clinical and experimental pharmacology and physiology*, 2006, 33 (11), 1022- 28.
- Lalit S. Doshi, Manoj K. Brahma, **Sufyan G. Sayyed**, *et al.*; Acute administration of GPR40 receptor agonist potentiates glucose-stimulated insulin secretion in vivo in rat. *Metabolism Clinical and Experimental*, 2009, 58 (3), 333- 43.
- Rathinasabapathy A., **Sufyan G. Sayyed**, *et al.*; 18F9 (4-(3,6-bis (ethoxycarbonyl)-4,5,6,7-tetrahydrothieno (2,3-c) pyridin-2-ylamino)-4-oxobutanoic acid) enhances insulin-mediated glucose uptake in vitro and exhibits antidiabetic activity in vivo in *db/db* mice. *Metabolism Clinical and Experimental*, 2009, 58 (10), 1503-16.

POSTER PRESENTATIONS

- **Sufyan G. Sayyed**, H. Hägele, O. P. Kulkarni, K. Endlich, S. Segerer, D. Eulberg, S. Klussmann, H.J. Anders; Podocyte release of SDF-1/CXCL12 contributes to glomerulosclerosis, podocyte loss, and albuminuria in type 2 diabetes. A novel pathomechanism of diabetic nephropathy. **American Society of Nephrology 2009, San Diego. (Poster selected for free talk presentation)**
- **Sufyan G. Sayyed**, Anil Bhanudas Gaikwad, Julia Lichtnekert, Onkar Kulkarni, Dirk Eulberg, Sven Klussmann, Kulbhushan Tikoo, Hans-Joachim Anders; Renal and cardiac histone H3 epigenetics in mice with type 2 diabetes and renal failure. **American Society of Nephrology 2009, San Diego.**
- **Sufyan G. Sayyed**, Anil Bhanudas Gaikwad, Julia Lichtnekert, Onkar Kulkarni, Dirk Eulberg, Sven Klussmann, Kulbhushan Tikoo, Hans-Joachim Anders; Epigenetische H3-Modifizierungen bei diabetischer Nephropathie werden durch MCP-1-Blockade verhindert. **Kongress für Nephrologie 2009, Göttingen.**
- Anil Bhanudas Gaikwad, **Sufyan G Sayyed**, Julia Lichtnekert, Hans-Joachim Anders; Nierenversagen bei Diabetes Typ II führt zu cardialen Histon-Modifizierungen. **Kongress für Nephrologie 2009, Göttingen.**
- **Sufyan G. Sayyed**, Anil Bhanudas Gaikwad, Julia Lichtnekert¹, Onkar Kulkarni¹, Dirk Eulberg, Sven Klussmann, Kulbhushan Tikoo, Hans Joachim Anders; CCL2 blockade prevents the development of diabetic nephropathy and alters the post-translational modification of histone H3 in type II diabetic mice. **World Congress Nephrology 2009, Milan.**
- **Sufyan G. Sayyed**, Anuj K Saini and Shyam S. Sharma, Effect of antioxidant on nerve conduction velocity, blood flow and nociception in diabetic neuropathy. *Indian Journal of Pharmacology, Volume 36, S-56.*

CONFERENCES ATTENDED

- International World Congress Nephrology, Milan, 2009
- XXXVIITH Annual conference of Indian Pharmacological Society 2005
- National symposium on medicine information held in August 2003
- Drug discovery and development in new millennium (Part one, Part two and Part three)

PERSONAL DETAILS

Date of Birth	07-07-1981
Nationality	Indian
Sex	Male
Marital Status	Single
Languages known	English, Hindi, Marathi, Urdu (and little bit of German)

REFERENCES

PD Dr. Hans-Joachim Anders

Internist Nephrologe Rheumatologe
Medizinische Poliklinik-Innenstadt
Klinikum der Universität München
Pettenkoferstr. 8a
D-80336 München
Tel. +49 (0) 89 51603583
Email: Hans-Joachim.Anders@med.uni-muenchen.de

Dr. S. S. Sharma

Associate Professor,
Dept of Pharmacology & Toxicology,
National Institute of Pharmaceutical Education & Research
(NIPER),
Sector-67, S. A. S. Nagar, Punjab-160 062
Email: sssharma@niper.ac.in

Dr. Kumar Nemmani

Assistant Director,
Dept of Pharmacology & Toxicology,
Nicholas Piramal Research Center (NPRC),
1, Nirlon complex, Off western Express highway,
Goregaon (E), Mumbai- 400 063.
Email: knemmani@nicholaspiramal.co.in

I here by declare that the details provided here are true to best of my knowledge.

SAYYED SUFYAN ALI